12-1-2023

Cell Surface and Plasma Biomarkers of Kaposi Sarcoma

Sara R. Privatt
University of Nebraska-Lincoln, saraprivatt@gmail.com

CELL SURFACE AND PLASMA BIOMARKERS OF KAPOSI SARCOMA

by

Sara R. Privatt

A DISSERTATION

Presented to the Faculty of

The Graduate College at the University of Nebraska

In Partial Fulfillment of Requirements

For the Degree of Doctor of Philosophy

Major: Biological Sciences

(Genetics, Cell, and Molecular Biology)

Under the Supervision of Professor Charles Wood

Lincoln, Nebraska

November 2023

CELL SURFACE AND PLASMA BIOMARKERS OF KAPOSI SARCOMA

Sara R. Privatt, Ph.D.

University of Nebraska, 2023

Adviser: Charles Wood

Kaposi sarcoma-associated herpesvirus is the etiological agent of several pathologies including Kaposi sarcoma, primary effusion lymphoma, and multicentric Castleman's disease. Here, we investigated both the tumor microenvironment (TME) in KS lesions as well as plasma from KSHV-infected individuals and how metabolic dysfunction and dysregulated cytokines might have a systemic effect on KS tumorigenesis. Based on previously published KS tumor transcriptomics, one aspect of our investigation involved characterizing cell surface glycoproteins with potential to serve as therapeutic targets against KSHV-infected cells or KS tumors or as biomarkers for disease. Expression patterns of such markers may also suggest the cellular origin of KS tumors.

We found that several surface proteins and endothelial lineage markers were overexpressed in KS biopsies compared to uninvolved skin. Colocalization with KSHV LANA was detected using multi-color immunofluorescence in KS tissues, *in vitro* cultures, and xenografts. The surface glycoproteins KDR, FLT4, UNC5A, ADAM12, and CD34 associated with LANA-positive cells but also perhaps with KSHV uninfected cells or those with KSHV antigen below detection limit in the TME. In KS tumors, most LANA-positive cells co-expressed markers of vascular as well as lymphatic endothelial lineages.

This contrasts with normal endothelial tissues and suggests that KSHV tumorigenesis promotes dedifferentiation to a more mesenchymal/progenitor phenotype or that KS results from initial infection of an endothelial (mesenchymal) progenitor cell type.

We next studied plasma metabolomics to conduct the first study to explore whether metabolic alterations induced by KSHV/HIV-1 co-infection or KS tumorigenesis could be detected in the plasma of affected subjects and whether different infection and disease states could be distinguished. Results from this preliminary study showed that asymptomatic and symptomatic subject groups exhibited distinct patterns in both polar and non-polar plasma metabolites. These findings suggested dysregulation in amino acid/urea cycle and purine metabolic pathways in KS disease progression, possibly influenced by viral infection. Overall, these findings indicate that more intensive investigation into the temporal patterns of metabolic dysregulation in KSHV infection/HIV co-infection and KS pathogenesis are justified.

Overall, the studies herein provided insights into the complex interplay between KSHV, the tumor microenvironment, plasma proteomics, and plasma metabolomics in the context of KS and related diseases.

ACKNOWLEDGMENTS

First and foremost, I would like to wholeheartedly thank all the participants of these studies for their generosity and willingness to be involved in this research as well as the study teams in Zambia and Tanzania, without their hard work and dedication none of the research described here would be possible. I would also like to thank the members of my committee for their unwavering support and patience: Dr. Eric Weaver, Dr. Jay Reddy, Dr. Peter Angeletti, and my advisors, Dr. John West, and Dr. Charles Wood. Additionally, I am grateful for the support of both past and present lab members of the Wood/West lab, especially Lisa Poppe, Sydney Bennett, Dicle Yalcin, Salum Lidenge and Zhou Liu; without them, none of this would have been possible.

PREFACE

Chapter 2 of this dissertation research has been published in *Cancers* (Privatt, et al, "Upregulation of Cell Surface Glycoproteins in Correlation with KSHV LANA in the Kaposi Sarcoma Tumor Microenvironment" (Published in *Cancers*, Apr, 2023).)

Chapter 3 of this dissertation research has been published in *Cancer & Metabolism* (Privatt, et al, "Comparative polar and lipid plasma metabolomics differentiate KSHV infection and disease states" (Published in *Cancer & Metabolism*, Aug, 2023).)

Chapter 5 of this dissertation research has been published in *Vaccine* (Privatt, et al, "Longitudinal quantification of adenovirus neutralizing responses in Zambian mother-infant pairs: Impact of HIV-1 infection and its treatment" (Published in *Vaccine*, Aug, 2019).)

Table of Contents

CHAPTER 1

LITERATURE REVIEW

Herpesviridae

The virus family Herpesviridae consists of over 200 enveloped, double-stranded DNA viruses (1). Nine herpesviruses have been shown to preferentially infect humans, however, herpesviruses have been isolated from a large range of animals. The nine human viruses, herpes simplex virus types 1 and 2 (HSV-1,2 or HHV-1,2), varicella zoster virus (VZV or HHV-3), Epstein Barr virus (EBV or HHV-4), human cytomegalovirus (HCMV or HHV-5), human herpes virus types 6A and 6B (HHV-6A/B), human herpes virus type 7 (HHV-7) and Kaposi sarcoma-associated herpesvirus (KSHV), also known as human herpes virus 8 (HHV-8), fall into three herpesvirus subfamilies: alpha, beta, and gamma. Worldwide, most adults harbor a persistent infection with several herpesviruses (1).

Alphaherpesvirinae is defined by characteristics like a variable host range, a relatively short reproductive cycle, rapid spread in culture, efficient destruction of infected cells, and the capacity to establish latent infections, primarily in sensory ganglia. It encompasses genera including *Simplexvirus* (HSV-1,2), and *Varicellovirus* (VZV) (2). The Betaherpesvirinae subfamily is characterized by a restricted host range, a relatively long reproductive cycle, and slow progression in cultured cells. Infected cells often become enlarged (cytomegaly), and carrier cultures are easily established. Betaherpesviruses can establish latency in various tissues, such as secretory glands, lymphoreticular cells, and kidneys. This subfamily comprises the genera

Cytomegalovirus, *Muromegalovirus*, *Proboscivirus*, and *Roseolovirus*, with examples like Human Cytomegalovirus (HCMV) and Human Herpesvirus 6 (HHV-6) (2).

There are two human viruses in the Gammaherpesvirinae family, EBV and KSHV (3), and these are two of the seven viruses known to cause human cancer. Over 90% of the world's adult population is estimated to be infected with EBV whereas KSHV has focal regions of high seroprevalence indicative of endemic infection (3-5). Initial infection of both EBV and KSHV occurs either in early childhood, during adolescence, or through sexual relations. Both viruses are primarily transferred through saliva from caregivers during childhood and through kissing or through blood transfusions or transplants (6, 7).

Viral Life Cycle

KSHV's genome is about 165kb long and encodes 90 protein-coding genes and 25 regulatory RNAs (1, 8). KSHV exhibits a complex viral life cycle that involves infection of various cell types, including endothelial cells, B cells, epithelial cells, dendritic cells, monocytes, and fibroblasts (5, 9). To gain entry into these cells, KSHV interacts with specific host cell surface receptors, such as integrins, cystine-glutamate transporters, heparan sulfate, and tyrosine protein kinase receptors (10). Viral binding triggers signal transduction cascades that allow the virus to enter the cell via endocytosis and be trafficked within the cytoplasm along acetylated microtubules to the nucleus (11).

KSHV primarily engages with heparan sulfate proteoglycans (HSPGs) present on the surface of most cells. This interaction serves to increase viral concentration on the

cell surface, thereby facilitating the infection process, as reviewed by van der Meuden et al (12). The viral glycoproteins gB and K8.1A are involved in this binding process (13). Moreover, the viral complement control protein (KCP), encoded by ORF4, also binds to HSPGs. The expression of human exostosin-1 (Ext1), an enzyme responsible for the glycosylation of heparan sulfate, plays a role in facilitating KSHV infection (12).

In terms of cellular entry receptors, KSHV engages a variety of receptors depending on the cell type. Some key receptors include DC-SIGN (Dendritic cell-specific intercellular adhesion molecule-3 grabbing non-integrin), Ephrin receptors, integrins, and xCT (glutamate/cysteine exchange transporter) (12, 13). These receptors facilitate KSHV entry into specific cell types. The interactions between these receptors and KSHV glycoproteins are critical for viral entry. Endothelial cells and fibroblasts are the primary targets for KSHV, with integrins and xCT playing a role in the entry process. In contrast, B cells, macrophages, dendritic cells, and monocytes are associated with KSHV-associated lymphoproliferative disorders, and receptors like DC-SIGN and Eph receptors are involved in infection (9, 12). The specific receptors and mechanisms can vary among different cell types.

Once inside the cell, the viral capsid releases the viral genome into the nucleus. The viral DNA circularizes and associates with cellular histones to form a chromatin-like structure (2). KSHV can then enter either a latent or lytic phase during its lifecycle. During the latent phase, KSHV establishes lifelong infection by expressing a set of latency-associated genes, including viral FLICE inhibitory protein (vFLIP), viral Cyclin

(vCyclin), latency-associated nuclear protein (LANA), kaposin, and several microRNAs (10, 14-17). The expression of these genes promotes cell survival and supports tumorigenesis as the gene products inhibit apoptosis and maintain latency. The viral genome, circularized in the nucleus, remains as an episome, tethered to the host chromosome by LANA. Several viral miRNAs contribute to cell reprogramming and prevent reactivation from latency (8, 18).

LANA is one of the most important KSHV proteins and plays a multifaceted role in the establishment of latency in KSHV infection. It recruits host machinery to the viral genome and vice versa, recruits DNA methyltransferases to silence cellular gene expression, recruits components of the Polycomb Repressive Complex (PRC) to repress KSHV lytic gene expression, stimulates protease-mediated cleavage of signal transducer and activator of transcription 6 (STAT6) to act as a transcriptional repressor of the host immune system, and promotes latent gene expression by recruiting human suppressor of variegation, enhancer-of-zeste, and trithorax domain-containing protein 1 (hSET1) for methylation of histone H3K4 which allows for active transcription of latency associated genes (10). LANA also removes heterochromatinic marks from latent and lytic promoters by recruiting lysine demethylase 3A (KDM3A). The SUMOylation of LANA is also thought to contribute to the formation of a complex that helps tether the viral episome to host cell chromosomes, promoting the establishment of latency. Additionally, arginine methylation facilitated by protein methyltransferase 1 (PRMT1) enhances LANA's binding to histones. These modifications underscore LANA's crucial

role as a master organizer in maintaining KSHV latency as reviewed by Broussard and Damania (10).

Several cellular signaling pathways and host factors play a crucial role in maintaining the virus in a latent state. One key pathway is the NF-κB signaling pathway, which is constitutively active in KSHV-infected cells. NF-κB transcription factors are activated by phosphorylation of the inhibitor protein IκBα, leading to transactivation of downstream target genes (12, 13). Activated NF-κB interacts with the replication and transcription activator (RTA) cofactor RBP-Jκ, restricting KSHV lytic activity. Two KSHV latent gene products, such as K15 and vFLIP, stimulate the NF-κB pathway, and a viral micro-RNA, miR-K1, further upregulates NF-κB by targeting IκBα mRNA (18). These interactions highlight the importance of the NF-κB pathway in the KSHV life cycle.

Another crucial pathway is the STAT3 signaling pathway, which is constitutively active in latently infected cells. Inhibition or disruption of STAT3 activity can lead to decreased levels of the transcriptional repressor KAP1, promoting lytic reactivation (15). Additionally, cellular immune sensors and interferon (IFN) responses contribute to the maintenance of KSHV latency (19). Proteins like IFI16 and immune defense proteins like ISG15 and IFIT family members are involved in restricting lytic gene expression (20). Host factors, both epigenetic and non-epigenetic, regulate the expression of the viral master switch protein RTA, preventing lytic reactivation (10, 15). This multifaceted control over RTA includes mechanisms such as epigenetic silencing, interference with RNA polymerase II phosphorylation, competitive binding, and miRNA regulation Our lab

has previously demonstrated that RTA induces autophagy within cells to increase lytic reactivation as well as can degrade cellular repressors of RTA such as K-RBP (15, 21, 22). The intricate web of interactions between host factors, cellular pathways, and viral genes underscores the importance of these processes in maintaining KSHV latency.

In contrast to the latent phase, the lytic phase of KSHV allows the virus to replicate and produce infectious progeny. This phase involves the expression of immediate-early (IE), delayed-early (DE), and late genes, with the key lytic protein being RTA (10, 23). The viral genome undergoes replication via a rolling circle mechanism, leading to the production of linear genomes that are packaged into capsids. While latent genes are expressed in most tumor cells, lytic genes and their encoded viral proteins are produced by a small subset of reactivated cells.

The reactivation of KSHV from latency is initiated by the expression of RTA, the master lytic switch protein. Once RTA reaches sufficient levels, it can outcompete LANA for binding to its major cofactor, recombination signal binding protein (RBP-Jκ), allowing it to transactivate numerous lytic genes (15). A critical promoter targeted by RTA is its own, forming a feed-forward loop that overcomes the repressive latent state and ensures an increase in lytic gene expression. Other lytic proteins, such as K8 and ORF57, cooperate with RTA to sustain this feed-forward loop and regulate the lytic cycle. RTA also serves as an E3 ubiquitin ligase, marking proteins like K-RBP and vFLIP for proteasomal degradation to promote lytic reactivation. The abundance of RTA is tightly

regulated by transcriptional growth factors like nuclear receptor coactivator 1 and virally expressed vSP-1, ensuring precise control of virus reactivation (24, 25).

RTA activation is responsive to environmental stimuli. Hypoxia, low oxygen levels, can stabilize hypoxia-inducible factor 1 subunit alpha (HIF-1α), which interacts with human transcription factors like X-box binding protein 1 (XBP-1) to transactivate the RTA promoter and induce KSHV lytic activity (26, 27). XBP1-s, an active form of XBP1 upregulated during B cell differentiation, is another cellular stimulus involved in controlling RTA expression. This responsiveness to environmental cues allows KSHV to sense and adapt to its surroundings through the interplay of viral and host factors, ultimately leading to reactivation from latency (28).

KSHV also employs various viral factors to specifically counteract viral sensing and antiviral defenses in the cellular intrinsic immune system. Viral interferon regulatory factor 1 (vIRF1) hinders the cGAS-STING-mediated IFNβ induction by blocking STING from binding TANK-binding kinase 1 (TBK1), which facilitates KSHV reactivation (29). Late lytic gene products target IFI16, a sensor of pathogenic DNA, for degradation, keeping the chromatin landscape open for lytic cycle activity (10). ORF63 inhibits the formation of inflammasome complexes, subverting their typical antiviral role and supporting KSHV reactivation. The mitochondrial anti-viral and the retinoic acid-inducible gene I pathways can slow down the progression of the lytic cycle, but others, such as toll-like receptors (TLRs), can trigger reactivation when stimulated by co-infection with other viruses (5, 19).

Clinical targeting of KSHV lytic reactivation and viral replication has been attempted in KS and MCD. In MCD, the viral replication inhibitors, zidovudine and valganciclovir, have shown effectiveness with a clinical response of over 80% (5, 19). However, their effectiveness in treating KS remains limited, highlighting the complexities of targeting KSHV infection and KS tumorigenesis in various clinical contexts. In summary, KSHV exhibits a dual life cycle involving latent and lytic phases, with latency promoting cell survival and tumorigenesis, while lytic replication allows the virus to produce infectious progeny (Figure 1.1) (5). Clinical efforts to target lytic replication have shown promise, however, this method does not address the need to KSHV-infected cells in latency and thus has had limited success.

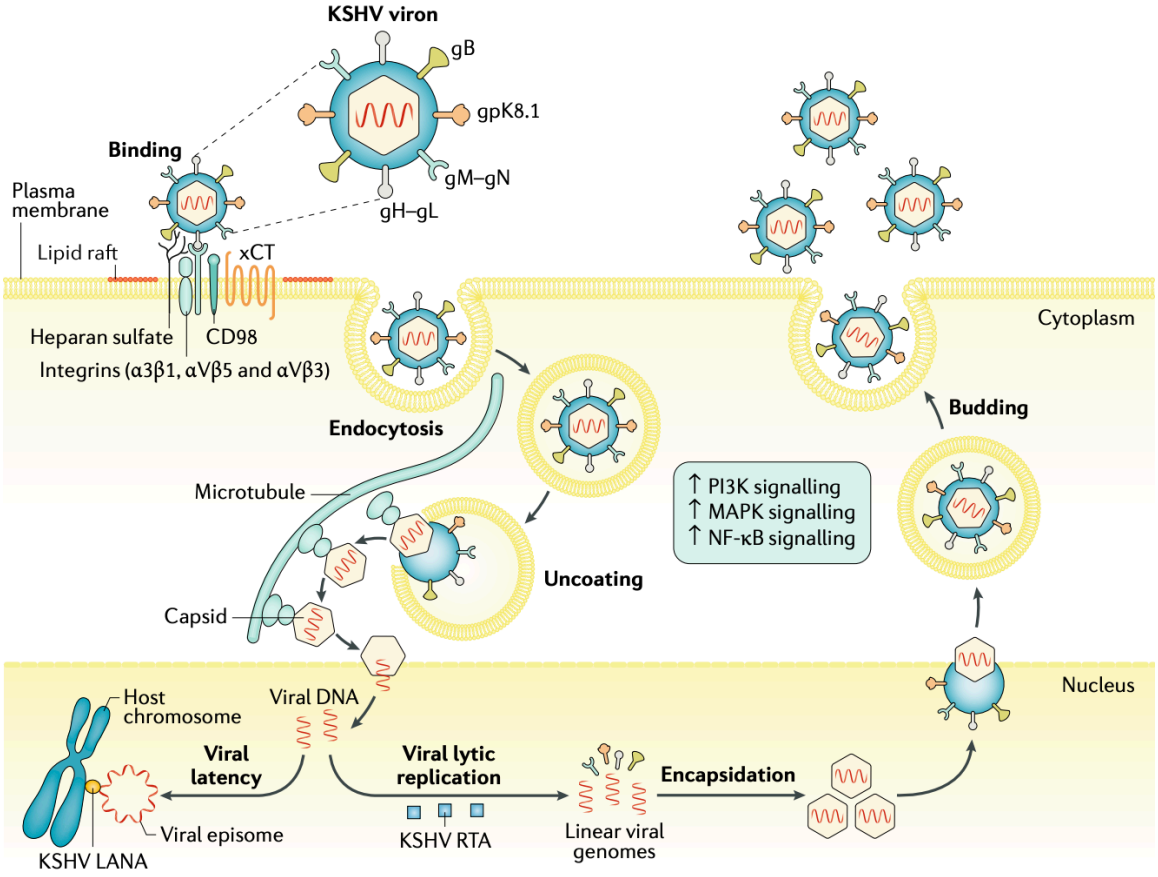

Figure 1.1. Adapted from Cesarman, et al (5). Viral life cycle of KSHV.

Associated pathologies (KS, MCD, PEL, KICS)

KSHV seroprevalence varies worldwide, with hotspots in sub-Saharan Africa, Mediterranean Italy and Sicily, Amazonia, and Western China (4, 30, 31). Currently, there are four pathologies associated with KSHV infection: Kaposi sarcoma (KS), Multicentric Castleman's disease (MCD), primary effusion lymphoma (PEL), and KSHV inflammatory cytokine syndrome (KICS) (5). MCD and PEL are visceral lymphoproliferative disorders of KSHV-infected or KSHV/EBV co-infected B cells whereas KS is a tumor that typically expresses endothelial cell markers and can present as

cutaneous, mucosal, and occasionally visceral disease (5). The cellular origin of KS is still under investigation but is thought to be from dedifferentiated endothelial cells or dysregulated mesenchymal stem cells due to their unique surface marker presentations (32).

Kaposi Sarcoma

The highly angiogenic cancer now known as Kaposi Sarcoma was first described in 1872 by Dr. Moritz Kaposi in the Mediterranean basin. an increase in incidence worldwide within the HIV-infected population in the early 1980s during the HIV epidemic leading to the discovery of its etiologic agent, KSHV, in 1994 by Chang *et al.* Until the HIV epidemic, KS was initially reported in elderly Mediterranean males of Jewish descent and was rarely reported outside the Mediterranean. KS is a highly angiogenic cancer with a dark purple or red presentation with spindle-like shaped cells. The typical histopathology of a KS lesion suggests that the majority of cells within the tumor are KSHV infected, however, the percentage of KSHV-infected cells can vary between 20 and 90% positive (33). This, along with the relatively small percentage of KSHV-infected individuals who develop cancer, suggests that KSHV infection is required for tumorigenesis, but additional co-factors are required.

Kaposi Sarcoma Presentations

There are currently four clinical types of KS based on demographics or other clinical characteristics of the affected: Classical (cKS), Endemic (EnKS), Epidemic KS (EpKS), and Iatrogenic KS (iKS). Classical KS is typically only seen in elderly men of

Mediterranean or Middle Eastern descent in the absence of HIV co-infection or immunosuppression. EnKS incidence varies greatly in Africa, rates in northern African countries have been recorded at 0.5-1.5 per 1000 person-years whereas SSA rates can be greater than 9 per 1000 person-years (5). EpKS is the most common type of KS and is found in HIV-positive individuals from Africa where the seroprevalence of KSHV infection is also the highest worldwide. Iatrogenic KS is also rare and is seen in transplant patients or individuals with an immunosuppressive disease.

Kaposi Sarcoma Global Prevalence and Burden

The global prevalence of both KSHV infection and KS presentation varies by region. The highest incidence of both virus and cancer is in sub-Saharan Africa (SSA) and specific regions of the Mediterranean basin and the HIV-positive population in South America (Figure 1.2). The seroprevalence of KSHV is significantly elevated in sub-Saharan Africa, with certain populations exhibiting prevalence rates exceeding 90%, in contrast to the Mediterranean region where prevalence ranges between 20% to 30%, and North America, where it is less than 10%. The geographical variation of KSHV infection has not been completely explained, however, a correlation with malaria and other parasitic infections may increase the rates of viral shedding in saliva has been observed (34). Genetic variations within KSHV subtypes and human genetics also likely play a role in population susceptibility, however, the important polymorphisms that play a crucial role in infection have yet to be elucidated (35).

Kaposi Sarcoma incidence is two to three times higher in men than women regardless of HIV status, although the driving factor for this disparity has yet to be identified. In 2017, a study by the AIDS-Defining Cancer Project Working Group spanned 57 countries and recruited over 200,000 patients. They reported that SSA was most affected by KS with a burden of 280 per 100,000 person-years as compared to 237 and 244 in North and South America respectively (36). The introduction of combination antiretroviral therapy (cART) in 1996 led to a significant decrease in AIDS-related KS, but the impact of cART in sub-Saharan Africa remains less clear due to limited data. While global AIDS-related KS incidence has decreased with cART, KS cases continue to occur among HIV-infected individuals. The prevalence and incidence patterns of KSHV in the era of HIV and cART may influence all forms of KS, but this area remains relatively underexplored. Notably, there are indications that classic KS risk groups are evolving, with some studies suggesting that fewer patients with Mediterranean backgrounds and an increased proportion of MSM are presenting with classical KS (37).

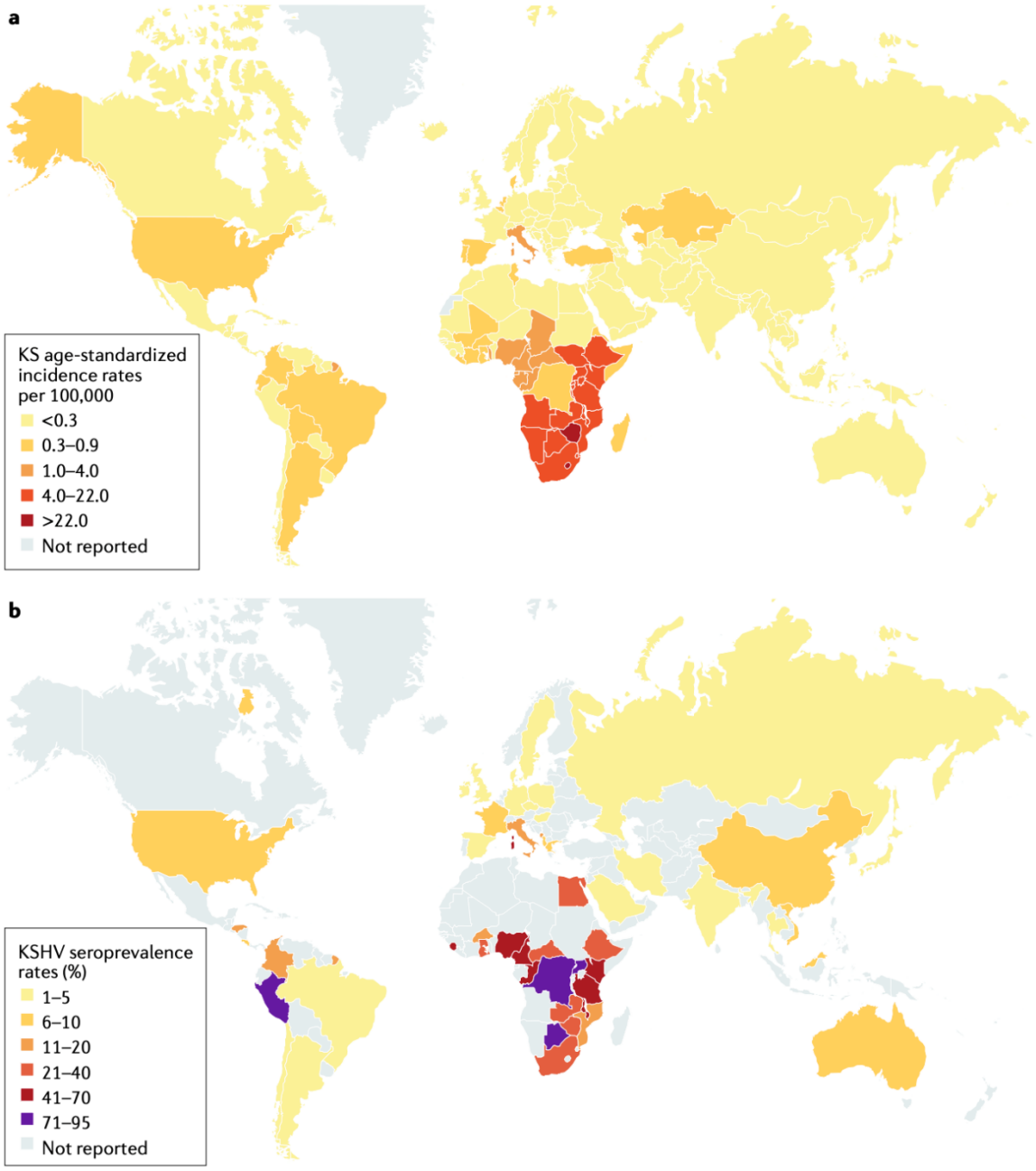

Figure 1.2. Adapted from Cesarman, et al (5). Global prevalence of KSHV and KS.

HIV-1 as a KSHV Co-factor

During the HIV epidemic, KS was categorized as an AIDS-defining malignancy as the incidence rate dramatically increased in the HIV-positive population. However, in

HIV-uninfected individuals, KS development often coincides with a form of immune suppression such as in transplant patients or elderly individuals (5). As previously mentioned, rates have decreased with HIV ART use, however, KS continues to be one of the top ten most prevalent cancers in sub-Saharan Africa (38). In coinfected individuals, HIV induces the production of various cytokines that affect KSHV's life cycle (39).

Multiple signaling pathways are involved in HIV-1-induced KSHV reactivation, including the PI3K/AKT, MAPK, and NF-κB pathways (40). HIV-1 Tat, a regulatory protein encoded by HIV, has been identified as a significant contributor to AIDS-KS. Tat is known to enhance KSHV lytic replication by modulating the JAK/STAT pathway through the induction of human interleukin-6 (IL-6) and its receptor (41-44). Additionally, Tat can activate pro-inflammatory and proliferative genes in KS, promoting angiogenesis and proliferation. HIV-1 Nef, another viral protein, plays a role in the oncogenesis of KSHV by cooperating with KSHV viral interleukin-6 (vIL-6) to facilitate angiogenesis and oncogenesis through manipulation of the AKT signaling pathway. These HIV viral proteins, in synergy with KSHV-encoded genes, influence the balance between KSHV latency and lytic production.

Furthermore, KSHV affects HIV by influencing its transmission and replication. KSHV receptor DC-SIGN is expressed on various immune cells, and KSHV-stimulated dendritic cells capture more HIV viral particles and enhance HIV-1 transport to CD4 T cells (45). KSHV-encoded genes, such as ORF50 and ORF45, can also activate HIV-1 replication, promoting a bidirectional interaction between the two viruses (46). KSHV

LANA and HIV Tat cooperate to transactivate HIV-1 LTR, further illustrating the complex interplay between these two viruses in coinfection scenarios.

Kaposi Sarcoma Histogenesis

Kaposi's Sarcoma is a multifactorial disease that arises from the interaction of various factors, requiring KSHV infection, a compromised immune system, and environmental factors for its development. Unlike many tumors with a monoclonal point of origin, KS has been suggested to be both monoclonal and, occasionally, oligoclonal (2, 47, 48). The monoclonal nature of KSHV suggests that a single viral variant may play a predominant role in the development of Kaposi's sarcoma (KS) tumors. This implies that a specific strain of the virus may have unique properties or adaptations that contribute to the oncogenic process. On the other hand, the oligoclonal nature indicates the presence of multiple viral variants, potentially contributing to the complexity and heterogeneity observed in KS tumors. Understanding the interplay between monoclonal and oligoclonal infections is crucial for deciphering the mechanisms of tumor development and persistence. Continued exposure to viral genes, disruption of cell cycle regulation, cytokine stimulation, and local inflammation are essential for the transformation of KSHV-infected endothelial cells into a neoplasm.

Several viral proteins contribute to KS oncogenesis. LANA-1, expressed during the latent phase, upregulates various factors that promote cell survival, inhibit apoptosis, and interfere with tumor suppression mechanisms (5, 10, 49). These LANA-induced factors include, but are not limited to, vFlip, vCyclin, beta-catenin, c-Myc, and

inhibition of p53, ultimately contributing to the survival and immortalization of future tumor cells (50). v-IL6, another viral protein, plays a pivotal role in angiogenesis, cell proliferation, and invasion through the downregulation of human caveolin-1 (CAV1) (44, 51). The downregulation of CAV1 leads to the formation of a STAT3-DNMT1 complex, which epigenetically silences the CAV1 promoter.

KS development involves angiogenesis which is the formation of new blood vasculature within the TME as opposed to non-angiogenic tumors which exploit pre-existing blood vessels in tissue. KS promotes the secretion of VEGF-A in normoxic conditions through several KSHV proteins, including LANA-1, vIRF3, and vGPCR (52-59). This promotes angiogenesis, where angiopoietin 2 significantly promotes KS through the ERK, JNK, and MAPK pathways (39, 40, 60). KSHV miRNAs also target THBS1, a regulator of angiogenesis and a suppressor of tumor-promoting proteins.

KSHV-infected endothelial cells experience increased vascular permeability due to the downregulation and degradation of VE-cadherin, resulting in the loss of endothelial cell junctions (61). This further promotes angiogenesis. MMPs, enzymes that remodel the extracellular matrix, facilitate angiogenesis by disrupting the basement membrane, allowing invasion and migration of endothelial and Kaposi spindle cells (62). vIRFs, LANA, k-bZIP, and other viral proteins play roles in downregulating the interferon pathway (63). vCCL proteins, originally known as vMIPs, downregulate the immune response, leading to chronic inflammation and suppression of the immune system (15, 19, 63).

The exact cellular origin for the spindle-like cells in KS lesions has yet to be elucidated. Cells in the KS tumor express many cell surface markers indicative of both endothelial cells (CD34, CD31, Prox-1, and LYVE-1) and mesenchymal stem cells (CD105, CD90, and CD73) regardless of KSHV infection status (32, 64-68). The co-expression of markers like CD34, Prox-1, CD90, and CD105 has led to two main hypotheses for the cellular origin of KS; the first is that circulating endothelial cells, which have been proposed by Lagunoff, et al to harbor latent KSHV, are incompletely differentiated into a lymphatic and vascular endothelial cell hybrid (64, 69-71). The second hypothesis is that KS lesions originate from infected mesenchymal stem cells that have undergone at least partial but perhaps indistinct mesenchymal to endothelial transition (MEndoT) (Figure 1.3) (32, 66, 72, 73).

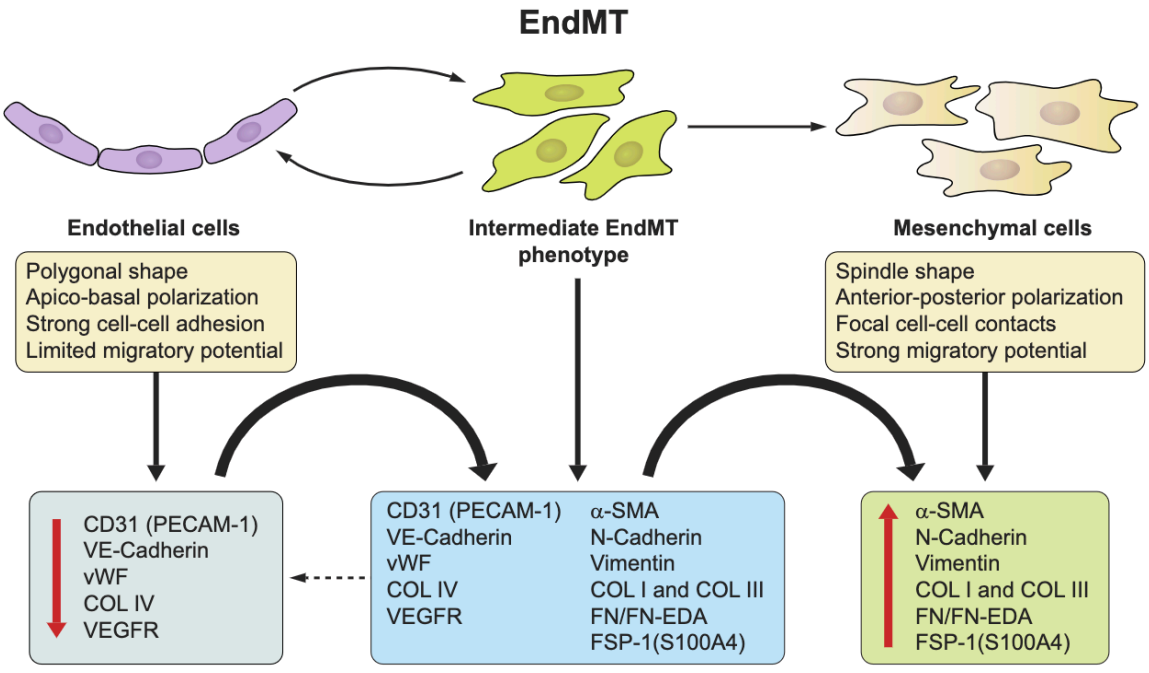

Figure 1.3. Adapted from Piera-Velazquez and Jimenez (73). Endothelial to mesenchymal transition.

Immune Responses to Kaposi Sarcoma

KSHV employs a multi-faceted approach to subvert the host's intrinsic and cellular immune responses as reviewed by Broussard, et al (19). This strategy begins with disrupting the host's ability to detect viral invasion, particularly through the manipulation of pattern recognition receptors (PRRs), which are essential for recognizing pathogens. KSHV impacts various PRRs, including Toll-like receptors (TLRs), NOD-like receptors (NLRs), and cytosolic DNA sensors. For instance, KSHV proteins interfere with TLR signaling pathways, preventing the activation of downstream antiviral responses (5). Moreover, the virus targets NLRs, which are cytosolic sensors for pathogen-associated molecular patterns (PAMPs). By disrupting these crucial sensors, KSHV avoids triggering the host's antiviral responses, a pivotal mechanism in maintaining persistent infection.

In addition to manipulating PRRs, KSHV interferes with the host's interferon response. Interferons play a critical role in inducing antiviral pathways and restricting viral replication. KSHV utilizes viral proteins such as vIRFs to inhibit interferon responses, which are important for activating immune defenses (5, 19). Additionally, the virus encodes various proteins that suppress the activation and signaling of interferon regulatory factors (IRFs), further hampering the host's ability to mount an effective immune response against the virus.

KSHV's manipulation of cellular immunity is not limited to intrinsic defenses. It extends to modulation of immune cells and cytokine signaling. The virus induces chronic

inflammation by promoting the secretion of pro-inflammatory cytokines, such as IL-6 and TNFα, while simultaneously elevating immunosuppressive cytokines like IL-10 (19, 74). This inflammatory milieu allows infected cells to thrive while crippling the host immune system. Furthermore, KSHV encodes viral homologs of cellular chemokines that influence the localization of immune cells, directing the immune response to favor the virus (19, 75, 76).

The virus also subverts cell-mediated immunity by disrupting immune cell recognition and cytotoxicity. KSHV proteins degrade MHC-I and MHC-II molecules, hindering the ability of CD8+ T cells and CD4+ T helper cells to recognize and eliminate infected cells (75). The loss or inhibition of T cell function can lead to viral reactivation and tumorigenesis. Both systemic KSHV-specific T cells and tumor-infiltrating T cells have a significant impact, and their role in controlling KSHV and KS is not yet fully understood. It has also been observed that KS patients have increased transcription as well as protein production of key T cell signaling cytokines such as CXCL9, 10, and 11 (77). However, despite the production of these cytokines, there is a marked absence of T cell infiltration within KS lesions; suggesting that KS lesions are creating the necessary signals for a cellular response but there is also a barrier preventing an effective T cell response.

Antibody responses to KSHV are challenging to assess due to the heterogeneity of the virus and its numerous antigens. Previous studies have described the development of antibodies against KSHV in early childhood where more than 60% of

children in Sub-Saharan Africa countries seroconvert by the age of 4 (76, 78, 79). Robust ELISAs using recombinant proteins have been developed to detect KSHV-specific antibodies, but there are no FDA-approved assays, and commercial options are limited. The levels of KSHV-specific antibodies are significantly higher in patients with KSHV-associated diseases (79, 80). A study by Labo et al identified several KSHV antigens that showed distinct reactivity patterns, allowing discrimination between infected and non-infected individuals (79). While the reasons for the diverse antibody responses are not entirely clear, the findings offer insights into KSHV infection, its natural history, and potential correlations with disease states. LANA was one of the most immunologically reactive KSHV proteins in the above experiment, a finding which was confirmed by Bennett et al utilizing a phage display platform VirScan to quantify antibody responses in KSHV-infected individuals (80).

To address the lack of neutralizing antibodies during asymptomatic KSHV infection, Poppe et al. investigated the role of non-neutralizing antibodies and their potential to mediate antibody-dependent cell cytotoxicity (ADCC) by an NK cell line (81). ADCC is a vital immune response mechanism in which effector cells, typically natural killer (NK) cells, recognize and eliminate target cells, such as infected or cancerous cells, that have been marked by antibodies (immunoglobulins). The process involves the binding of the antibodies' Fc region to Fc receptors (CD16) on the surface of NK cells, resulting in NK cell activation. Once activated, NK cells release cytotoxic granules containing perforin and granzymes, inducing apoptosis in the target cell (82). ADCC plays

a crucial role in immune defense against pathogens and tumor cells, as it enhances the elimination of antibody-coated targets, contributing to the body's ability to combat infections and malignancies. However, Poppe et al. demonstrated that KSHV seropositive individuals possess antibodies capable of mediating ADCC, but this ability was observed in only approximately 35% of seropositive individuals, who demonstrated significantly higher ADCC activity compared to seronegative controls. These findings are in contrast to other herpesviruses like HCMV, HSV-1, and EBV, where the majority of seropositive individuals appear to have ADCC-mediating antibodies (81). The study found no correlation between ADCC responses and KS status or disease progression, suggesting that ADCC-mediating antibodies alone might not protect against KS development.

Kaposi Sarcoma Transcriptomic Dysregulation

In recent years, attention has been focused on understanding KS lesions at a mRNA transcript level to identify the changes associated with KSHV infection and KS development (71, 74). Studies by Tso et al. and Lidenge et al. compared transcriptomic profiles of EpKS, EnKS, and uninvolved skin (74, 77). The research involved sequencing skin tissues from KS patients and contralateral uninfected tissues and revealed that KS tumor tissues have highly variable gene expression patterns, irrespective of HIV-1 co-infection. Interestingly, the study found that KS lesions show both latent and lytic KSHV gene expression, but this pattern is not influenced by HIV-1 co-infection or antiretroviral therapy (ART). However, despite higher HIV-1 viral loads and a longer duration of KS in

endemic KS (EnKS) patients, gene expression changes did not correlate significantly with these factors. Moreover, the study found that KS tumors exhibit metabolic changes involving glycolysis and altered lipid metabolism that are central to KS tumorigenesis, and these changes appear to be independent of ART or direct HIV-1 infection (Figure 1.4) (77).

The transcriptomic profiles from KS lesions have also been compared to most of the commonly used *in vitro* cell lines for KSHV infection (83). Even though glucose and lipid dysregulation seen in the tumors have also been suggested from in vitro infection studies, the overall transcriptomic comparison revealed only about 10% overlap between transcriptomic changes seen in KS tumors and those in cell lines. This, suggests that the current *in vitro* models cannot accurately mimic the changes that are seen *in vivo* and that further studies in human tissues are needed to answer questions regarding KSHV and KS, or the use of mouse models that can be reflective of human KS lesions (77).

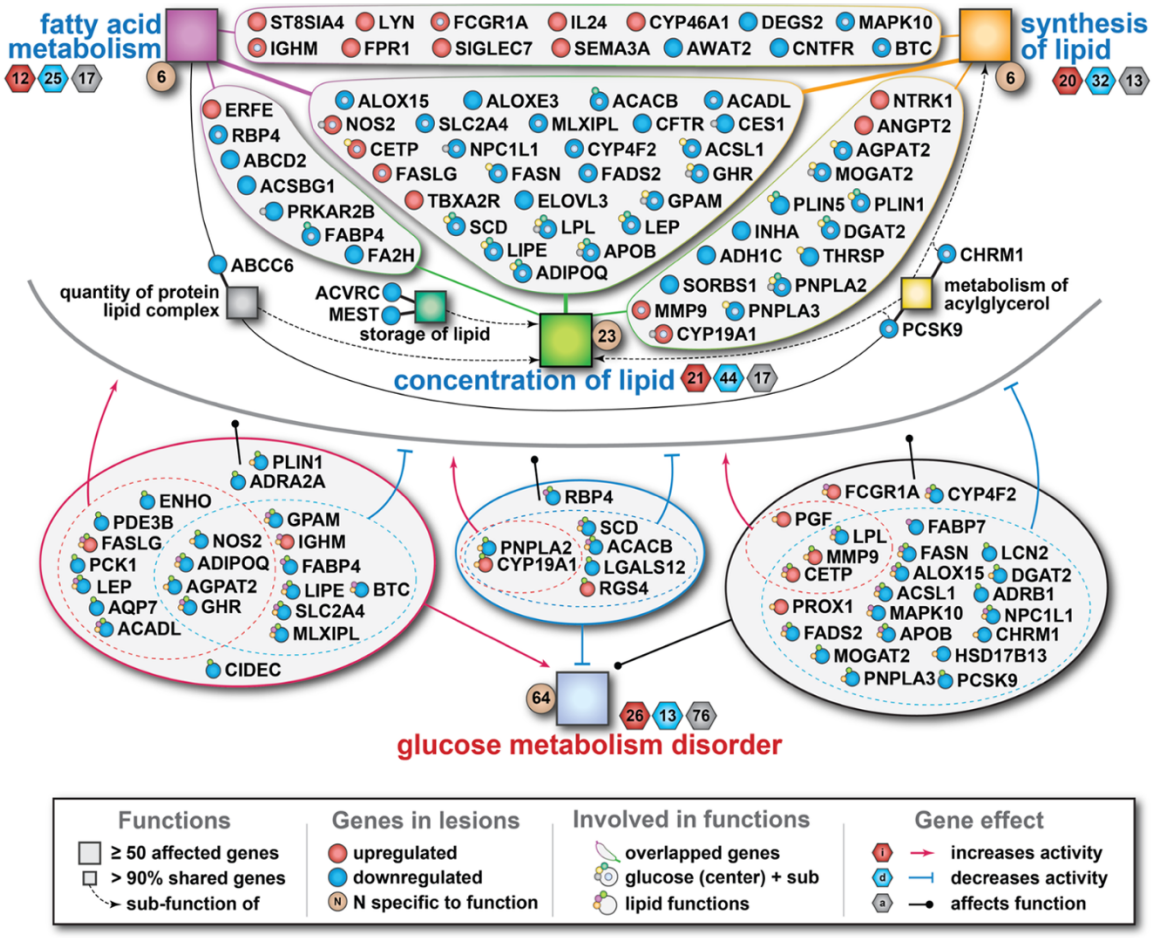

Figure 1.4. Adapted from Tso, et al (77). Dysregulated genes involved in fatty acid metabolism and glucose metabolism disorder in KS tissue.

Kaposi Sarcoma Metabolism

KS tumors exhibit unique metabolic characteristics that distinguish them from surrounding healthy tissues (74, 84). Studies have shown that both glycolysis and fatty acid synthesis are highly active in KS tumors, leading to increased glucose consumption and lipid production. This metabolic shift, known as the Warburg effect, is a hallmark of cancer cells and contributes to their growth and survival (85-87). In KS, it appears that KSHV manipulates host cell metabolism to its advantage. For instance, KSHV-encoded

proteins can stimulate glycolysis and enhance glucose uptake, promoting an environment conducive to viral replication (88, 89).

Furthermore, KS tumors exhibit increased levels of glutaminolysis, a metabolic pathway involving the conversion of glutamine into energy and biomass for cell growth (74). Glutaminolysis is crucial for KSHV-infected cells, as it provides the necessary substrates for viral DNA synthesis (83, 90-92). Some studies have suggested that inhibiting glycolysis or glutaminolysis can disrupt KSHV replication, making these metabolic pathways potential targets for therapeutic intervention (19, 90). While the exact mechanisms of how KSHV modulates cellular metabolism in KS are still not fully understood, metabolic reprogramming plays a crucial role in KSHV infection and KS pathogenesis (26, 85-89, 92-94). Understanding these metabolic alterations may provide new insights into the development of targeted therapies for KS, thus we sought to identify metabolic markers of KS pathogenesis.

Research Aims

Even in regions where the KSHV infection rate exceeds 90%, only a small population of individuals progress to cancer development. Many studies have tried to identify the drivers of tumorigenesis but have been restricted to suboptimal cell models and limited access to African patient samples. Very little is known about how changes to human gene expression as a result of long-term KSHV infection or KS disease progression affect the overall tumor microenvironment. It is important to explore the

effects that change in cellular gene expression and metabolism have on the overall environment and how different features are correlated to KS progression.

Thus, our primary hypothesis is as follows: Comparative transcriptomics and metabolomics between Kaposi Sarcoma patients and KSHV-infected individuals will identify biomarkers of KS disease development and progression that can be tested using in vitro and ex vivo models. This hypothesis was tested in the following aims:

- Identification and validation of upregulated human cell surface markers as indicators of KS or as targets for anti-tumor therapy.
- Analysis of endothelial cell phenotype based on transcriptomics and protein expression to elucidate the cellular origin of KS lesions.
- Identification of differential polar and non-polar plasma metabolites in KSHV-infected asymptomatic individuals and KS patients.
- Integration of plasma metabolomics and KS lesion transcriptomics for the identification of important pathways in KS disease progression.
- Comparison of cytokine profiles between EpKS and asymptomatic KSHV+HIV+ individuals by plasma proteomics approaches.

References

1. Knipe D, Howley P, Griffin D, Lamb R, Martin M, Roizman B, et al. Fields Virology: Volumes 1 & 2. Philadelphia, PA, USA.: Lippincott Williams & Wilkins; 2013.

2. Liu L. Fields Virology, 6th Edition. Clinical Infectious Diseases. 2014;59(4):613-.

3. Weed DJ, Damania B. Pathogenesis of Human Gammaherpesviruses: Recent Advances. Curr Clin Microbiol Rep. 2019;6(3):166-74.

4. Grabar S, Costagliola D. Epidemiology of kaposi's sarcoma. Cancers2021.

5. Cesarman E, Damania B, Krown SE, Martin J, Bower M, Whitby D. Kaposi sarcoma. Nat Rev Dis Primers. 2019;5(1):9.

6. Crabtree KL, Wojcicki JM, Minhas V, Smith DR, Kankasa C, Mitchell CD, et al. Risk factors for early childhood infection of human herpesvirus-8 in Zambian children: the role of early childhood feeding practices. Cancer Epidemiol Biomarkers Prev. 2014;23(2):300-8.

7. Dunmire SK, Verghese PS, Balfour HH, Jr. Primary Epstein-Barr virus infection. J Clin Virol. 2018;102:84-92.

8. Vilimova M, Contrant M, Randrianjafy R, Dumas P, Elbasani E, Ojala PM, et al. Cis regulation within a cluster of viral microRNAs. Nucleic Acids Res. 2021;49(17):10018-33.

9. Chandran B. Early events in Kaposi's sarcoma-associated herpesvirus infection of target cells. J Virol. 2010;84(5):2188-99.

10. Broussard G, Damania B. Regulation of KSHV Latency and Lytic Reactivation. Viruses2020.

11. Kumar B, Chandran B. KSHV Entry and Trafficking in Target Cells-Hijacking of Cell Signal Pathways, Actin and Membrane Dynamics. Viruses. 2016;8(11).

12. van der Meulen E, Anderton M, Blumenthal MJ, Schafer G. Cellular Receptors Involved in KSHV Infection. Viruses. 2021;13(1).

13. Connolly SA, Jardetzky TS, Longnecker R. The structural basis of herpesvirus entry. Nat Rev Microbiol. 2021;19(2):110-21.

14. Vladimirova O, Soldan S, Su C, Kossenkov A, Ngalamika O, Tso FY, et al. Elevated iNOS and 3'-nitrotyrosine in Kaposi's Sarcoma tumors and mouse model. Tumour Virus Res. 2023;15:200259.

15. Sandhu PK, Damania B. The regulation of KSHV lytic reactivation by viral and cellular factors. Current Opinion in Virology2022.

16. Nabiee R, Syed B, Ramirez Castano J, Lalani R, Totonchy JE. An Update of the Virion Proteome of Kaposi Sarcoma-Associated Herpesvirus. Viruses. 2020;12(12).

17. Yan L, Majerciak V, Zheng ZM, Lan K. Towards Better Understanding of KSHV Life Cycle: from Transcription and Posttranscriptional Regulations to Pathogenesis. Virologica Sinica2019.

18. Mishra R, Kumar A, Ingle H, Kumar H. The Interplay Between Viral-Derived miRNAs and Host Immunity During Infection. Front Immunol. 2019;10:3079.

19. Broussard G, Damania B. KSHV: Immune Modulation and Immunotherapy. Frontiers in Immunology2020.

20. Gonzalez-Perez AC, Stempel M, Chan B, Brinkmann MM. One Step Ahead: Herpesviruses Light the Way to Understanding Interferon-Stimulated Genes (ISGs). Front Microbiol. 2020;11:124.

21. Wen HJ, Yang Z, Zhou Y, Wood C. Enhancement of autophagy during lytic replication by the Kaposi's sarcoma-associated herpesvirus replication and transcription activator. J Virol. 2010;84(15):7448-58.

22. Yang Z, Yan Z, Wood C. Kaposi's sarcoma-associated herpesvirus transactivator RTA promotes degradation of the repressors to regulate viral lytic replication. J Virol. 2008;82(7):3590-603.

23. Manners O, Murphy JC, Coleman A, Hughes DJ, Whitehouse A. Contribution of the KSHV and EBV lytic cycles to tumourigenesis. Curr Opin Virol. 2018;32:60-70.

24. Jaber T, Yuan Y. A virally encoded small peptide regulates RTA stability and facilitates Kaposi's sarcoma-associated herpesvirus lytic replication. J Virol. 2013;87(6):3461-70.

25. Aneja KK, Yuan Y. Reactivation and Lytic Replication of Kaposi's Sarcoma-Associated Herpesvirus: An Update. Front Microbiol. 2017;8:613.

26. Singh RK, Lang F, Pei Y, Jha HC, Robertson ES. Metabolic reprogramming of Kaposi's sarcoma associated herpes virus infected B-cells in hypoxia. PLoS Pathog. 2018;14(5):e1007062.

27. Singh RK, Bose D, Robertson ES. HIF1alpha-Regulated Expression of the Fatty Acid Binding Protein Family Is Important for Hypoxic Reactivation of Kaposi's Sarcoma-Associated Herpesvirus. J Virol. 2021;95(12).

28. Perillo B, Di Donato M, Pezone A, Di Zazzo E, Giovannelli P, Galasso G, et al. ROS in cancer therapy: the bright side of the moon. Exp Mol Med. 2020;52(2):192-203.

29. Ma Z, Jacobs SR, West JA, Stopford C, Zhang Z, Davis Z, et al. Modulation of the cGAS-STING DNA sensing pathway by gammaherpesviruses. Proc Natl Acad Sci U S A. 2015;112(31):E4306-15.

30. Motlhale M, Sitas F, Bradshaw D, Chen WC, Singini MG, de Villiers CB, et al. Epidemiology of Kaposi's sarcoma in sub-Saharan Africa. Cancer Epidemiol. 2022;78:102167.

31. Ragi SD, Moseley I, Ouellette S, Rao B. Epidemiology and Survival of Kaposi's Sarcoma by Race in the United States: A Surveillance, Epidemiology, and End Results Database Analysis. Clin Cosmet Investig Dermatol. 2022;15:1681-5.

32. Li Y, Zhong C, Liu D, Yu W, Chen W, Wang Y, et al. Evidence for Kaposi Sarcoma Originating from Mesenchymal Stem Cell through KSHV-induced Mesenchymal-to-Endothelial Transition. Cancer Res. 2018;78(1):230-45.

33. Privatt SR, Ngalamika O, Zhang J, Li Q, Wood C, West JT. Upregulation of Cell Surface Glycoproteins in Correlation with KSHV LANA in the Kaposi Sarcoma Tumor Microenvironment. Cancers (Basel). 2023;15(7).

34. Nalwoga A, Webb EL, Chihota B, Miley W, Walusimbi B, Nassuuna J, et al. Kaposi's sarcoma-associated herpesvirus seropositivity is associated with parasite infections in Ugandan fishing communities on Lake Victoria islands. PLoS Negl Trop Dis. 2019;13(10):e0007776.

35. Moorad R, Juarez A, Landis JT, Pluta LJ, Perkins M, Cheves A, et al. Whole-genome sequencing of Kaposi sarcoma-associated herpesvirus (KSHV/HHV8) reveals evidence for two African lineages. Virology. 2022;568:101-14.

36. IeDEA AI-dCPWGf, EuroCoord Ci. Comparison of Kaposi Sarcoma Risk in Human Immunodeficiency Virus-Positive Adults Across 5 Continents: A Multiregional Multicohort Study. Clin Infect Dis. 2017;65(8):1316-26.

37. Denis D, Seta V, Regnier-Rosencher E, Kramkimel N, Chanal J, Avril MF, et al. A fifth subtype of Kaposi's sarcoma, classic Kaposi's sarcoma in men who have sex with men: a cohort study in Paris. J Eur Acad Dermatol Venereol. 2018;32(8):1377-84.

38. Sharma R, Aashima, Nanda M, Fronterre C, Sewagudde P, Ssentongo AE, et al. Mapping Cancer in Africa: A Comprehensive and Comparable Characterization of 34 Cancer Types Using Estimates From GLOBOCAN 2020. Front Public Health. 2022;10:839835.

39. Dandachi D, Morón F. Effects of HIV on the Tumor Microenvironment. Advances in Experimental Medicine and Biology. 12632020.

40. Noorolyai S, Shajari N, Baghbani E, Sadreddini S, Baradaran B. The relation between PI3K/AKT signalling pathway and cancer. Gene. 2019;698:120-8.

41. Privatt SR, Braga CP, Johnson A, Lidenge SJ, Berry L, Ngowi JR, et al. Comparative polar and lipid plasma metabolomics differentiate KSHV infection and disease states. Cancer Metab. 2023;11(1):13.

42. Yang WS, Lin TY, Chang L, Yeh WW, Huang SC, Chen TY, et al. HIV-1 Tat Interacts with a Kaposi's Sarcoma-Associated Herpesvirus Reactivation-Upregulated Antiangiogenic Long Noncoding RNA, LINC00313, and Antagonizes Its Function. J Virol. 2020;94(3).

43. Zeng Y, Zhang X, Huang Z, Cheng L, Yao S, Qin D, et al. Intracellular Tat of human immunodeficiency virus type 1 activates lytic cycle replication of Kaposi's sarcoma-associated herpesvirus: role of JAK/STAT signaling. J Virol. 2007;81(5):2401-17.

44. Giffin L, Yan F, Ben Major M, Damania B. Modulation of Kaposi's sarcoma-associated herpesvirus interleukin-6 function by hypoxia-upregulated protein 1. J Virol. 2014;88(16):9429-41.

45. Liu W, Qin Y, Bai L, Lan K, Wang JH. Kaposi's-sarcoma-associated-herpesvirus-activated dendritic cells promote HIV-1 trans-infection and suppress CD4(+) T cell proliferation. Virology. 2013;440(2):150-9.

46. Thakker S, Verma SC. Co-infections and Pathogenesis of KSHV-Associated Malignancies. Front Microbiol. 2016;7:151.

47. Indave Ruiz BI, Armon S, Watanabe R, Uttley L, White VA, Lazar AJ, et al. Clonality, Mutation and Kaposi Sarcoma: A Systematic Review. Cancers (Basel). 2022;14(5).

48. Duprez R, Lacoste V, Briere J, Couppie P, Frances C, Sainte-Marie D, et al. Evidence for a multiclonal origin of multicentric advanced lesions of Kaposi sarcoma. J Natl Cancer Inst. 2007;99(14):1086-94.

49. Uppal T, Banerjee S, Sun Z, Verma SC, Robertson ES. KSHV LANA--the master regulator of KSHV latency. Viruses. 2014;6(12):4961-98.

50. Verma SC, Lan K, Robertson E. Structure and function of latency-associated nuclear antigen. Curr Top Microbiol Immunol. 2007;312:101-36.

51. Li W, Wang Q, Qi X, Guo Y, Lu H, Chen Y, et al. Viral interleukin-6 encoded by an oncogenic virus promotes angiogenesis and cellular transformation by enhancing STAT3-mediated epigenetic silencing of caveolin 1. Oncogene. 2020;39(23):4603-18.

52. Liu Y, Li Y, Wang Y, Lin C, Zhang D, Chen J, et al. Recent progress on vascular endothelial growth factor receptor inhibitors with dual targeting capabilities for tumor therapy. J Hematol Oncol. 2022;15(1):89.

53. Maslowska K, Halik PK, Tymecka D, Misicka A, Gniazdowska E. The Role of VEGF Receptors as Molecular Target in Nuclear Medicine for Cancer Diagnosis and Combination Therapy. Cancers (Basel). 2021;13(5).

54. Melincovici CS, Bosca AB, Susman S, Marginean M, Mihu C, Istrate M, et al. Vascular endothelial growth factor (VEGF) - key factor in normal and pathological angiogenesis. Rom J Morphol Embryol. 2018;59(2):455-67.

55. Kerr DA, Busarla SVP, Gimbel DC, Sohani AR, Nazarian RM. mTOR, VEGF, PDGFR, and c-kit signaling pathway activation in Kaposi sarcoma. Hum Pathol. 2017;65:157-65.

56. Simons M, Gordon E, Claesson-Welsh L. Mechanisms and regulation of endothelial VEGF receptor signalling. Nat Rev Mol Cell Biol. 2016;17(10):611-25.

57. Miettinen M, Rikala MS, Rys J, Lasota J, Wang ZF. Vascular endothelial growth factor receptor 2 as a marker for malignant vascular tumors and mesothelioma: an immunohistochemical study of 262 vascular endothelial and 1640 nonvascular tumors. Am J Surg Pathol. 2012;36(4):629-39.

58. Bruns AF, Bao L, Walker JH, Ponnambalam S. VEGF-A-stimulated signalling in endothelial cells via a dual receptor tyrosine kinase system is dependent on co-ordinated trafficking and proteolysis. Biochem Soc Trans. 2009;37(Pt 6):1193-7.

59. Andre T, Kotelevets L, Vaillant JC, Coudray AM, Weber L, Prevot S, et al. Vegf, Vegf-B, Vegf-C and their receptors KDR, FLT-1 and FLT-4 during the neoplastic progression of human colonic mucosa. Int J Cancer. 2000;86(2):174-81.

60. Cirone M. Cancer cells dysregulate PI3K/AKT/mTOR pathway activation to ensure their survival and proliferation: mimicking them is a smart strategy of gammaherpesviruses. Critical Reviews in Biochemistry and Molecular Biology2021.

61. Qian LW, Greene W, Ye F, Gao SJ. Kaposi's sarcoma-associated herpesvirus disrupts adherens junctions and increases endothelial permeability by inducing degradation of VE-cadherin. J Virol. 2008;82(23):11902-12.

62. Rivera-Soto R, Damania B. Modulation of Angiogenic Processes by the Human Gammaherpesviruses, Epstein-Barr Virus and Kaposi's Sarcoma-Associated Herpesvirus. Front Microbiol. 2019;10:1544.

63. Rusu-Zota G, Manole OM, Gales C, Porumb-Andrese E, Obada O, Mocanu CV. Kaposi Sarcoma, a Trifecta of Pathogenic Mechanisms. Diagnostics (Basel). 2022;12(5).

64. Pyakurel P, Pak F, Mwakigonja AR, Kaaya E, Heiden T, Biberfeld P. Lymphatic and vascular origin of Kaposi's sarcoma spindle cells during tumor development. Int J Cancer. 2006;119(6):1262-7.

65. Ntikoudi E, Pergaris A, Kykalos S, Politi E, Theocharis S. The Role of PROX1 in Neoplasia: A Key Player Often Overlooked. Diagnostics (Basel). 2022;12(7).

66. Ding Y, Chen W, Lu Z, Wang Y, Yuan Y. Kaposi's sarcoma-associated herpesvirus promotes mesenchymal-to-endothelial transition by resolving the bivalent chromatin of PROX1 gene. PLoS Pathog. 2021;17(9):e1009847.

67. Fiedler U, Christian S, Koidl S, Kerjaschki D, Emmett MS, Bates DO, et al. The sialomucin CD34 is a marker of lymphatic endothelial cells in human tumors. Am J Pathol. 2006;168(3):1045-53.

68. AbuSamra DB, Aleisa FA, Al-Amoodi AS, Jalal Ahmed HM, Chin CJ, Abuelela AF, et al. Not just a marker: CD34 on human hematopoietic stem/progenitor cells dominates vascular selectin binding along with CD44. Blood Adv. 2017;1(27):2799-816.

69. Choi D, Park E, Kim KE, Jung E, Seong YJ, Zhao L, et al. The Lymphatic Cell Environment Promotes Kaposi Sarcoma Development by Prox1-Enhanced Productive Lytic Replication of Kaposi Sarcoma Herpes Virus. Cancer Res. 2020;80(15):3130-44.

70. Dimaio TA, Lagunoff M. KSHV Induction of Angiogenic and Lymphangiogenic Phenotypes. Front Microbiol. 2012;3(MAR):102.

71. Bruce AG, Barcy S, DiMaio T, Gan E, Garrigues HJ, Lagunoff M, et al. Quantitative Analysis of the KSHV Transcriptome Following Primary Infection of Blood and Lymphatic Endothelial Cells. Pathogens. 2017;6(1).

72. Naipauer J, Mesri EA. The Kaposi's sarcoma progenitor enigma: KSHV-induced MEndT-EndMT axis. Trends Mol Med. 2023;29(3):188-200.

73. Piera-Velazquez S, Jimenez SA. Endothelial to Mesenchymal Transition: Role in Physiology and in the Pathogenesis of Human Diseases. Physiol Rev. 2019;99(2):1281-324.

74. Lidenge SJ, Kossenkov AV, Tso FY, Wickramasinghe J, Privatt SR, Ngalamika O, et al. Comparative transcriptome analysis of endemic and epidemic Kaposi's sarcoma (KS) lesions and the secondary role of HIV-1 in KS pathogenesis. PLoS Pathog. 2020;16(7):e1008681.

75. Lidenge SJ, Tso FY, Ngalamika O, Kolape J, Ngowi JR, Mwaiselage J, et al. Lack of CD8(+) T-cell co-localization with Kaposi's sarcoma-associated herpesvirus infected cells in Kaposi's sarcoma tumors. Oncotarget. 2020;11(17):1556-72.

76. Lidenge SJ, Tso FY, Mortazavi Y, Ngowi JR, Shea DM, Mwaiselage J, et al. Viral and Immunological Analytes are Poor Predictors of the Clinical Treatment Response in Kaposi's Sarcoma Patients. Cancers (Basel). 2020;12(6).

77. Tso FY, Kossenkov AV, Lidenge SJ, Ngalamika O, Ngowi JR, Mwaiselage J, et al. RNA-Seq of Kaposi's sarcoma reveals alterations in glucose and lipid metabolism. PLoS Pathog. 2018;14(1):e1006844.

78. Olp LN, Minhas V, Gondwe C, Poppe LK, Rogers AM, Kankasa C, et al. Longitudinal analysis of the humoral response to Kaposi's sarcoma-associated herpesvirus after primary infection in children. J Med Virol. 2016;88(11):1973-81.

79. Labo N, Miley W, Marshall V, Gillette W, Esposito D, Bess M, et al. Heterogeneity and breadth of host antibody response to KSHV infection demonstrated by systematic analysis of the KSHV proteome. PLoS Pathog. 2014;10(3):e1004046.

80. Bennett SJ, Yalcin D, Privatt SR, Ngalamika O, Lidenge SJ, West JT, et al. Antibody epitope profiling of the KSHV LANA protein using VirScan. PLoS Pathog. 2022;18(12):e1011033.

81. Poppe LK, Wood C, West JT. The Presence of Antibody-Dependent Cell Cytotoxicity-Mediating Antibodies in Kaposi Sarcoma-Associated Herpesvirus-Seropositive Individuals Does Not Correlate with Disease Pathogenesis or Progression. J Immunol. 2020;205(10):2742-9.

82. Narvekar A, Pardeshi A, Jain R, Dandekar P. ADCC enhancement: A conundrum or a boon to mAb therapy? Biologicals. 2022;79:10-8.

83. Sanchez EL, Pulliam TH, Dimaio TA, Thalhofer AB, Delgado T, Lagunoff M. Glycolysis, Glutaminolysis, and Fatty Acid Synthesis Are Required for Distinct Stages of Kaposi's Sarcoma-Associated Herpesvirus Lytic Replication. J Virol. 2017;91(10).

84. Lidenge SJ, Tso FY, Ngalamika O, Ngowi JR, Mortazavi Y, Kwon EH, et al. Similar Immunological Profiles Between African Endemic and Human Immunodeficiency Virus

Type 1-Associated Epidemic Kaposi Sarcoma (KS) Patients Reveal the Primary Role of KS-Associated Herpesvirus in KS Pathogenesis. J Infect Dis. 2019;219(8):1318-28.

85. Bian X, Liu R, Meng Y, Xing D, Xu D, Lu Z. Lipid metabolism and cancer. J Exp Med. 2021;218(1).

86. Lo AK, Dawson CW, Young LS, Lo KW. The role of metabolic reprogramming in gamma-herpesvirus-associated oncogenesis. Int J Cancer. 2017;141(8):1512-21.

87. Sanchez EL, Lagunoff M. Viral activation of cellular metabolism. Virology2015.

88. Ali ES, Ben-Sahra I. Regulation of nucleotide metabolism in cancers and immune disorders. Trends Cell Biol. 2023.

89. Liu X, Zhu C, Wang Y, Wei F, Cai Q. KSHV Reprogramming of Host Energy Metabolism for Pathogenesis. Frontiers in Cellular and Infection Microbiology2021.

90. Wang Z, Liu F, Fan N, Zhou C, Li D, Macvicar T, et al. Targeting Glutaminolysis: New Perspectives to Understand Cancer Development and Novel Strategies for Potential Target Therapies. Front Oncol. 2020;10:589508.

91. Lagunoff M. Activation of cellular metabolism during latent Kaposi's Sarcoma herpesvirus infection. Current Opinion in Virology2016.

92. Sanchez EL, Carroll PA, Thalhofer AB, Lagunoff M. Latent KSHV Infected Endothelial Cells Are Glutamine Addicted and Require Glutaminolysis for Survival. PLoS Pathog. 2015;11(7):e1005052.

93. Choi UY, Lee JJ, Park A, Zhu W, Lee HR, Choi YJ, et al. Oncogenic human herpesvirus hijacks proline metabolism for tumorigenesis. Proc Natl Acad Sci U S A. 2020;117(14):8083-93.

94. Lange PT, Lagunoff M, Tarakanova VL. Chewing the fat: The conserved ability of DNA viruses to hijack cellular lipid metabolism. Viruses2019.

CHAPTER 2

UPREGULATION OF CELL SURFACE GLYCOPROTEINS IN CORRELATION WITH KSHV LANA IN THE KAPOSI SARCOMA TUMOR MICROENVIRONMENT

Abstract

HIV-associated epidemic Kaposi sarcoma (EpKS) remains one of the most prevalent cancers in sub-Saharan Africa despite the widespread uptake of anti-retroviral therapy and HIV-1 suppression. In an effort to define potential therapeutic targets against KS tumors, we analyzed previously published KS bulk tumor transcriptomics to identify cell surface biomarkers. In addition to upregulated gene expression (>6-fold) in the EpKS tumor microenvironment, biomarkers were selected for correlation with KSHV latency-associated nuclear antigen (LANA) expression. The cell surface glycoprotein genes identified were KDR, FLT4, ADAM12, UNC5A, ZP2, and OX40, as well as the endothelial lineage determinants Prox-1 and CD34. Each protein was evaluated for its expression and co-localization with KSHV LANA using multi-color immunofluorescence in KS tissues, KSHV-infected L1T2 cells, uninfected TIVE cells, and murine L1T2 tumor xenografts. Five surface glycoproteins (KDR, FLT4, UNC5A, ADAM12, and CD34) were associated with LANA-positive cells but were also detected in uninfected cells in the KS microenvironment. *In vitro* L1T2 cultures showed evidence of only FLT4, KDR, and UNC5A, whereas mouse L1T2 xenografts recapitulated human KS cell surface expression profiles, with the exception of CD34 and Prox-1. In KS tumors, most LANA-positive cells

co-expressed markers of vascular as well as lymphatic endothelial lineages, suggesting KS-associated dedifferentiation to a more mesenchymal/progenitor phenotype.

Introduction

Kaposi Sarcoma-associated herpesvirus (KSHV), the etiologic agent of Kaposi Sarcoma (KS), pulmonary effusion lymphoma (PEL), multicentric Castleman's disease (MCD), and KSHV-induced inflammatory cytokine syndrome (KICS), was discovered in 1994 by Chang and Moore (1, 2). The incidence of KS varies depending on geographical location, lifestyle choices, and HIV-1 coinfection status (3, 4). KS occurs at a high prevalence in sub-Saharan Africa (SSA), isolated regions of South America, and the Mediterranean basin (5, 6). KS presents in four distinct forms: classical KS, observed in elderly Mediterranean men; iatrogenic KS, associated with therapeutic immunosuppression in organ transplantation; endemic KS (EnKS), in African individuals without human immunodeficiency virus (HIV-1) co-infection; and epidemic KS (EpKS), in the HIV-1 infected (3, 7). Based on clinical presentation during the early HIV epidemic, where KS became the most prevalent cancer in the HIV-infected individuals, EpKS was considered an acquired immune deficiency syndrome (AIDS)-defining disease (8). The widespread use of ART treatment, including in SSA, and the resulting increase in HIV-1 suppression has led to decreased EpKS incidence in the US and Europe. Yet, both EpKS and EnKS continue to occur at a high incidence. KS is still one of the most incident cancers in SSA, and EpKS continues to present at a high incidence in the HIV-infected, despite plasma viral load suppression (6, 9).

KS is a highly vascularized cutaneous lesion characterized by the slit vasculature and spindle morphology of growth deregulated cells, which are seemingly of endothelial origin (10, 11). Previously published bulk transcriptomic data from 24 KS tumors compared to cognate normal skin biopsies revealed an increased expression of transcripts related to the vascular endothelial growth factor (VEGF) pathways, namely, FLT4 and KDR, which are receptors for VEGF C/D and B, respectively (12, 13). The upregulation of FLT4 has also been observed in some KSHV-infected endothelial cell lines (14). *In vitro* findings from KSHV-infected primary endothelial cells linked the expression of FLT4 with an increased expression of the transcription factor Prox-1, a lineage-defining marker of lymphatic endothelial cells (15, 16). An alternate endothelial cell marker CD34, also found on hematopoietic stem cells, is known to be robustly expressed in KS lesions, (17, 18). These heterogeneous findings raise questions about the cellular origin of KS tumor cells and the tissue-specific driver pathways of tumorigenesis.

Despite KSHV being discovered over 25 years ago, models of sustained infection are few, and those of tumorigenesis are even more limited. Fixed human tissues are not conducive for mechanistic studies or for evaluating biomarkers for therapeutic potential; thus, we are exploring the validity of KSHV-infectable telomerase immortalized vein endothelial cells (TIVE) and the long-term KSHV-infected L1T2 cell line (19, 20) in recapitulating *in vivo* KS tumor microenvironment characteristics. Consistent with observations from human KS lesions, tumors derived from L1T2 cells have variable

percentages of KSHV-infected spindle cells throughout the tumor (20). Here, we explore the extent to which tumor cell surface marker phenotypes in L1T2 xenografts reflect those from human KS lesions.

We describe the identification of a panel of highly upregulated cell surface glycoproteins from data mining of our previous comparative human KS transcriptomics as well as the validation and expression of the identified panel in KS tissues, KSHV-infected cell lines *in vitro*, and cell line explants in NSG mice. We also explore the alternative endothelial cellular origins of KS lesions and demonstrate the extent to which explant KSHV-infected cell lines and explant models recapitulate the human KS microenvironment and expression patterns.

Materials and Methods

Patient Sample Collection

Approval to conduct this study was obtained from the review boards of Tanzania National Institute for Medical Research, Ocean Road Cancer Institute (ORCI), University of Zambia Biomedical Research Ethics Committee; the University of Nebraska-Lincoln (UNL); and the Louisiana State University Health Sciences Center—New Orleans (LSUHSC-NO) IRBs. Sample collection for this study was as described in Lidenge et al. (12). Informed consent was obtained from all subjects involved in the study.

Compliance

All animal experiments for generating KS cell line xenograft models were reviewed and approved by the UNL Institutional Animal Care and Use Committee

(IACUC) protocol (ID 1812). All personnel who were involved with the mice studies underwent training in appropriate methods to accomplish these procedures.

Cell Culture

L1T2 cells, obtained from ATCC, were cultured in DMEM supplemented with 10% FBS and 1% penicillin/streptomycin and passaged every 3–4 days. At the onset of this project, L1T2 cells were available for purchase from ATCC but are no longer available despite having been demonstrated to maintain long-term KSHV infection and to induce tumors upon xenotransplantation into immunodeficient mice (20). TIVE cells, kindly provided by Rolf Renne, were cultured in Medium 199 supplemented with 20% FBS, 1% penicillin/streptomycin, 1% 200 mM L-Glutamine, and 30 mg Endothelial Cell Growth Factor (Sigma, Burlington, MA, USA) and reportedly lack the capacity to produce tumors in immunodeficient mice (19). The media were changed two times per week, and the cells were split 1:2 when the culture reached ~60% confluency.

L1T2 Murine Xenograft Generation

The protocols for the preparation and xenografting of mice with human tissues or cell lines have been previously published (21). Briefly, 6–8-week-old *NOD-scid IL2Rgamma^{null}* (NSG) mice were acquired from Jackson Labs, Bar Harbor, ME, USA (Stock Number 005557). The animals were housed in negative pressure individually HEPA-filtered microisolator racked caging. Environmental controls in-cage and in-facility were monitored and maintained by a centralized computer network. All procedures were carried out in a Class II Type A2 biological safety cabinet. To maintain a liquid state, 100

µL of growth factor-depleted Matrigel (BD Biosciences, San Jose, CA, USA) was mixed with 1×10^6 L1T2 cells (ATCC® VR1802, Manassas, VA, USA) in 100 µL cold-PBS and injected subcutaneously into the flank of each irradiated NSG mouse. The mice were observed daily for palpable tumors. Tumor growth was followed by caliper measurements of volume (length, depth, and width) until sacrifice. The mice were anesthetized with isoflurane (5% induction, 2% maintenance) during the xenograft transplantation process, and then tumor growth was monitored by a caliper. During euthanasia, the tumor and major organs such as the spleen, liver, and lung were excised; half of each tissue was frozen in liquid nitrogen immediately after dissection, and the other half was fixed in 10% neutral-buffered formalin for pathological and molecular analyses.

Immunohistochemistry (IHC)

Formalin-fixed, paraffin-embedded (FFPE), KS tumor biopsy specimens were sectioned into adjacent 6 µm-thick sections for protein detection, as described in Tso et al. (22). Briefly, the slides were deparaffinized in xylene and rehydrated in graded ethanol washes, followed by 30 min treatment with 2% hydrogen peroxide in methanol to quench endogenous peroxidase activity. The slides then underwent antigen retrieval in sodium citrate solution pH 6.0 for 15 min at 98 °C. The slides were blocked for 30 min using Bloxall (Vector Labs, Newark, CA, USA), followed by primary antibody application and overnight incubation at 4 °C. The antibodies used for IHC were as follows: mouse anti-LANA (Leica, Deer Park, IL, USA, 1:100), rat anti-LANA (Abcam, Boston, MA, USA,

1:100), mouse-anti CD34 (Invitrogen, Boston, MA, USA 1:200), rabbit-anti Prox-1 (Abcam, 1:500), rabbit-anti KDR (ProteinTech, Rosemont, IL, USA, 1:1500), rabbit-anti FLT4 (Invitrogen, 1:800), rabbit-anti ADAM12 (Invitrogen, 1:500), rabbit-anti UNC5A (ProteinTech, 1:300), rabbit-anti OX40 (Novus, Centennial, CO, USA 1:500), rabbit-anti ZP2 (Invitrogen, 1:5000). The slides were then washed, and the species-appropriate HRP-labeled polymeric secondary reagent was applied for 30 min at RT, followed by the addition of diaminobenzidine for chromogen deposition. Hematoxylin was used for counterstaining.

Dual-Immunofluorescence (IF)

Dual IF was used to visualize protein colocalization. As described in the IHC protocol, adjacent slides were deparaffinized, followed by antigen retrieval in sodium citrate solution for 15 min at 98 °C, and then blocked for 30 min using Bloxall (Vector Labs). Primary antibodies were added, and the slides were incubated at 4 °C overnight. The primary antibodies used are as follows: rat anti-LANA (Abcam, 1:100), mouse-anti CD34 (Invitrogen, 1:200), rabbit-anti Prox-1 (Abcam, 1:500), rabbit-anti KDR (ProteinTech,1:200), rabbit-anti FLT4 (Invitrogen, 1:100), rabbit-anti ADAM12 (Invitrogen, 1:100), rabbit-anti UNC5A (ProteinTech, 1:100), rabbit-anti OX40 (Novus, 1:100), and rabbit-anti ZP2 (Invitrogen, 1:100). After washing, the slides were incubated with their corresponding secondary antibody (chicken anti-rat AF647 (Invitrogen, 1:100), donkey anti-mouse AF488 (Invitrogen, 1:100), donkey anti-rabbit AF488 (Invitrogen, 1:100), donkey anti-rabbit AF647 (Invitrogen, 1:100)) for 2 h at RT. The slides were then

counterstained with 300 nM DAPI for 30 min at RT and mounted using Fluoro-gel (Electron Microscopy Sciences, Hatfield, PA, USA).

Imaging

IHC imaging was performed using the Motic EasyScan One. IF imaging and cell quantification were performed using the BZX Fluorescence Microscope and the Keyence Hybrid Cell Quantification software version 1.1.1.8.

Statistical Analysis

Pearson's correlation coefficients were used to identify transcript correlations. Non-parametric Kruskal–Wallis with Dunn's multiple comparisons tests were used in GraphPad Prism v9 to compare protein expression within KS tumors.

Results

Identification of Glycoprotein Transcripts That Correlate with KSHV LANA

Using the transcriptomic dataset described in Lidenge et al. (2020) (12), we identified six transcripts that were uniformly upregulated by more than 6-fold in all KS tumors as compared to cognate normal skin controls (Figure 2.1 A and B). These transcripts encode empirically demonstrated or informatically implied membrane-associated proteins. Their expression was correlated with the presence of KSHV latently infected cells, as measured by LANA expression. The expression of LANA was correlated with the extent of KSHV infection (KSHV viral burden) within the KS tumor (r_p = 0.6166). Despite variable transcriptomic expression (on average 1.40-fold upregulated), CD34 was included for lineage discrimination since it has been detected previously in KS

lesions at the protein level and is a marker for vascular endothelial cells and hematopoietic stem cells (18, 23). Prox-1, a nuclear marker for lymphatic endothelial cells, was included for lineage discrimination; it was upregulated 21.52-fold in KS tumors and highly correlated with KSHV LANA (16). Prox-1 has also been implicated in KSHV maintenance in cell culture models and may also contribute to lytic reactivation (15). KDR, also known as VEGF receptor 2, and FLT4, also known as VEGF receptor 3, were both highly upregulated by 6.19- and 12.60-fold, respectively. CD34, Prox-1, FLT4, and KDR are associated with endothelial cell signaling, vascularization, and angiogenesis during tumor formation (3, 11, 15, 24).

Additional notable upregulated transcripts encoding cell surface proteins were the metalloproteinase ADAM12 (7.19-fold upregulated), the netrin receptor UNC5A (16.89-fold upregulated), the tumor necrosis factor receptor OX40 (6.59-fold upregulated), and the major subunit of the zona pellucida sperm receptor ZP2 (7.71-fold upregulated). UNC5A, OX40, and ZP2 were highly correlated with KSHV LANA expression; however, ADAM12, despite the strong upregulation in KS versus uninvolved skin, showed no significant correlation with LANA and the KSHV latency program. This short list of transcriptomically implied cell surface markers of KS was evaluated for protein expression in human KS lesions, TIVE and L1T2 cell lines, and L1T2-derived mouse xenograft tumors to determine whether the proteins were KSHV-infection-associated or markers of the KS tumor microenvironment.

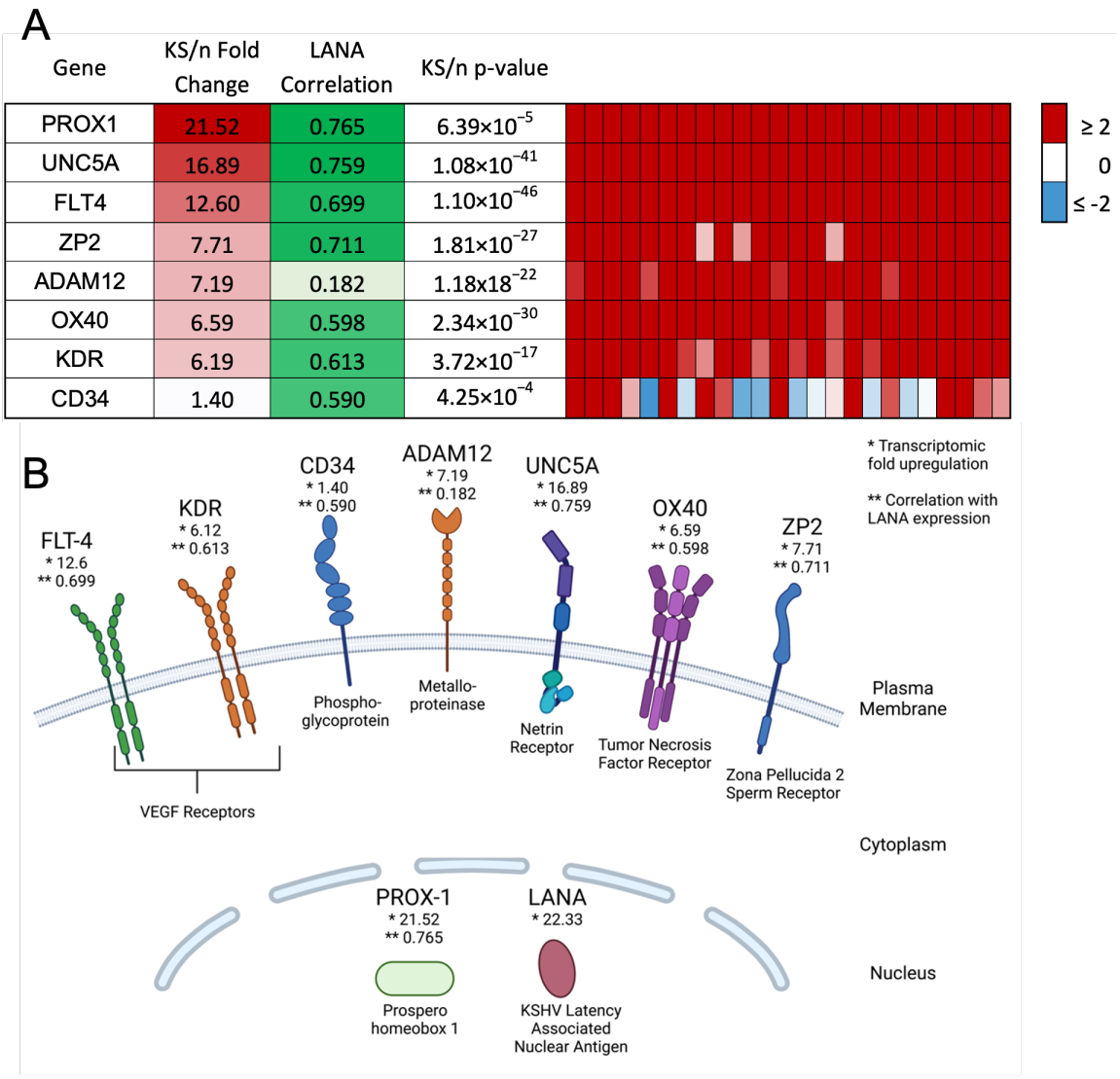

Figure 2.1. Identification of potential biomarkers with high upregulation in KS tumors and high correlation with LANA expression. (A) Overall fold change, correlation with LANA expression, and p-value are shown, as well as transcript expression within each individual KS lesion. (B) Diagram indicating the cellular location of markers at the protein level. Created using BioRender.com. * indicates the transcriptomic fold upregulation of KS tissues over normal human skin. ** indicates the correlation with LANA expression in the KS lesions.

Validation of Protein Expression in KS Tissues

It has been well demonstrated that transcript expression values calculated from bulk transcriptomics do not always accurately reflect protein abundance in tissues (25, 26). Thus, we sought to determine the extent of the expression and localization of each protein in KS tumors using immunohistochemistry. KS tumor biopsies were sectioned and stained for LANA expression to identify regions with demonstrable KSHV infection (Figure 2.2 A). Representative images from adjacent slides are shown in Figure 2.2 B–K for each identified protein and isotype control. KDR, FLT4, Prox-1, CD34, ADAM12, and UNC5A were all robustly expressed throughout the KS tumors. Staining intensity was similar across multiple lesions regardless of the extent of LANA expression or its intensity, both of which were variable across KS lesions (27). OX40 and ZP2 were not detected, which is consistent with the lack of T cells in KS lesions and with the highly restricted, tissue-specific expression and function of ZP2, respectively (27). The efficacy of the ZP2 and OX40 antibodies was confirmed using human ovary and human lymph node tissues, respectively. Protein expression was also evaluated in normal skin using dual immunofluorescence, where low to no staining of the identified markers was detected (Figure 2.3 A-J).

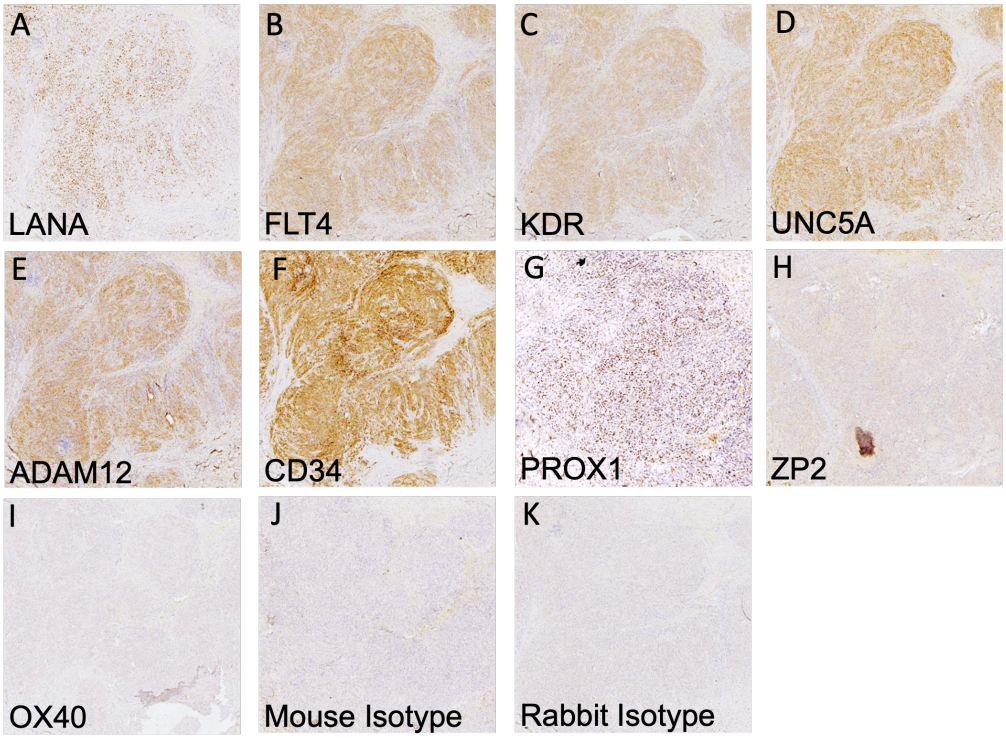

Figure 2.2. IHC detection of all human cell markers and KSHV LANA. (A–G) Positive staining is indicated by HRP staining within human KS tissues of the indicated surface marker and KSHV LANA protein. (H,I) There was no detection of ZP2 and OX40 proteins despite robust transcript detection. (J,K) Mouse and rabbit isotype controls. IHC images were taken at 10X magnification.

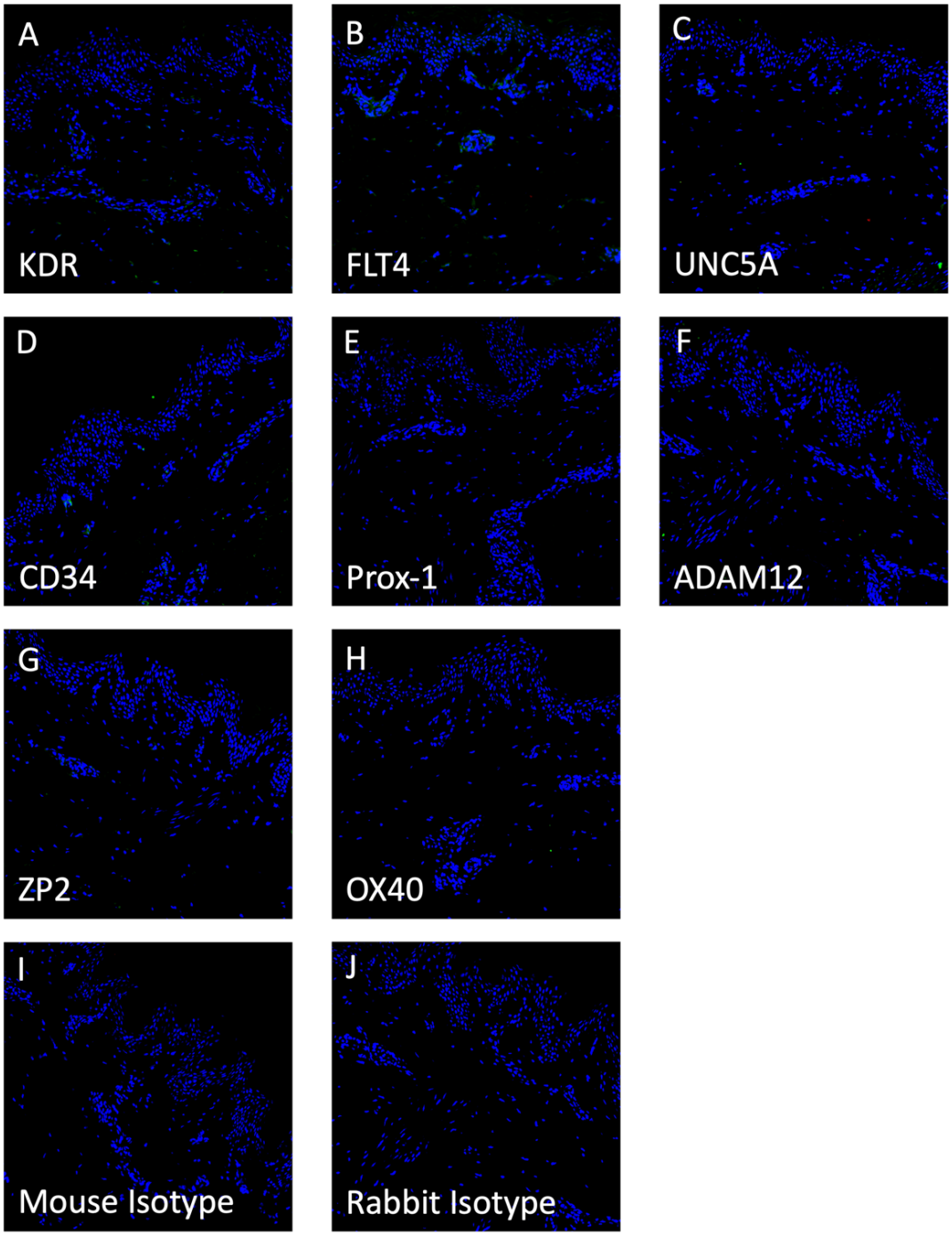

Figure 2.3. Dual immunofluorescence for all markers in normal human skin tissue. LANA is denoted as red and the surface marker in question is green. No LANA staining and minimal staining of the surface markers were observed. Images were taken at 20X magnification.

Highly Expressed Proteins Are Not Exclusive to KSHV-Infected Tumor Cells

Having demonstrated the upregulated expression of several transcriptomically implicated cell surface proteins in regions of KS tissue harboring demonstrably KSHV-infected cells, we next sought to determine whether those proteins were directly co-localized with LANA (i.e., KSHV infection) or, alternately if they were upregulated cell markers in the tumor environment. We conducted dual immunofluorescence assays with each identified protein and LANA. The same antibody clones used for IHC were used for IF to minimize sensitivity differences based on epitope recognition between approaches. Representative images are shown in Figure 2.4 A–F. The surface-associated proteins, KDR, FLT4, CD34, UNC5A, and ADAM12, were all robustly expressed throughout the lesions but were not exclusive to LANA-positive cells. Prox-1, a protein localized in the nucleus, was detected in most LANA+ cells but was also observed in some LANA– cells (Figure 2.4 C). Consistent with the IHC results, OX40 and ZP2 remained undetectable by dual IF (Figure 2.5 A-D).

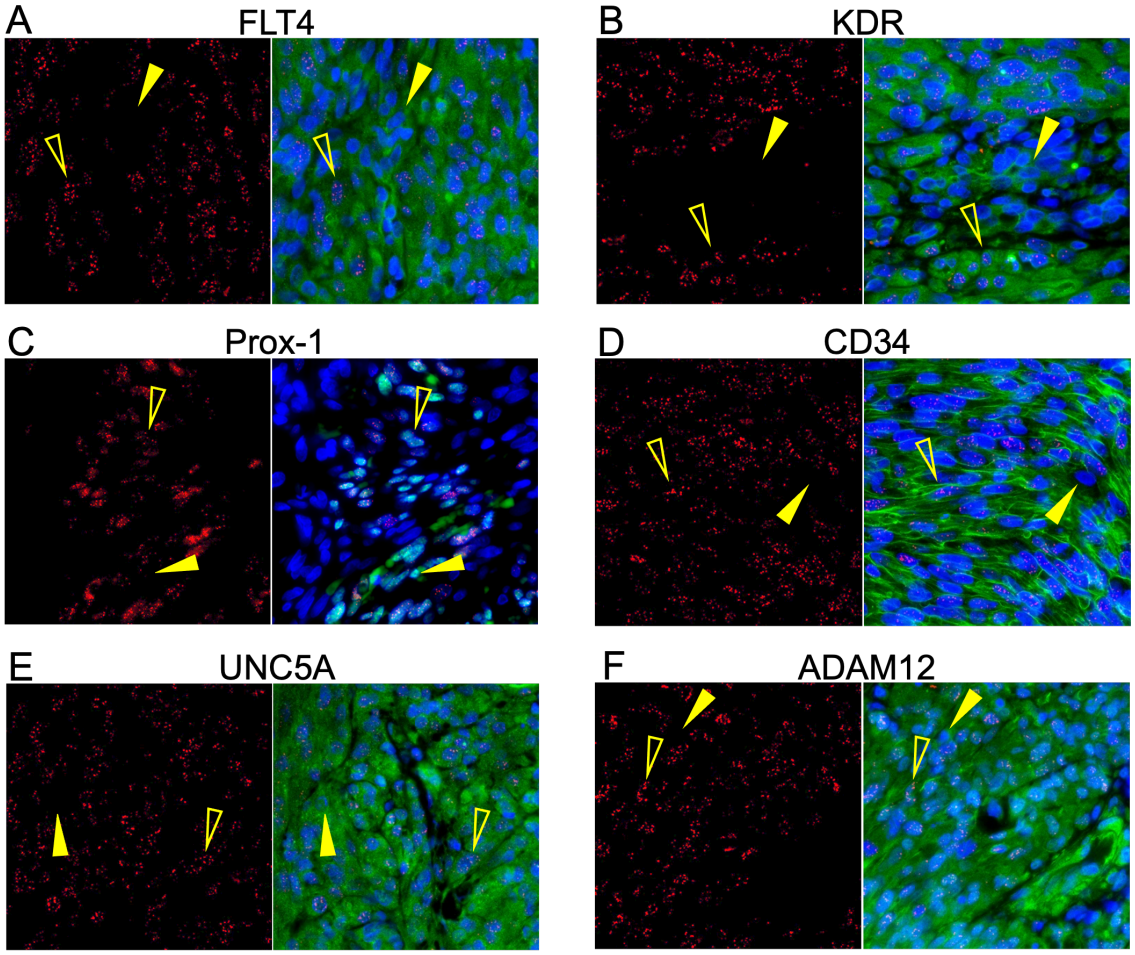

Figure 2.4. Six of the potential markers are robustly translated into protein within KS tumors. (A–F) Dual IF of the co-expression of LANA and the indicated potential KS biomarker. FLT4, KDR, UNC5A, ADAM12, CD34, and Prox-1 had robust expression in the KS lesions and were not exclusively detected in LANA-positive cells. ZP2 and OX40 were not detected at the protein level in KS lesions despite high transcriptomic expression. LANA is denoted as red, and the surface marker in question is green. Open yellow arrows indicate LANA-positive cells, and closed arrows indicate LANA-negative cells.

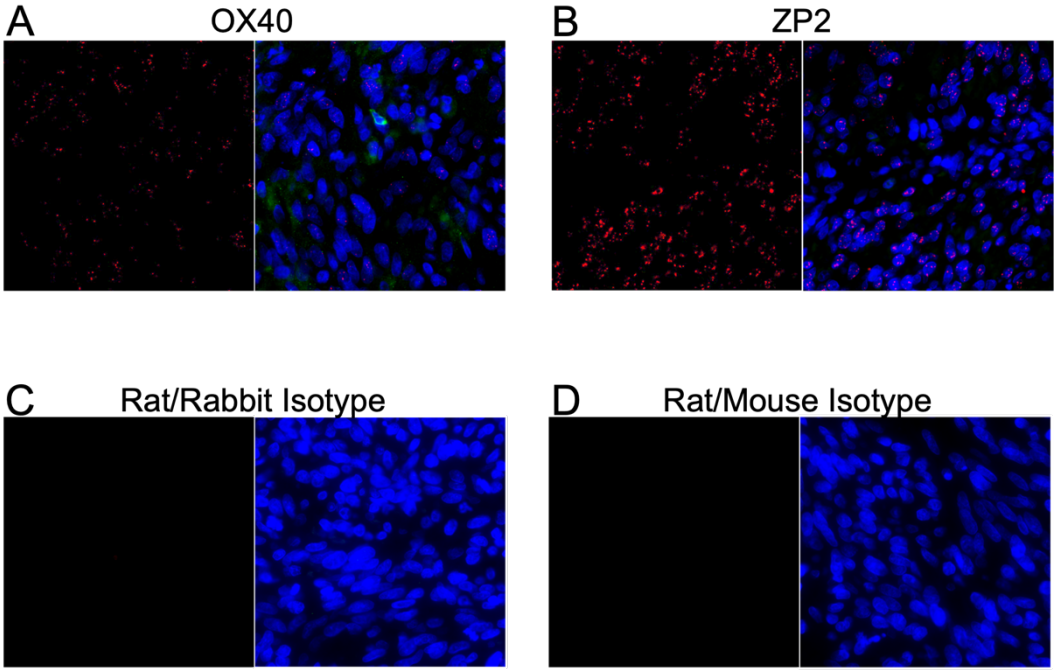

Figure 2.5. Dual immunofluorescence for OX40, ZP2, and isotype controls of KS tissue. A) OX40; B) ZP2; C) rat and rabbit isotype control; D) rat and mouse isotype control. LANA is denoted as red and the surface marker in question is green. Images were taken at 20X magnification.

Cells in KS Lesions Co-Express Prox-1 and CD34

We next analyzed the frequency of the co-localization of Prox-1 and CD34, proteins which are normally part of distinct endothelial cell lineages and, therefore, are not typically expressed on the same cells. We evaluated 16–20 fields from 5 different lesions (N = 83) for staining patterns of Prox-1, CD34, and LANA expression. This revealed that 25% of tumor cells were CD34+/Prox-1+, 26% CD34+ only, and 4% Prox-1+ only (Figure 2.6 A, E). We also calculated the degree to which the endothelial markers were colocalized with KSHV infection, as denoted by LANA staining. The KS tumors were 22% Prox-1+/LANA+, 14% Prox-1+ only, and 7% LANA+ only. We also observed that 66% of the cells in the KS tumors were CD34+, but only 34% of the tumor cells were also

LANA+, and less than 6% were LANA+ only (Figure 2.6 B,C,F,G). The five KS tumors all varied in the percentage of LANA-positive cells, which highlights the heterogeneity of KS lesions when evaluating for biomarkers (Figure 2.6 D). The cell counting software does not allow for the quantification of three markers at once; however, staining for LANA, CD34, and Prox-1, as shown in Figure 2.7 A–F, demonstrated a mixture of cell phenotypes and variable staining patterns. Together, IHC staining and IF colocalization data indicate that the majority of cells in KS tumors co-express markers of both vascular endothelial and lymphatic endothelial lineages, suggesting that the lesions are lineage indistinguishable or may have de-differentiated to a progenitor-like phenotype.

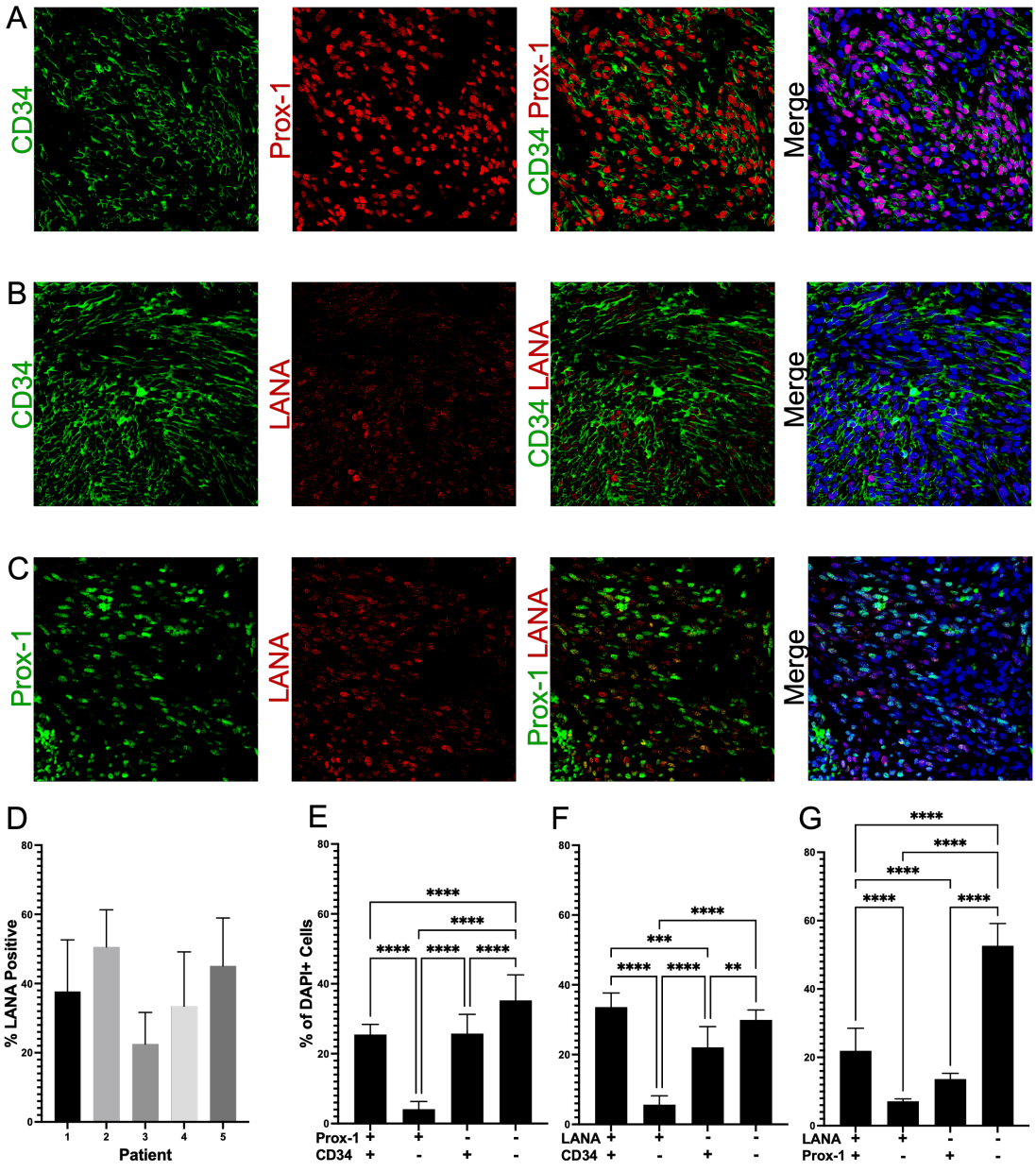

Figure 2.6. Colocalization of distinct endothelial lineage markers suggests KS tumors are dedifferentiating to an HSC phenotype. (A) Colocalization of Prox-1 and CD34, (B) Colocalization of LANA and CD34, and (C) Colocalization of Prox-1 and LANA. (D) Variation in the percentages of LANA-positive cells in five different KS lesions, which contributes to the quantification variation of cellular phenotypes across tissues. (E–G) Quantification of expression within KS tumors; about 25% of the tumor is double-positive for Prox-1 and CD34; greater than 50% of the tumor is CD34-positive, but only about 50% of these cells are also LANA-positive. Images were acquired at 20X

magnification. Non-parametric Mann–Whitney U test was used to determine statistical differences. Significance levels are $p < 0.01$ **, $p < 0.001$ ***, $p < 0.0001$ ****.

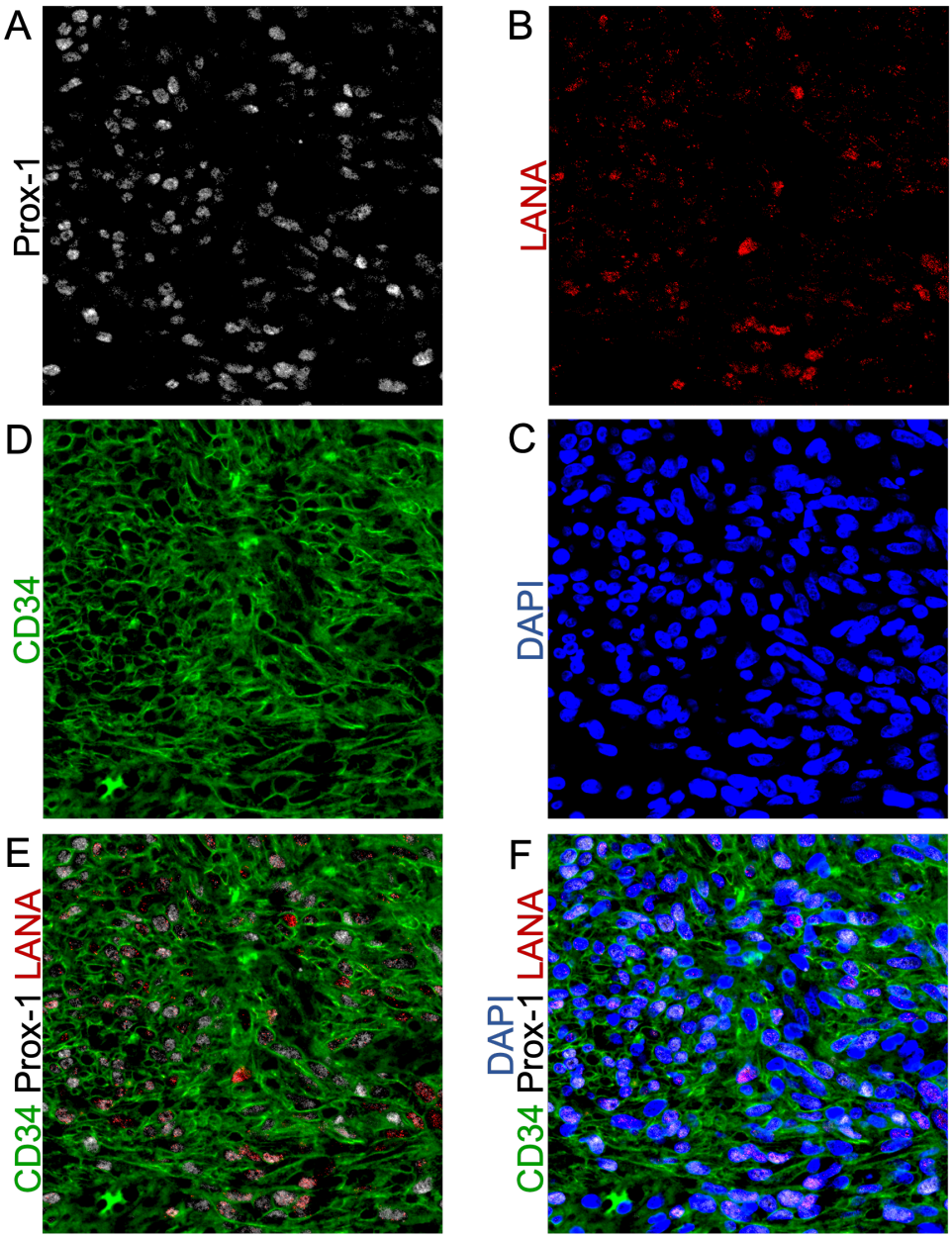

Figure 2.7. Triple-stained IF shows the heterogeneous expression of KSHV-LANA and the endothelial lineage markers Prox-1 and CD34. (A) Prox-1 staining; (B) LANA staining; (C) nuclear DAPI staining; (D) CD34 staining; (E) Co-localization of KSHV-LANA, Prox-1, and CD34; (F) Co-localization of KSHV-LANA, Prox-1, and CD34 with nuclear DAPI staining. Images were acquired at 20X magnification.

Limited Protein Expression in KSHV-Infected Endothelial Cell Lines

Since mechanistic studies for investigating potential roles for these cell surface proteins in defining and contributing to the KS tumor microenvironment require model systems that faithfully mimic the *in vivo* (human) tumor microenvironment, we then tested the KSHV-infected cell line, L1T2, and its uninfected endothelial cell counterpart, TIVE. L1T2 is a heterogeneous cell line derived from KSHV-infected TIVE cells implanted into mice, as described in Roy et al. (2013), where it was reported that tumors reminiscent of KS develop and recapitulate the protein expression phenotypes of KS tumors (20). There was a low but detectable protein expression of KDR, FLT4, and UNC5A in the *in vitro* cultured L1T2 cells but not in the uninfected TIVE cells, which were uniformly negative (Figure 2.8 A–F). The endothelial lineage markers CD34 and Prox-1, as well as ADAM12, were not detectable in either L1T2 or TIVE cells (Figure 2.8 G–L). We also observed an overall low frequency of KSHV-infected cells in the L1T2 culture. Isotype controls are seen in Figure 2.9 A-D. Since only three out of six markers readily detected in human KS tumors were detected in L1T2 *in vitro*, this finding, coupled with the lack of transcriptomic concordance between KS and cell infection models, highlights the challenges and limitations of recapitulating KS tumor biology with cell culture models of KSHV infection and KS tumorigenesis (13).

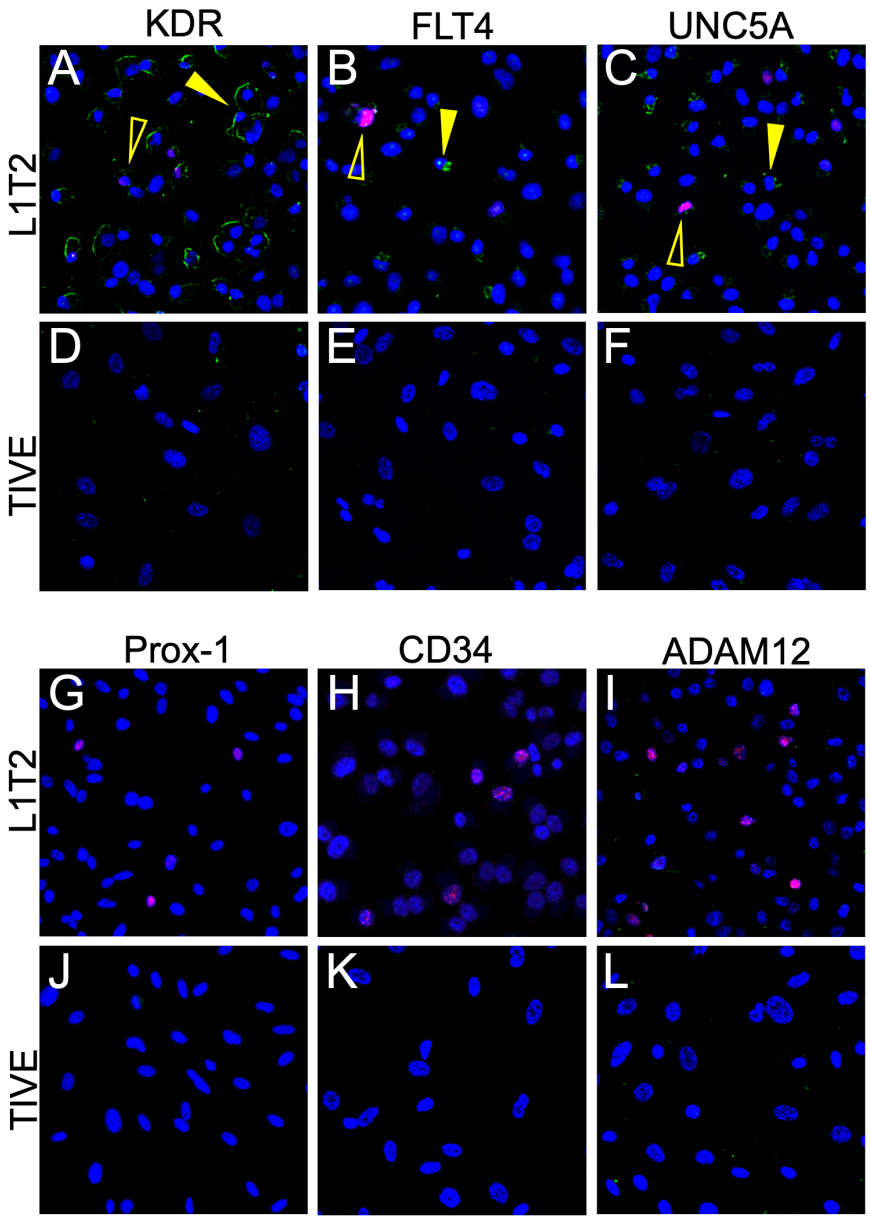

Figure 2.8. Dual IF of KSHV-infected L1T2 and uninfected TIVE cells shows the expression of KDR, FLT4, and UNC5a but not ADAM12 or the endothelial markers. (A–L) Dual IF of the co-expression of LANA and the indicated potential KS biomarker. ADAM12, CD34, and Prox-1 were not detected in either cell line. FLT4, KDR, and UNC5A had low to moderate expression in the KS lesions and were not exclusively detected in LANA-positive cells. LANA is denoted as red, and the surface marker in question is green. Open yellow arrows indicate LANA-positive cells, and closed arrows indicate LANA-negative cells. Images were acquired at 20X magnification.

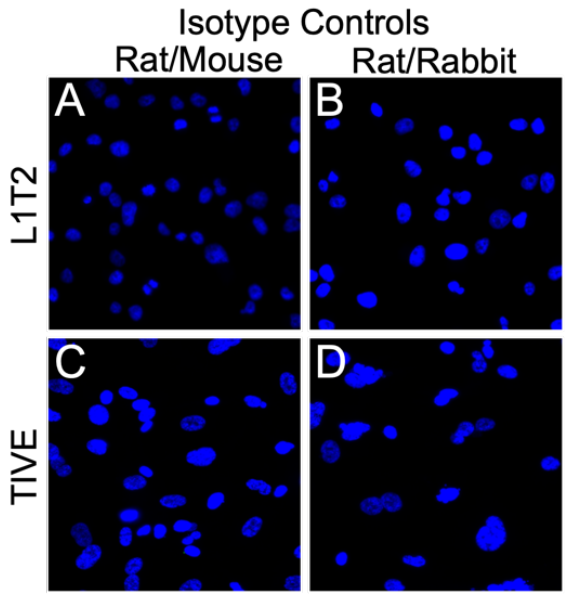

Supplemental Figure 2.9. Negative staining of isotype controls in L1T2 and TIVE cells. A and C) Rat and mouse isotype control; B and D) rat and rabbit isotype control. Images were taken at 20X magnification.

L1T2-Derived Xenografts Reflect the Protein Expression Observed in Human KS Tissues

Nevertheless, L1T2 cells readily form KS-like lesions with increased numbers of KSHV-infected cells when transplanted into mice; thus, we tested for the presence of the KS tumor microenvironment cell surface markers to evaluate the extent to which xenografts recapitulate the human KS tumor environment. The FLT4, KDR, and UNC5A proteins were detected at high levels within the L1T2 xenografts, mirroring the human KS tumor expression patterns (Figure 2.10 A–C). Surprisingly, despite not being detected in the L1T2 cell line, ADAM12 was also highly expressed in xenografted L1T2 (Figure 2.10 D). As with L1T2 *in vitro* cultures, CD34 and Prox-1 were not detected in the xenografts, suggesting that the L1T2 cell line and mouse xenografts, despite KSHV infection, are not differentiated endothelial cells (Figure 2.10 E, F). We also evaluated the expression of

LANA and the human surface markers in the spleens of the tumor-bearing mice, where no cross-reactive staining was observed except for low levels of ADAM12 (Figure 2.11 A-H). Isotype controls for the L1T2 xenografts are shown in Figure 2.12 A and B. In summary, we detected the partial recapitulation of KS tumor microenvironment cell surface protein expression within the xenograft tissues where FLT4, KDR, UNC5A, and ADAM12 mirrored the levels detected in the human KS tumors. However, the lack of endothelial lineage markers in both pre-implant and post-implant L1T2 cells may limit the applicability of this model for the investigation of KS origins.

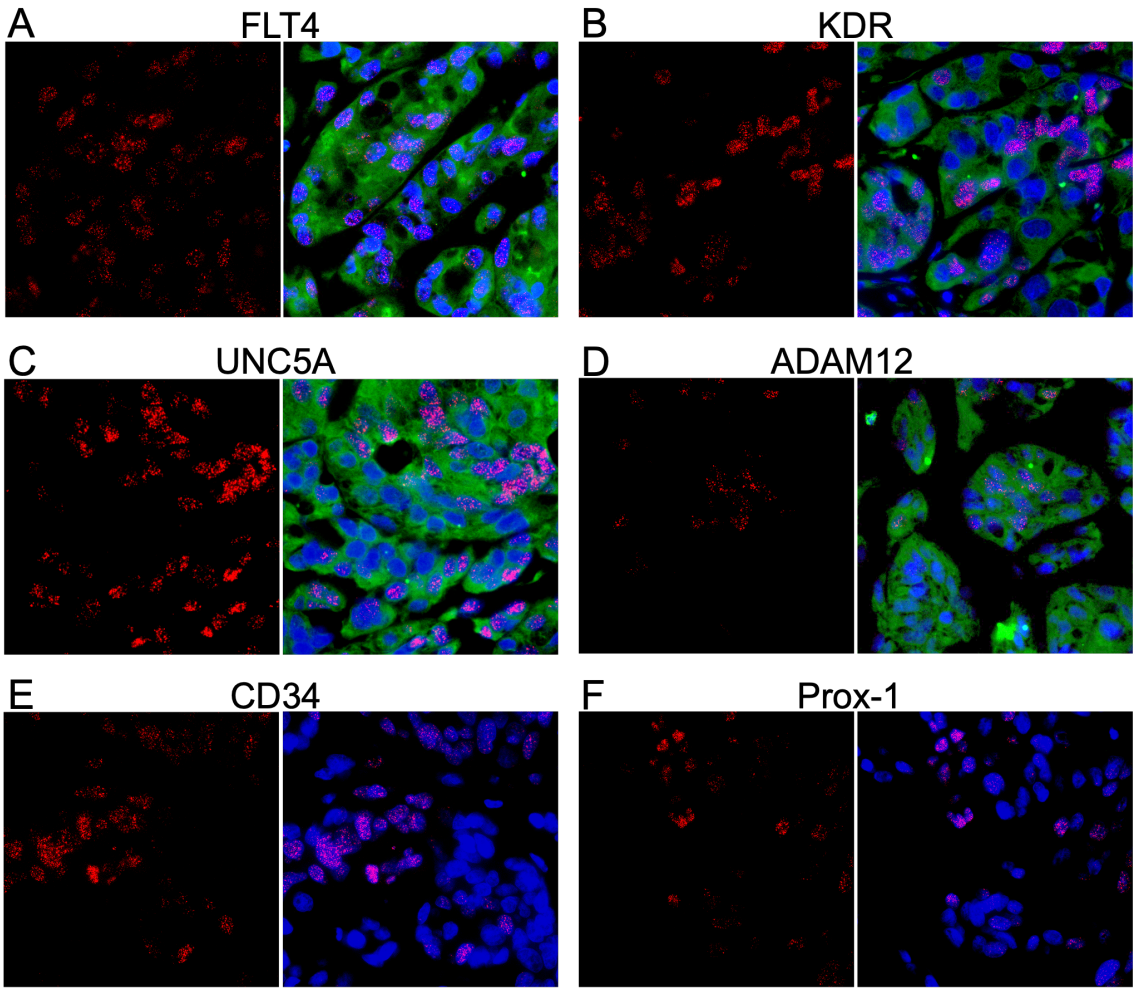

Figure 2.10. Dual IF demonstrating the colocalization of markers and LANA in mouse xenograft tissue. (A–F) Dual IF of the co-expression of LANA and the indicated potential KS biomarker. FLT4, KDR, UNC5A, and ADAM12 had robust expression in the KS lesions and were not exclusively detected in LANA-positive cells. CD34 and Prox-1 were not detected at the protein level. LANA is denoted as red, and the surface marker in question is green. Images were acquired at 20X magnification.

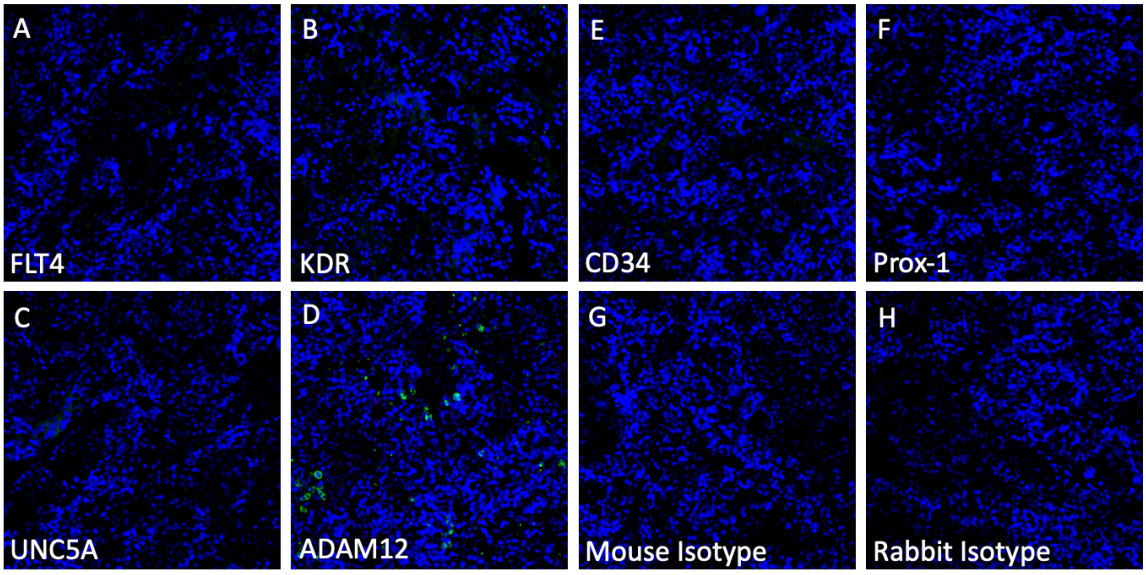

Figure 2.11. Dual immunofluorescence for all markers in L1T2 derived tumor-bearing mouse spleens. LANA is denoted as red and the surface marker in question is green. No LANA staining and minimal staining of the surface markers were observed. Images were taken at 20X magnification.

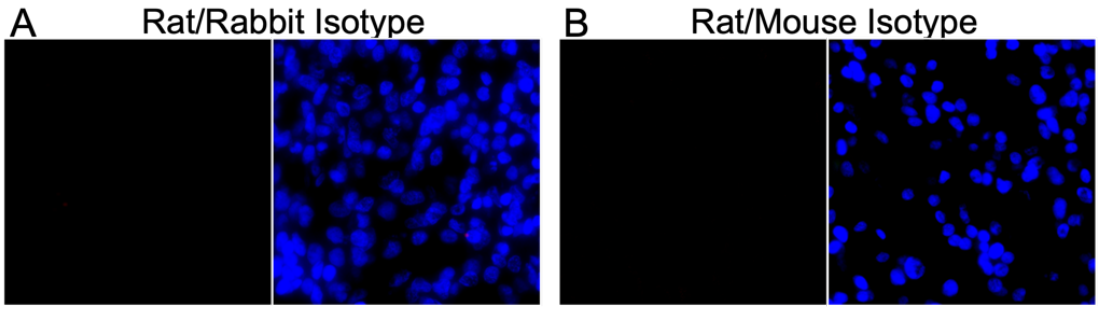

Figure 2.12. L1T2-derived mouse xenograft isotype controls. A) rat and rabbit isotype control; B) rat and mouse isotype control. Images were taken at 20X magnification.

Discussion

The lack of *in vivo* models that accurately reflect the phenotypes and behaviors of cells in human KS lesions is an impediment to studies of KSHV infection, KS tumorigenesis, and pathogenesis, as well as to the preclinical evaluation of potential treatments. To address these impediments, and to further refine our understanding of the KS tumor microenvironment, we utilized previously published gene expression profiles from 24 KS lesions, each subjected to subtractive comparison with autologous non-involved skin. We identified a subset of seven highly upregulated transcripts that correlated with KSHV LANA expression, six of which were predicted to be present on the cell surface of at least some component lineage within KS tumors. These cell surface markers might be potential biomarkers of latent infection with KSHV or of KS-transformed cells and could be potential targets for KS therapy. Alternately, these markers, which were not elevated in uninvolved skin, might be induced in bystander cells by the processes of infection or transformation. Other markers, such as the transcription factor Prox-1, were investigated for their potential to refine our appreciation of the specific endothelial cell lineage(s) that comprise KS tumors. Here, in correlation with transcriptome data, we demonstrated the detectable protein expression of KDR, FLT4, UNC5A, ADAM12, CD34, and Prox-1 in the human KS tumor microenvironment. Despite significantly upregulated RNA expression in KS tumors, neither OX40 nor ZP2 proteins were detected. The absence of the former is consistent with its typical expression as a co-stimulatory molecule on T cells, which we have reported as largely absent in the vicinity of KSHV-infected cells in KS biopsies (27). The

failure to verify ZP2 is likewise unsurprising given that it is typically expressed almost exclusively in the human ova (28). Thus, both upregulated transcripts may undergo some form of post-transcriptional regulation that limits/prevents their translation in the constituent cells of the KS microenvironment, as has been demonstrated in transcriptomic–proteomic decoupling in other studies (25, 29).

ADAM12, Prox-1 and CD34, were expressed at elevated levels in KS lesions versus normal skin. We compared the extent to which the KSHV-uninfected TIVE, KSHV-infected L1T2 cells, and the L1T2-derived mouse xenograft tissues recapitulated the KS tumor protein expression phenotypes. In contrast to KS lesions, ADAM12, Prox-1 and CD34 were not detectable in either the TIVE or L1T2 cell lines; however, ADAM12 was evident via IF in L1T2 xenografts. The metalloproteinase ADAM12 has been shown to be connected to hypoxia as well as T-cell mediated TGFβ activation, leading to cell death and sustained inflammation (30, 31). The activation of TGFβ has been demonstrated to be through the stabilization and recruitment of TGFβ receptor II, which was also upregulated in our KS transcriptomics (32). The lack of T-cell infiltration in KS lesions and the robust ADAM12 expression in both human KS lesions and the L1T2 mouse xenografts make ADAM12 an interesting potential target and biomarker.

Despite some lineage marker data supporting both vascular and lymphatic endothelial origins of KS, this remains speculation due to inconsistency in systems and the lack of a *de novo* transformation model. Evidence from in vitro infections of vascular and lymphatic endothelial cells suggests that lymphatic endothelial cells (Prox-

1+/CD34−) are more susceptible to KSHV infection and long-term episomal maintenance than vascular endothelial cells (Prox-1−/CD34+) (15). However, in the current study, we found that 25% of the KS tumor cells were co-expressing CD34 and Prox-1 which implies two scenarios that cannot, at this time, be distinguished. In the first, dedifferentiation events occurring during infection or tumorigenesis could result in an infected cell type with a more primordial/progenitor endothelial lineage lacking distinct lineage commitment markers. This type of dedifferentiation has been reported in other cancers and cancer virus infections (33, 34). An alternate concept involves the KSHV infection of mesenchymal stem cells that undergo differentiation or perhaps variable differentiation to endothelial phenotype(s) based on other factors (10, 35). This transition has been suggested to be associated with the KSHV-driven activation of Prox-1 (15). The co-expression of CD34 and Prox-1 may support this concept but might suggest an incomplete or heterogeneous switch from mesenchymal to endothelial cells, where heterogeneous protein expression phenotypes may derive from unique and, to date, undefined microenvironmental determinants in KS tumors. Colon cancer has also been shown to contain endothelial cells which co-express both CD34 and Prox-1, which may suggest that the co-expression of these lineage markers is a result of tumorigenesis in endothelial tumors (36). However, currently, it remains unclear in KS whether the microenvironment defines the tumor phenotype or, rather, the tumor phenotype defines the tumor microenvironment.

There is much interest in generating *in vivo* models that more completely reflect the human KS tumor environment since endothelial cell lines, the most time- and cost-effective choice, have been shown to only reflect about 10% of the transcriptomic changes seen in KS lesions (13). Here, we revealed that while TIVE cells lack the cell markers of KS, the KSHV-infected L1T2 cell line derived from them did not fully gain protein expression phenotypes evident in KS, since only 50% of the validated protein markers were evident. *In vivo* animal models may be more likely to recapitulate the KS microenvironment; however, tumor generation has proven difficult and inconsistent using both cell line and human KS tumor xenografts. Furthermore, while FLT4, KDR, UNC5A, and ADAM12 were detected in the L1T2 mouse xenografts in concert with human tumor results, we did not detect either endothelial cell marker (Prox-1 and CD34) in those grafts, which may indicate that the L1T2 cell line has lost its endothelial cell attributes in culture. Thus, as we have shown in the comparison of human transcriptomics to those from infected cell lines, protein expression profiles are also differential between KS patient tumors and cell lines/mouse models.

The consistency in the transcriptomic expression of the selected markers indicated that our sample size is robust enough to be representative and generalizable. Consistency was also evident at the protein level, where the detectable markers were consistently found in all tissues evaluated, albeit with variation in the signal magnitude from field to field depending on the cellularity, the cell types, and the number of KSHV-infected cells. Additionally, many of these markers, namely, KDR, FLT4, and UNC5A, are

involved in other types of cancers, making these markers non-exclusive to KS tumorigenesis (11, 24, 37). The specific role of these proteins in KS lesions has yet to be fully explored. The two VEGF receptors, KDR and FLT4, are currently being explored for targeted inhibition therapy to reduce immune modulation and immunosuppression in the tumor environment (38). These studies have, to date, produced inconclusive results and require more exploration with *in vivo* models to ascertain the effects of therapy on KS tumorigenesis.

Conclusions

We show the robust expression of potential candidate therapeutic targets, KDR and FLT4, as well as newly identified biomarkers, UNC5A and ADAM12, expressed consistently in KS tissues. Our current study also highlights the importance of validating transcriptomic data at the protein level, since the OX40 and ZP2 glycoproteins were not detectable despite 6.59- and 7.71-fold upregulation in gene expression, respectively. We also showed, through the robust upregulation of the expression of KDR and FLT4 in L1T2 versus TIVE cells, that L1T2-derived mouse xenografts could be a model for studying pathways, such as VEGF activation in KSHV infection and neoplasia, but they cannot be used to resolve the endothelial origin of KS, as they lack appropriate lineage markers. Further evaluation in additional cell lines, lineages, and animal models is needed to identify the conditions that more completely recapitulate the human KS tumor microenvironment and the landscape of the cellular membrane proteins.

Acknowledgments

The authors acknowledge all participants of this study and the supporting clinical and laboratory staff at the University Teaching Hospitals in Lusaka, Zambia.

References

1. Chang Y, Cesarman E, Pessin MS, Lee F, Culpepper J, Knowles DM, et al. Identification of herpesvirus-like DNA sequences in AIDS-associated Kaposi's sarcoma. Science. 1994;266(5192):1865-9.

2. PS M, Y C. Detection of herpesvirus-like DNA sequences in Kaposi's sarcoma in patients with and those without HIV infection. The New England journal of medicine. 1995;332(18).

3. Cesarman E, Damania B, Krown SE, Martin J, Bower M, Whitby D. Kaposi sarcoma. Nat Rev Dis Primers. 2019;5(1):9.

4. Ragi SD, Moseley I, Ouellette S, Rao B. Epidemiology and Survival of Kaposi's Sarcoma by Race in the United States: A Surveillance, Epidemiology, and End Results Database Analysis. Clin Cosmet Investig Dermatol. 2022;15:1681-5.

5. Grabar S, Costagliola D. Epidemiology of kaposi’s sarcoma. Cancers2021.

6. Motlhale M, Sitas F, Bradshaw D, Chen WC, Singini MG, de Villiers CB, et al. Epidemiology of Kaposi's sarcoma in sub-Saharan Africa. Cancer Epidemiol. 2022;78:102167.

7. AE G, CM V. The epidemiology of cancers in human immunodeficiency virus infection and after organ transplantation. Seminars in oncology. 2015;42(2).

8. Friedman-Kien AE. Disseminated Kaposi's sarcoma syndrome in young homosexual men. Journal of the American Academy of Dermatology. 1981;5(4):468-71.

9. Ngalamika O, Munsaka S, Lidenge SJ, West JT, Wood C. Antiretroviral Therapy for HIV-Associated Cutaneous Kaposi's Sarcoma: Clinical, HIV-Related, and Sociodemographic Predictors of Outcome. AIDS Res Hum Retroviruses. 2021;37(5):368-72.

10. P P, F P, AR M, E K, T H, P B. Lymphatic and vascular origin of Kaposi's sarcoma spindle cells during tumor development. International journal of cancer. 2006;119(6).

11. Kerr DA, Busarla SVP, Gimbel DC, Sohani AR, Nazarian RM. mTOR, VEGF, PDGFR, and c-kit signaling pathway activation in Kaposi sarcoma. Hum Pathol. 2017;65:157-65.

12. Lidenge SJ, Kossenkov AV, Tso FY, Wickramasinghe J, Privatt SR, Ngalamika O, et al. Comparative transcriptome analysis of endemic and epidemic Kaposi's sarcoma (KS) lesions and the secondary role of HIV-1 in KS pathogenesis. PLoS Pathog. 2020;16(7):e1008681.

13. Tso FY, Kossenkov AV, Lidenge SJ, Ngalamika O, Ngowi JR, Mwaiselage J, et al. RNA-Seq of Kaposi's sarcoma reveals alterations in glucose and lipid metabolism. PLoS Pathog. 2018;14(1):e1006844.

14. Hirakawa S, Hong YK, Harvey N, Schacht V, Matsuda K, Libermann T, et al. Identification of vascular lineage-specific genes by transcriptional profiling of isolated blood vascular and lymphatic endothelial cells. Am J Pathol. 2003;162(2):575-86.

15. Choi D, Park E, Kim KE, Jung E, Seong YJ, Zhao L, et al. The Lymphatic Cell Environment Promotes Kaposi Sarcoma Development by Prox1-Enhanced Productive Lytic Replication of Kaposi Sarcoma Herpes Virus. Cancer Res. 2020;80(15):3130-44.

16. Ntikoudi E, Pergaris A, Kykalos S, Politi E, Theocharis S. The Role of PROX1 in Neoplasia: A Key Player Often Overlooked. Diagnostics (Basel). 2022;12(7).

17. Kanitakis J, Narvaez D, Claudy A. Expression of the CD34 antigen distinguishes Kaposi's sarcoma from pseudo-Kaposi's sarcoma (acroangiodermatitis). Br J Dermatol. 1996;134(1):44-6.

18. Russell Jones R, Orchard G, Zelger B, Wilson Jones E. Immunostaining for CD31 and CD34 in Kaposi sarcoma. J Clin Pathol. 1995;48(11):1011-6.

19. An FQ, Folarin HM, Compitello N, Roth J, Gerson SL, McCrae KR, et al. Long-term-infected telomerase-immortalized endothelial cells: a model for Kaposi's sarcoma-associated herpesvirus latency in vitro and in vivo. J Virol. 2006;80(10):4833-46.

20. Roy D, Sin SH, Lucas A, Venkataramanan R, Wang L, Eason A, et al. mTOR inhibitors block Kaposi sarcoma growth by inhibiting essential autocrine growth factors and tumor angiogenesis. Cancer Res. 2013;73(7):2235-46.

21. Wang LX, Kang G, Kumar P, Lu W, Li Y, Zhou Y, et al. Humanized-BLT mouse model of Kaposi's sarcoma-associated herpesvirus infection. Proc Natl Acad Sci U S A. 2014;111(8):3146-51.

22. Tso FY, Sawyer A, Kwon EH, Mudenda V, Langford D, Zhou Y, et al. Kaposi's Sarcoma-Associated Herpesvirus Infection of Neurons in HIV-Positive Patients. J Infect Dis. 2017;215(12):1898-907.

23. AbuSamra DB, Aleisa FA, Al-Amoodi AS, Jalal Ahmed HM, Chin CJ, Abuelela AF, et al. Not just a marker: CD34 on human hematopoietic stem/progenitor cells dominates vascular selectin binding along with CD44. Blood Adv. 2017;1(27):2799-816.

24. Melincovici CS, Bosca AB, Susman S, Marginean M, Mihu C, Istrate M, et al. Vascular endothelial growth factor (VEGF) - key factor in normal and pathological angiogenesis. Rom J Morphol Embryol. 2018;59(2):455-67.

25. Liu Y, Beyer A, Aebersold R. On the Dependency of Cellular Protein Levels on mRNA Abundance. Cell. 2016;165(3):535-50.

26. Koussounadis A, Langdon SP, Um IH, Harrison DJ, Smith VA. Relationship between differentially expressed mRNA and mRNA-protein correlations in a xenograft model system. Sci Rep. 2015;5:10775.

27. Lidenge SJ, Tso FY, Ngalamika O, Kolape J, Ngowi JR, Mwaiselage J, et al. Lack of CD8(+) T-cell co-localization with Kaposi's sarcoma-associated herpesvirus infected cells in Kaposi's sarcoma tumors. Oncotarget. 2020;11(17):1556-72.

28. Litscher ES, Wassarman PM. Zona Pellucida Proteins, Fibrils, and Matrix. Annu Rev Biochem. 2020;89:695-715.

29. Wegler C, Olander M, Wisniewski JR, Lundquist P, Zettl K, Asberg A, et al. Global variability analysis of mRNA and protein concentrations across and within human tissues. NAR Genom Bioinform. 2020;2(1):lqz010.

30. Liu Y, Bockermann R, Hadi M, Safari I, Carrion B, Kveiborg M, et al. ADAM12 is a costimulatory molecule that determines Th1 cell fate and mediates tissue inflammation. Cell Mol Immunol. 2021;18(8):1904-19.

31. Wang R, Godet I, Yang Y, Salman S, Lu H, Lyu Y, et al. Hypoxia-inducible factor-dependent ADAM12 expression mediates breast cancer invasion and metastasis. Proc Natl Acad Sci U S A. 2021;118(19).

32. Atfi A, Dumont E, Colland F, Bonnier D, L'Helgoualc'h A, Prunier C, et al. The disintegrin and metalloproteinase ADAM12 contributes to TGF-beta signaling through interaction with the type II receptor. J Cell Biol. 2007;178(2):201-8.

33. Ding Y, Chen W, Lu Z, Wang Y, Yuan Y. Kaposi's sarcoma-associated herpesvirus promotes mesenchymal-to-endothelial transition by resolving the bivalent chromatin of PROX1 gene. PLoS Pathog. 2021;17(9):e1009847.

34. Li Y, Zhong C, Liu D, Yu W, Chen W, Wang Y, et al. Evidence for Kaposi Sarcoma Originating from Mesenchymal Stem Cell through KSHV-induced Mesenchymal-to-Endothelial Transition. Cancer Res. 2018;78(1):230-45.

35. Bruce AG, Barcy S, DiMaio T, Gan E, Garrigues HJ, Lagunoff M, et al. Quantitative Analysis of the KSHV Transcriptome Following Primary Infection of Blood and Lymphatic Endothelial Cells. Pathogens. 2017;6(1).

36. Fiedler U, Christian S, Koidl S, Kerjaschki D, Emmett MS, Bates DO, et al. The sialomucin CD34 is a marker of lymphatic endothelial cells in human tumors. Am J Pathol. 2006;168(3):1045-53.

37. Simons M, Gordon E, Claesson-Welsh L. Mechanisms and regulation of endothelial VEGF receptor signalling. Nat Rev Mol Cell Biol. 2016;17(10):611-25.

38. Maslowska K, Halik PK, Tymecka D, Misicka A, Gniazdowska E. The Role of VEGF Receptors as Molecular Target in Nuclear Medicine for Cancer Diagnosis and Combination Therapy. Cancers (Basel). 2021;13(5).

CHAPTER 3

COMPARATIVE POLAR AND LIPID PLASMA METABOLOMICS DIFFERENTIATE KSHV INFECTION AND DISEASE STATES

Abstract

Kaposi sarcoma (KS) is a neoplastic disease etiologically associated with infection by the Kaposi sarcoma-associated herpesvirus (KSHV). KS manifests primarily as cutaneous lesions in individuals due to either age (Classical KS), HIV infection (Epidemic KS), or tissue rejection preventatives in transplantation (Iatrogenic KS), but can also occur in individuals, predominantly in sub-Saharan Africa (SSA), lacking any obvious immune suppression (Endemic KS). The high endemicity of KSHV and human immunodeficiency virus-1 (HIV) co-infection in Africa results in KS being one of the top 5 cancers there. As with most viral cancers, infection with KSHV alone is insufficient to induce tumorigenesis. Indeed, KSHV infection of primary human endothelial cell cultures, even at high levels, is rarely associated with long-term culture, transformation, or growth deregulation, yet infection *in vivo* is sustained for life. Investigations of immune mediators that distinguish KSHV infection, KSHV/HIV co-infection, and symptomatic KS disease have yet to reveal consistent correlates of protection against or progression to KS. In addition to viral infection, it is plausible that pathogenesis also requires an immunological and metabolic environment permissive to the abnormal endothelial cell growth evident in KS tumors. In this study, we explored whether plasma

metabolomes could differentiate asymptomatic KSHV-infected individuals with or without HIV co-infection, and symptomatic KS from each other.

To investigate how metabolic changes may correlate with co-infections and tumorigenesis, plasma samples derived from KSHV seropositive sub-Saharan African subjects in three groups; A) asymptomatic (lacking neoplastic disease) with KSHV infection only, B) asymptomatic co-infected with KSHV and HIV, and C) symptomatic with clinically diagnosed KS were subjected to analysis of lipid and polar metabolite profiles.

Polar and non-polar plasma metabolic differentials were evident in both comparisons. Integration of the metabolic findings with our previously reported KS transcriptomics data suggests dysregulation of amino acid/urea cycle and purine metabolic pathways, in concert with viral infection in KS disease progression. This study is, to our knowledge, the first to report human plasma metabolic differentials between *in vivo* KSHV infection and co-infection with HIV, as well as differentials between co-infection and Epidemic KS.

Introduction

Kaposi sarcoma (KS) is a neoplastic disease first characterized in elderly Mediterranean men by the Hungarian physician Moritz Kaposi (1-3). The disease occurs endemically at high incidence in sub-Saharan Africa as well as parts of the Mediterranean basin, and in specific regions of South America (4-6). In association with the acquired immune deficiency syndrome (AIDS) pandemic, KS came to be widely

recognized as an AIDS-defining condition. In fact, prior to the isolation of Kaposi sarcoma-associated herpesvirus (KSHV) or human herpesvirus-8 (HHV-8), it was the abnormally high incidence of this rare sarcoma amongst men who have sex with men (MSM) that triggered the search for the infectious agent that ultimately became the human immunodeficiency virus-1 (HIV) in the 1980s (7). We now know that KS requires infection with the gammaherpesvirus KSHV (1). There are four forms of KS, all of which are attributable to KSHV infection, growth dysregulation, and abnormal angiogenesis in endothelial cells. This includes classic KS (cKS), as originally observed in elderly Mediterranean men, endemic KS (EnKS) – in men, women, and children lacking HIV co-infection, iatrogenic KS (iKS) – resulting from chemical immunosuppression in organ transplantation, and epidemic KS (EpKS) – resulting from HIV co-infection (4, 8, 9). In addition, KSHV infection is also linked to B-cell neoplastic diseases such as primary effusion lymphoma (PEL), multicentric Castleman's disease (MCD), and KSHV-induced inflammatory cytokine syndrome (KICS) (4).

Although KSHV seroprevalence is low in the US and Europe, it is significantly higher in specific populations such as MSM and those co-infected with HIV (10). Antiretroviral therapies (ART) have been highly successful in the US and Europe in reducing the incidence of EpKS, consistent with a role for immune dysfunction in KS development. Treatment responses vary depending on age, staging, visceral involvement, co-infections and comorbidities, and other sociodemographic variables (11, 12). Unfortunately, KS presentation is often advanced in sub-Saharan Africa, despite

HIV viral suppression. The response rate of such advanced patients to treatment with chemotherapy is ~50% in Zambia, of whom an additional 50% succumb to recurrence within a year. Currently, there are no prognostic markers or tests that can provide any indication of likely treatment success or failure, other than the HIV disease staging parameters and the AIDS clinical trials group (ACTG) initiated tumor/immune/system (T/I/S) staging criteria often being used. Moreover, no markers are reliable indicators of the transition from asymptomatic to symptomatic presentation or of protection against such progression.

Recent transcriptomics studies comparing tumor biopsy gene expression to that of normal skin from the same individuals have revealed several salient KS features (13, 14). First, HIV transcripts are rarely detected in KS tumor tissue, suggesting HIV gene products are not direct drivers of tumorigenesis. Second, EpKS and EnKS upregulate or downregulate a majority of the same genes and do so in the same direction, differing only in the greater magnitude of that dysregulation in EnKS. This finding implies that HIV lowers the threshold for malignant transformation. Moreover, gene dysregulation in EpKS is shared between subjects with undetectable HIV plasma viral load and those with active HIV replication. Whether such dysregulation of expression is communicated into detectable plasma metabolite differentials is one of the objectives of the investigation here. Our previous RNA-Seq data revealed significant changes in glucose metabolism, the Krebs (tricarboxylic acid) cycle, and multiple aspects of lipid metabolism. Additionally, the data suggested activation of redox balance to promote cell growth as

opposed to virus-induced dysregulation. Increases in angiogenesis pathways and evidence of immune signaling consistent with attempted T-cell recruitment were all associated with KS tumorigenesis (15, 16). Our follow-up studies have, however, failed to identify a robust immune infiltration of KS tumors, and limited cytokine differences were detectable between EnKS and EpKS with the differentials predominantly in immune-regulatory, suppressive, or Th2-skewing, as opposed to hyper-inflammatory, categories (17, 18).

Previous studies investigating the effects of KSHV infection on cell metabolism have been restricted to *in vitro* infections over a short time course. Dysregulation of glycolysis, fatty acid synthesis, and glutaminolysis was evident during both latency and lytic reactivation (19-22). Glycolysis and glutaminolysis were suggested to be essential for KSHV viral replication *in vitro* and inhibition of these pathways prevented the generation of new infectious virus (23). In human tissue, the relationships between virus replication and KS disease progression are less apparent since in most KS tissues, gene expression from the latency locus predominates. Limited cellular transcriptomic overlap (10%) between KS tissues and telomerase-immortalized human microvascular endothelial (TIME) cells, a commonly used *in vitro* infection model, has been previously reported (13). Nevertheless, the most predominantly shared pathway between *in vitro* models and KS tumors was glucose metabolism disorder, reflective of widespread metabolic reprogramming commonly observed in viral infection and cancer.

The lack of data characterizing *in vivo* KSHV/HIV co-infection-associated, and KS-specific metabolic dysregulation underscored a need to assess potential diagnostic and prognostic implications of metabolic dysregulation in KSHV-induced neoplastic disease. In this study comparisons of polar and non-polar (lipid) plasma metabolites in KSHV infection versus co-infection with HIV (KSHV+/HIV- vs. KSHV+/HIV+), and between asymptomatic co-infection with symptomatic KS (KSHV+/HIV+ vs. EpKS) were conducted to preliminarily determine if differentials metabolites among them existed. This approach defined metabolites unique to co-infection and tumorigenesis that may have potential as marker panels for disease staging and treatment outcome. Moreover, the integration of tumor transcriptomics with the plasma metabolome pointed to specific pathways that become additively or synergistically dysregulated in the pathogenetic transition of KSHV infection to malignant disease with or without the contribution of HIV co-infection. An increased appreciation of these KS pathogenetic pathways may provide a framework for novel combinatorial approaches perhaps with dose-sparing regimens to target the viral, metabolic, oncologic, and immunologic aspects of the KS disease.

Materials and Methods

Sample Collection

24 participants (>18 years old) were recruited from the Ocean Road Cancer Institute (ORCI), Tanzania as described in Lidenge et al. (14). Participants (both genders) were 18 years and older. Whole blood was collected in EDTA tubes followed by plasma isolation by centrifugation at 400 x *g* for 5 minutes. Plasma was stored at -80°C until

shipment. HIV viral load and CD4 quantification were performed as described in Lidenge et al. (17). This study was approved by the review boards of the Tanzania National Institute for Medical Research, Ocean Road Cancer Institute, the University of Nebraska Medical Center, the University of Nebraska–Lincoln, and the Louisiana State University Health Sciences Center.

Sample Extraction

From each individual, 20µL of plasma was used to generate polar and non-polar (lipid) metabolite fractions. Each plasma sample was transferred to a 1.5mL Eppendorf tube, and 500µL of methanol and 30µL of ribitol (2mg/mL in water, used as an internal standard) was added as a spike control. Samples were vigorously mixed, incubated for 15 minutes at 70°C, and centrifuged at 14,000 x *g* for 10 minutes. The supernatant (500µL) was transferred to a new tube with 250µL of chloroform and 500µL of water and mixed vigorously for 1 minute. To separate polar and nonpolar phases the samples were centrifuged at 1,500 x *g* for 15 minutes and each phase was transferred to separate tubes. Extracted polar metabolites (upper aqueous phase, 500µL) were dried in a speed vacuum before derivatization and GC-MS analysis. Extracted non-polar lipid metabolites (lower chloroform phase, 200µL) were dried under a constant nitrogen stream and dissolved in 50µL of methanol just before LC-MS global lipid profiling analysis. In addition to the samples, blanks and quality control samples were prepared for both LC and GC-MS platforms. A blank sample was prepared without the addition of plasma but underwent all the extraction steps for the elimination of potential

contaminants coming from non-biological background sources (solvents, tubes etc.) during the sample processing and preparation. Quality control (QC) samples were prepared by mixing equal aliquots of each sample and injected between biological samples to evaluate sensitivity, stability, and reproducibility of the LC and GC-MS acquisition platforms. Samples were analyzed in random order.

Lipid profiling

Lipid analyses were carried out using an Agilent 1200 Series High-Performance Liquid Chromatography (HPLC) system coupled to a high-resolution/accuracy Fourier-Transform Ion Cyclotron Resonance (FT-ICR) 7.05T Mass Spectrometer (MS) (Bruker Daltonics, Germany). An aliquot of 5µL of the methanol resuspended, dried chloroform extraction was injected onto an ACE 5 C8-300 column (2.1 x 100 mm) column and lipids were separated in a linear gradient elution at a flow rate of 0.1 mL/min. The mobile phases consisted of A: 0.1% formic acid and 10 mM ammonium acetate in Milli-Q water; and B: 0.1% formic acid and 10 mM ammonium acetate in acetonitrile/ isopropanol (50/50; v/v). The gradient was set as follow: T= 0 minutes: 30% B; T= 1 minute: 30% B; T= 25 minutes: 100% B; T= 45 minutes: 100% B; T= 47 minutes: 30% B; and T= 60 minutes: 30% B (column re-equilibration). Data was collected in positive mode in a scan range of 244 - 1,800 m/z and 0.2 s of ion accumulation time with estimated resolving power of 78,000 (at m/z 400). A capillary voltage of 4,500 V, and end plate offset of -500 V was used. Dry temperature and gas flow were set at 180°C and 4 L/min, respectively. CompassXport v. 3.0.6. (Bruker Daltonics, Germany) software was used to convert LC-

MS data to a general mzXML format and further processed with the mzMine software package for peak detection, deconvolution, normalization, and alignment (24).

Profiling of polar metabolites

For polar analysis, dried samples were derivatized by addition of 40µL Methoxyamine hydrochloride (20mg/mL in pyridine), incubated in a shaker for 2 hours at 37°C, followed by the addition of 70µL N-Trimethylsilyl-N-methyl trifluoroacetamide (MSTFA, 1mL, and 20µL Fatty Acid Methyl Esters (FAME)) and incubation in a shaker for an additional 30 minutes at 37°C. After cooling to room temperature, the samples were centrifuged at 14,000 x *g*, for 10 minutes and 90µL of supernatant was transferred into a 200µL conical base inert glass insert inside a 2mL amber autosampler glass vial (Agilent Technologies, Germany). MS acquisitions were done using 7200 GC-QTOF system (Agilent) and an HP-5MS UI column (30 m, 0.25 mm, and 0.25 mm; Agilent). The temperature gradient included a starting temperature of 80°C held for 2 minutes, increasing at a rate of 15°C per minute to 350°C followed by a final hold for 6 minutes (total run time of 26 minutes). The ion source temperature was set to 250°C, while the scanning mass range was set to 60 - 600 m/z. Acquired data were converted to .abf using AbfConverter and further processed by MS-Dial 4.12 (25).

Data analysis

Following data processing, excel files (containing *m/z* values, retention times, and peak areas information for each feature) were generated and exported from MZmine and MS-Dial. Missing values were imputed using K-nearest neighbors (KNN)

and auto-scaled prior to data analyses. Multivariate and univariate statistical analyses were performed using MetaboAnalyst software v5.0 (26, 27). Using the auto-scaled data from Metaboanalyst, heatmaps were generated using the R package Pheatmap v1.0.12 in RStudio v2022.02.3 with R v4.2.0.

Principal component analysis (PCA) and Kruskal-Wallace analysis were used to visualize the variation of datasets between groups (GraphPad Prism v9). Polar and non-polar data were combined and comparisons between two groups were performed, and volcano plots were constructed. In addition, Wilcoxon ranked-sum analysis with and without a Bonferroni correction were applied. Polar features were tentatively identified using the public Fiehn database search on MS-Dial before statistical analysis (28). Nonpolar features with a significant threshold of $p<0.05$ and a fold-change (FC) threshold of 1.5 (log2 FC of 0.585< or >0.585) were tentatively identified on the Human Metabolome Database (HMDB) with a mass tolerance of 10 ppm selecting $M+H^+$, $M+NH_4^+$ as the positive ion adducts for non-polar metabolites (29). KEGG IDs were obtained for polar and non-polar tentatively identified metabolites and used to check pathways affected based on the conditions analyzed, using *Homo sapiens* as the organism. In cases where multiple ions could be annotated to the same feature (due to different adducts or ppm), they were counted additively to the predicted pathway classification where at least 2 metabolites were used for the enrichment analysis.

Pathway Analyses Integrating Metabolomics and Transcriptomics Data

Pathway analyses were completed in Metaboanalyst v5.0 using the Joint Pathway Analysis tool (30). Briefly, significantly changed genes and metabolites were entered without their corresponding fold changes. Gene symbols that did not have a match were removed. The parameters chosen were degree-centrality and integrated metabolic pathways (regulatory pathways were not considered). Transcriptomic data used for pathway analyses in this report were previously published by Lidenge et al. (14). Of this data, genes that possessed a significant threshold of $p < 0.05$ (raw p.value) and a fold change (FC) > 2 for KS/control (or lesion/normal skin) or an FC >1.5 for KS origin (EnKS vs. EpKS) were included. For metabolomics data, identified metabolites with a minimum FC of 2 (FC > 2 or <0.5) and a raw p-value < 0.05 were used for pathway analyses. Pathways that were not relevant to humans were excluded in reporting final results (i.e. porphyrin and chlorophyll which is common for plants).

For the KSHV+/HIV+ vs. EpKS pairwise comparison, metabolomic data was integrated with comparative transcriptomic data that subtracted normal skin gene expression from that of the KS lesion from 24 subjects used. The integration was conducted to seek insight into KS progression/development biomarkers and how these changes might be reflected in the more accessible plasma.

Results

Overall analysis and data overview

Twenty-four KSHV samples were included in the study (Table 3.1). Of those, 11 samples were KS symptomatic (9 **Ep**idemic and 2 **En**demic), and 13 samples were

asymptomatic and segregated into groups based on KSHV and HIV serostatus; 7 $KSHV^{+}/HIV^{+}$ and 6 $KSHV^{+}/HIV^{-}$. In addition, 5 US-collected $KSHV^{-}/HIV^{-}$ serum samples were used as controls to monitor variations in technical processing and for quality assurance purposes but were not included in group/pairwise analyses since they are unlikely to be appropriate comparators for parameters (diet, lifestyle etc.) beyond KSHV or HIV infection status factors. Quality Control (QC) samples, representing a pool of all samples analyzed, were used to evaluate technical variation and chromatographic shifts during both LC-MS and GC-MS analyses. The overview of the project workflow is summarized in Figure 3.1. Following processing, normalization, and scaling, MetaboAnalyst and Prism v9 were used to produce PCA plots, volcano plots, and other statistical analyses.

Table 3.1. Cohort characteristics. There were no significant differences between group Ages or CD4 Counts within the HIV+ patients. NA, not applicable; ND, not detectable; NR, no record.

Group	Study ID	Age	Gender	HIV VL/mL	CD4 Count
EnKS	*21147*	*39*	*Male*	*NA*	*NA*
EnKS	*21182*	*57*	*Male*	*NA*	*NA*
EpKS	21117	38	Female	3,450	130
EpKS	21119	39	Male	ND	264
EpKS	21120	56	Male	14,500	482
EpKS	21121	42	Male	6,310	30
EpKS	21145	26	Male	NR	422
EpKS	21161	38	Male	148,000	710
EpKS	21204	58	Male	ND	261
EpKS	21220	30	Female	NR	67
EpKS	21228	38	Female	NR	333
KSHV+HIV-	21525	48	Male	NA	256
KSHV+HIV-	21526	50	Male	NA	310
KSHV+HIV-	21527	54	Male	NA	931

KSHV+HIV-	21528	55	Male	NA	303
KSHV+HIV-	21559	33	Female	NA	1054
KSHV+HIV-	21562	33	Female	NA	1398
KSHV+HIV+	21570	36	Female	NR	500
KSHV+HIV+	21575	34	Male	NR	675
KSHV+HIV+	21578	38	Male	NR	316
KSHV+HIV+	21579	43	Male	NR	240
KSHV+HIV+	21580	48	Female	NR	295
KSHV+HIV+	21582	34	Female	NR	594
KSHV+HIV+	21583	35	Female	NR	124

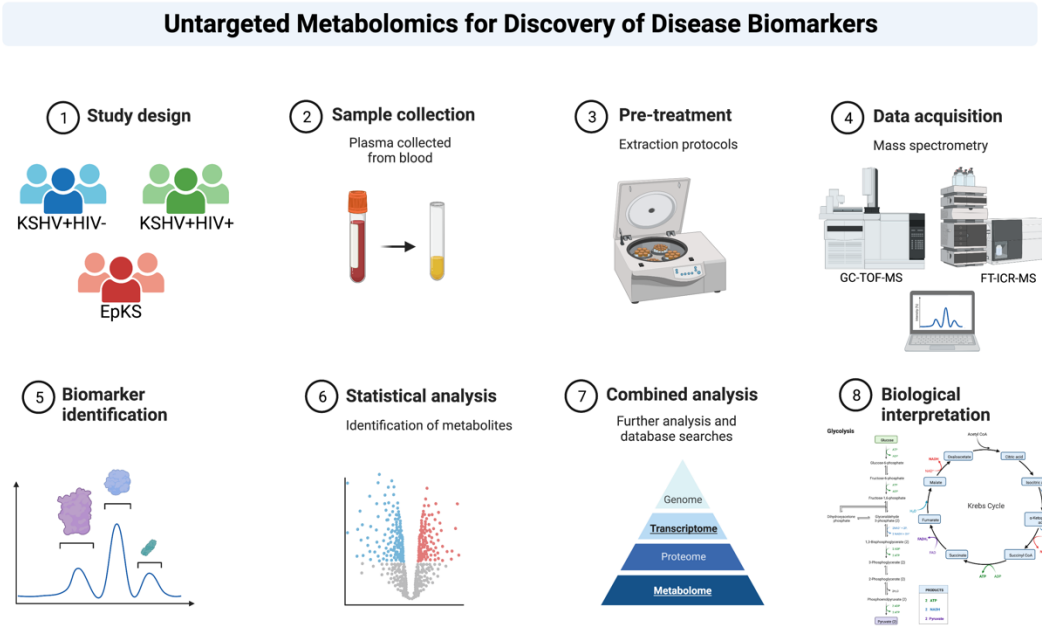

Figure 3.1. Overview of project design. The 22 individuals were divided into ASY KSHV+HIV- (N=6), ASY KSHV+HIV+ (N=7), and SYM EpKS (N=9) groups. Metabolites were extracted from plasma, acquired by GC-TOF-MS and FT-ICR-MS, and then analyzed for biological relevance.

An initial analysis evaluating technical variation showed well-defined clusters of QC samples for both LC- and GC-MS platforms and indicated good reproducibility and reliability of generated data (Figure 3.2 A and B, respectively). Further analyses were therefore carried out without QC samples. PCA plots of lipid and polar metabolites

revealed separation between the KS group and asymptomatic groups (Figure 3.3 A and B). Further clustering analysis showed a well-defined separation between the KS and the asymptomatic individuals in both the lipid and polar metabolites (Figure 3.3 C and D). Interestingly, two KSHV+/HIV+ samples (21579 and 21580), clustered with SYM samples in lipid analysis. This may reflect the transition from asymptomatic to symptomatic presentation. Consistent with previous transcriptomic profiling, the two EnKS cases clustered within the EpKS profiles suggesting the plasma metabolite profile is driven primarily by the symptomatic KS disease presentation as opposed to HIV infection status. However, the small sample number prevented us from conducting statistically valid pairwise comparisons between EnKS and EpKS samples. Despite their overall similarity, to avoid potential confusion, the EnKS metabolite profiles have been excluded from analyses hereafter and we will only present EpKS analysis.

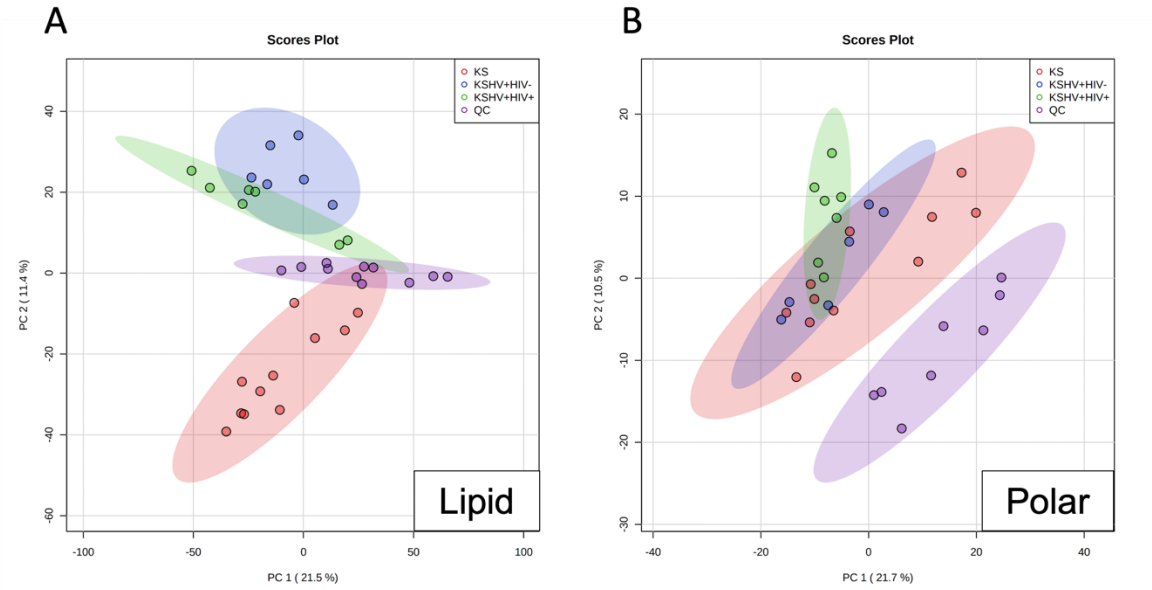

Figure 3.2. PCA plots demonstrating QC sample (purple) separation from symptomatic and asymptomatic individuals.

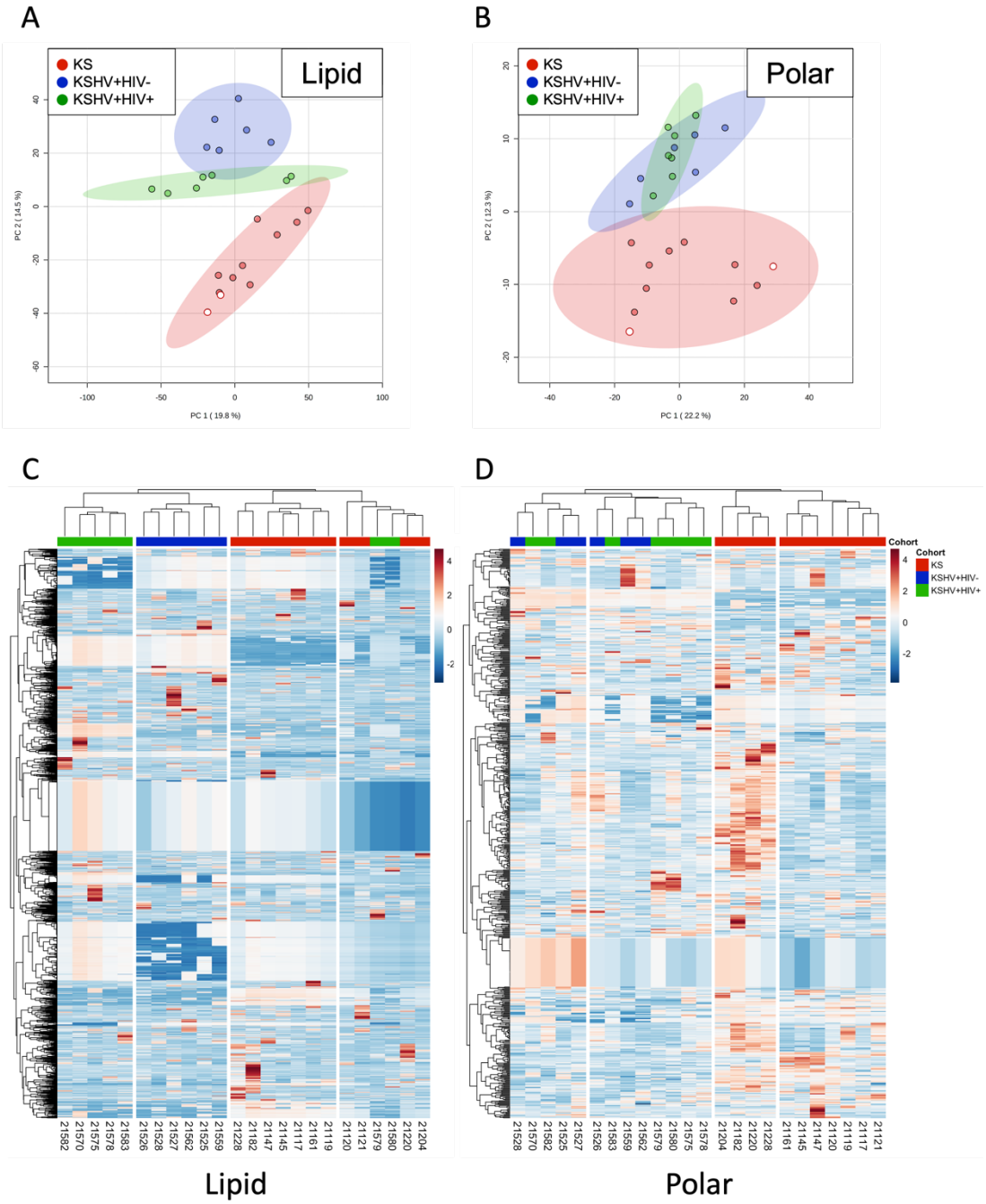

Figure 3.3. Plasma samples from KS patients are different from KSHV-infected asymptomatic controls. A. PCA analysis of the lipid profiles and B. polar metabolites, from all three groups reveal segregation of the KS subjects' metabolites. C. Hierarchal

clustering and heatmaps of all detected lipids, and D. All detected polar metabolites using Pearson Coefficient and complete clustering. Red, KS cohort; blue, KSHV+HIV- cohort; green, KSHV+HIV+ cohort. Endemic KS cases (HIV-negative) are indicated in the PCA plots by open red circles.

Analysis of Differential Polar Profiles

In asymptomatic KSHV-infected individuals, factors such as HIV co-infection increase the risk of progressing to malignancy (EpKS). Multivariate analysis of $KSHV^{+}HIV^{+}$ vs $KSHV^{+}HIV^{-}$ showed partial segregation between groups for polar features (Figure 3.4 A) suggesting a relatively minor impact of HIV+ coinfection on changes in overall profiles. Wilcoxon rank-sum tests, however, revealed 55 significantly changed polar features underlying the segregation between the $KSHV^{+}HIV^{+}$ and $KSHV^{+}HIV^{-}$ groups (p-value <0.05) with a fold change of -0.585< or >0.585. Of the 55 identified features, only 12 could be confirmed using the Fiehn database for GC-MS. Of the 12 discriminant features, 4 metabolites were upregulated in the context of HIV co-infection, and 8 were decreased (Table 3.2).

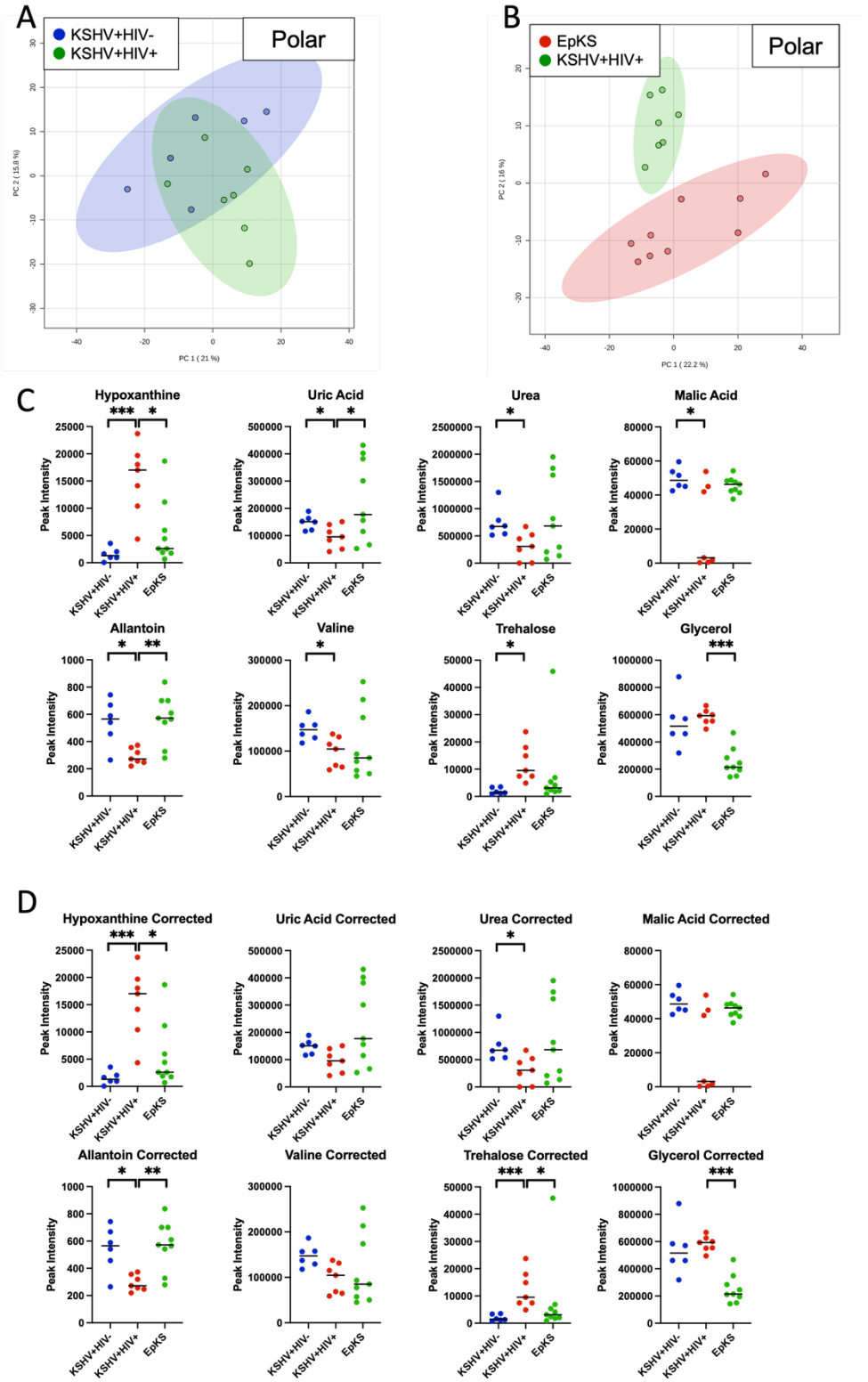
A
KSHV+HIV-
KSHV+HIV+
Polar
PC 1 (21 %)
PC 2 (15.8 %)
B
EpKS
KSHV+HIV+
Polar
PC 1 (22.2 %)
PC 2 (16 %)
C
Hypoxanthine
Uric Acid
Urea
Malic Acid
Allantoin
Valine
Trehalose
Glycerol
Peak Intensity
KSHV+HIV-
KSHV+HIV+
EpKS
D
Hypoxanthine Corrected
Uric Acid Corrected
Urea Corrected
Malic Acid Corrected
Allantoin Corrected
Valine Corrected
Trehalose Corrected
Glycerol Corrected

Figure 3.4. Pair-wise comparisons reveal differential features driving segregation. A. Separation of polar metabolite profiles between KSHV+HIV- and KSHV+HIV+ cohorts. B. Polar metabolite profiles of EpKS and KSHV+HIV+ cohorts separate completely. C. Wilcoxon rank-sum tests of 8 selected differential metabolites without Bonferroni corrections. D. Wilcoxon rank-sum tests of 8 selected differential metabolites with Bonferroni corrections. Upon correction, uric acid and valine were no longer significantly different despite showing significance in the uncorrected analysis. Red, KS cohort; blue, KSHV+HIV- cohort; green, KSHV+HIV+ cohort. *P<0.05, **P<0.01, ***P<0.001.

To investigate whether plasma metabolite differentials were evident between symptomatic EpKS and asymptomatic $KSHV^{+}HIV^{+}$ co-infection, an unsupervised PCA analysis was performed (Figure 3.4 B). The resulting separate clusters indicate significant changes in polar metabolic profiles based on the transition from co-infection to symptomatic disease. This segregation was confirmed by pairwise analysis (Wilcoxon rank-sum tests) that revealed 89 significantly different polar features. These included 14 metabolites that were identifiable and confirmed using the Fiehn database, 9 of which were upregulated in EpKS and 5 were downregulated. The most differential identified metabolite was glycerol which is central in both carbohydrate and lipid metabolism (Table 3.2).

Table 3.2. Differentially identified metabolites for the two pair-wise comparisons. Analysis was performed using Wilcoxon Rank-Sum tests.

Metabolite Name	**KSHV+HIV+/KSHV+HIV-**	**EpKS/KSHV+HIV+**
	p-value	***p-value***
Serine	0.001	-
Decanoic acid	0.014	-
Urea	0.014	-
Valine	0.022	-
4-Hydroxyphenylacetic acid	0.035	-

Bicine	0.035	-
Malic acid	0.035	-
Glycerol	-	0.001
Dehydroabietic acid	-	0.001
Benzoic acid	-	0.012
Citramalic acid	-	0.012
Palmitic acid	-	0.012
Fumaric acid	-	0.023
Heptadecanoic acid	-	0.031
Cerotinic acid	-	0.042
Hypoxanthine	0.001	0.016
Trehalose	0.001	0.016
Allantoin	0.014	0.003
Pyrophosphate Meox2	0.022	0.023
Uric acid	0.022	0.042

Combined results from both comparisons revealed 20 significantly differential and identifiable polar metabolites, 7 of which were attributable to the presence/absence of HIV co-infection (the $KSHV^{+}HIV^{+}$ vs $KSHV^{+}HIV^{-}$ comparison), and another 8 that were differential based on the presence or absence of neoplastic disease (the EpKS vs $KSHV^{+}HIV^{+}$ comparison). 5 differential polar metabolites were common to both comparisons suggesting interconnectivity between co-infection-associated metabolic changes and pathways involved in KSHV tumorigenesis. Distribution and trends of the most relevant metabolites for both groups are shown in Figure 3.4 C and D indicating an important role of purine metabolism in both ASY KSHV infection and KS tumorigenesis.

Analysis of Differential Lipid Profiles

Multivariate analysis of lipid metabolites showed well-defined clustering in both $KSHV^{+}HIV^{-}$ *vs*. $KSHV^{+}HIV^{+}$ and $KSHV^{+}HIV^{+}$ *vs*. EpKS comparisons (Figure 3.5 A and B, respectively). Because the signal was collected in MS-only mode, no structural details are available and potential metabolite ID(s) can only be reported by atomic composition without specific details of side chain length, double bond position, or similar. Tentative identification of individual features was done by matching measured m/z with the predicted molecular mass of metabolites in the Human Metabolome Database (HMDB). For some features, multiple IDs corresponded and therefore these features are designated as molecular classes rather than specific compounds. Using this approach, a total of 204 and 229 differential lipids between KSHV+HIV+ and KSHV+HIV-, and between EpKS and KSHV+HIV+ individuals, respectively, were tentatively identified/classified. These represent 32 different lipid classes as summarized in Figure 3.5 C. Although some of these classes are plant specific, they are listed as they can reflect dietary and/or lipid uptake specifics or potentially reflect the known impact of HIV on gut integrity and microbial translocation that presumably also applies to metabolite translocation.

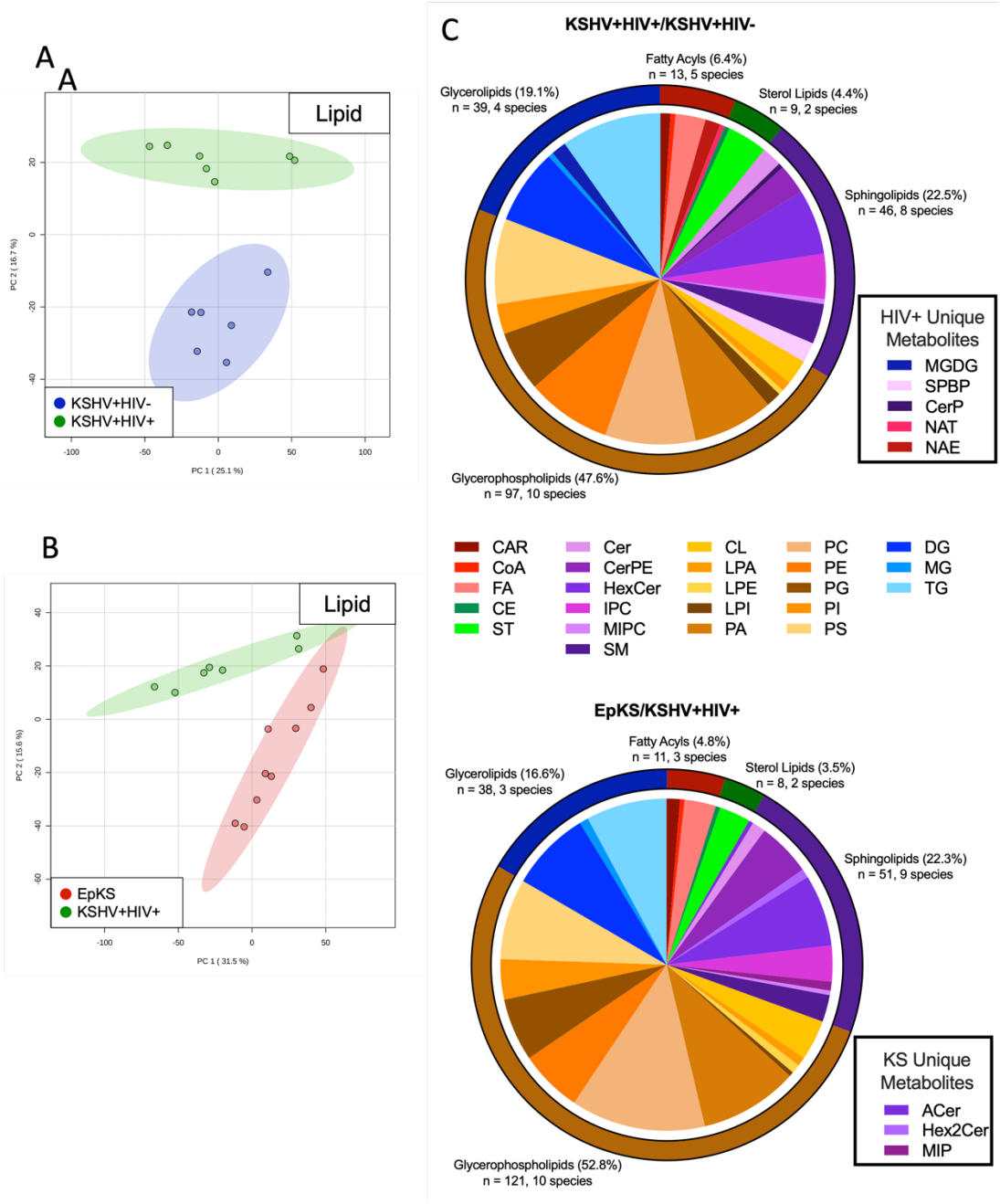

Figure 3.5. A pairwise comparison of lipid profiles highlights both common and distinct differential lipid families. PCA plots of lipid metabolite profiles between A. KSHV+HIV- and KSHV+HIV+ cohorts and B. EpKS and KSHV+HIV+ cohorts showing complete separation. Red, KS cohort; blue, KSHV+HIV- cohort; green, KSHV+HIV+ cohort. C. Breakdown of differential lipid metabolites from both pairwise comparisons. Each wedge represents a lipid class. Comparison unique metabolites are highlighted in the boxes to the right.

Because of the seminal roles sphingolipids and glycerophospholipids play in viral structure, replication cycles, viral curvature, viral assembly, and viral entry into target cells, the dynamics of their metabolites are of particular interest in KSHV infection and disease. While the number of identified sphingolipids was not different between comparisons, monogalactosyldiacylglycerols (MGDG), sphingoid base-phosphates (SPBP), and ceramide-phosphates (CerP) were differential in the asymptomatic comparison but acyl ceramides (ACer), dihexosylceramides (Hex2Cer), and Mannosyl-phosphoramides (MIP) replaced these as differential families in the KS vs. KSHV+HIV+ comparison. The proportion of dysregulated glycerophospholipids increased in neoplasia but not in response to HIV co-infection. Interestingly, one of the highly differential molecules for both comparisons is cardiolipin, indicating a potential impact on mitochondrial membranes and their integrity in either immune cells or potentially affected tissue (31).

Correlation between identified metabolites and KS transcriptomics

In previously published work, both glycolysis and lipid metabolism pathways were highly dysregulated at the transcriptomic level (13). We next integrated our transcriptomic and metabolomic data to evaluate the extent to which dysregulated gene expression in KS tumor tissue was being reflected in plasma metabolite profiles and to gain preliminary insight into the potentially dysregulated pathways. For this analysis, the differential polar metabolites from the EpKS vs. KSHV+HIV+ comparison were analyzed in conjunction with all cellular transcripts evincing > 2-fold differential

expression between KS tumor and normal uninvolved skin in comparisons from 24 individuals (N=1104 transcripts). KEGG pathway analysis revealed the most correlative, dysregulated pathways to be amino acid synthesis, purine, and pyruvate metabolism (Figure 3.6 A). A more detailed analysis revealed a combination of up-and down-regulated metabolites and genes (Figure 3.6 B), particularly in the metabolism of uric acid, that may be explained by the downregulation of purine nucleoside phosphorylase (*PNP)*, the enzyme which breaks down hypoxanthine.

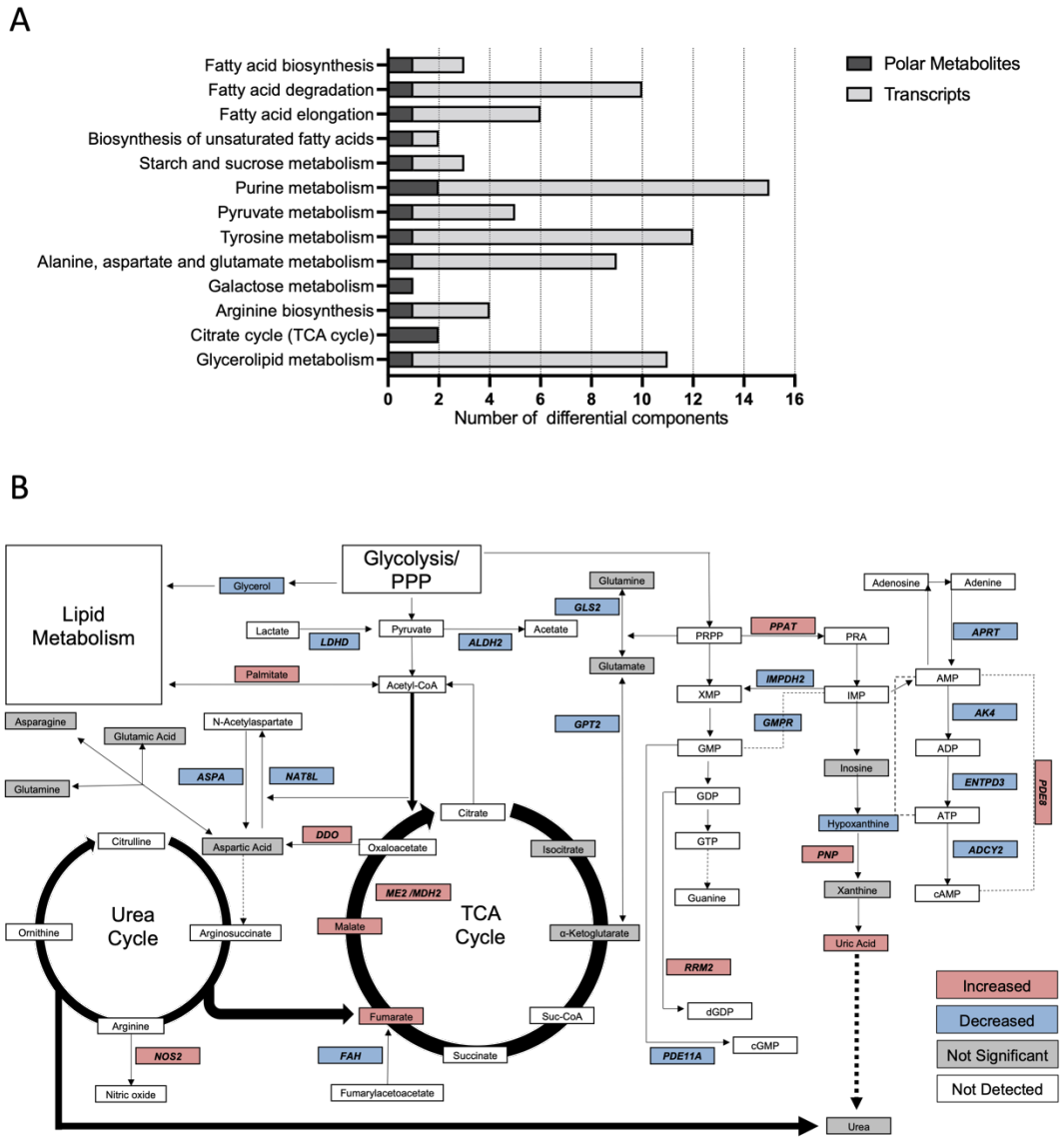

Figure 3.6. Pathway analysis integrating expression differentials from KS transcriptomics with differential polar metabolites between KS and KSHV+HIV+ individuals. For visualization purposes, the authors have focused on pathways in which both genes and metabolites were identified to link metabolic and gene expression phenotypes. A. Pathway analyses were completed using the MetaboAnalyst Joint Pathway Analysis tool in Metaboanalyst v5.0 (27). For metabolomics data, identified metabolites with a minimum FC of 2 (FC>2 or <0.5) and a raw p-value < 0.05 were used for pathway analyses. Included transcriptomics data was derived from a previously published report in which the transcriptomic profile of healthy skin was compared to cutaneous KS lesions (14). B. A summary of significantly changed genes and metabolites within central carbon, purine, and urea metabolism is depicted. Genes and metabolites related to lipid

metabolism have not been included due to redundancy and space limits. Red and blue colored boxes indicate increased and decreased detection, respectively, while grey boxes indicate metabolites that were detected in this study but were not significantly different. Genes are bold and italicized.

Discussion

In this study, plasma provides a partial, albeit dilute, conduit of information that reflects to some extent the pathogenesis associated-metabolic profiles of KSHV-affected cells and tissue(s). Overall, distinct metabolic profiles from each of the three experimental groups were identified with a clear separation between symptomatic and asymptomatic individuals. Most of the differential features were identified from the lipid (non-polar) fraction suggesting significant effects in lipid metabolism, a finding consistent with the highly dysregulated pathways highlighted from transcriptomics of KS tumors (13). Although the lipidomics method employed here could not reveal the exact structures of these featured molecules, the molecular mass of precursor ions and retention time were used to identify their atomic composition and lipid classes. We are using this preliminary data to reduce the complexity of future KSHV/KS lipid analyses that would also include tumor tissue and employ a more targeted $MS^{-}MS$ approach that would support complete characterization. Glycerophospholipids and sphingolipids represented more than 75% of the differential lipids (Figure 3.6). In cancer, lipid metabolism plays a crucial role in membrane rearrangement, energy production, and signaling molecules, and cancer cells are well known for their increased uptake, scavenging, and *de novo* synthesis leading to the presence of unusual and/or exogenous lipids (32). This is reflected by the identification of 229 differential lipids in KS samples

indicating increased uptake and *de novo* synthesis. However, transcriptomics suggested a profound downregulation in most lipid pathways including anabolic, catabolic, and lipid storage domains. Thus, the metabolomic data may imply more of a lipid scavenging role of the KS tumor regarding lipid utilization, especially since the tumor cells are not robustly replicating KSHV and therefore are not likely producing lipids in an effort to support viral assembly components. Additionally, MIP was detected in KS samples which can be indicative of dysregulated signaling pathways such as the phosphoinositide 3-kinase-protein kinase B (PI3K–AKT) pathway and can directly affect the activity of lipogenic enzymes and thus the lipid composition, particularly phosphatidylinositol (PI) (33, 34). Increased lipogenesis can be also suggested by decreased levels of glycerol which together with glycerol-3-P represents an essential precursor for glycerophospholipids biogenesis. In fact, Villumsen et al. found differential diglyceride (DG) and triglyceride (TG) metabolites associated with metabolism disorders within HIV-infected individuals, supporting our findings that HIV infection and subsequent tumorigenesis both alter the plasma lipidome (35).

The polar fraction was analyzed by GC-MS, allowing in some cases to support the confirmed identification of altered metabolic features. Many changes were related to energy/redox balance and purine metabolism both of which converge to support low-level viral replication and cancerous growth due to metabolic reprogramming (36). Within the purine metabolism pathway, hypoxanthine and uric acid were significantly affected by cancer development where hypoxanthine was decreased, and uric acid was

significantly increased in the EpKS group. This correlates with the previous finding of 13 dysregulated genes from those pathways identified by transcriptomic analysis (Figure 3.6). Other studies have also identified decreased levels of hypoxanthine as being indicative of cancer progression in colorectal cancer and lung cancer (37, 38).

Reprogramming of energy metabolism and redox balance are hallmarks of tumorigenesis in general (39). High demand for ATP and increased levels of reactive oxygen species (ROS), together with hypoxic conditions in tumor tissue, lead to the Warburg effect, a balancing act involving glycolysis generating ATP, and the Pentose Phosphate Pathway (PPP) maintaining reducing power together with supplying precursors for purine metabolism (36). Cancer cells exhibit higher levels of ROS production and consequently increased levels of ROS scavenging (40). Trehalose, detected as differentially increased in KSHV+/HIV+ versus KSHV+HIV- plasma, is well known for its antioxidant properties with anti-inflammatory and cancer-inhibitory effects (41). In addition, it targets and inhibits the mTOR pathway, thereby inducing autophagy and reducing viral entry in human primary macrophages and CD4+ T cells (41). The increase of trehalose in KSHV+/HIV+ and a slight increase in EpKS samples compared to KSHV+/HIV- samples may reflect an attempt to limit HIV infection, but since trehalose cannot be synthesized by human metabolism, its levels must reflect an HIV-associated availability which may be associated with loss of gut integrity (42). In EpKS, the trehalose levels could be decreased by its utilization in tumor energy metabolism and attempted redox balance.

The Warburg effect as induced by viral infections and cancer can also induce metabolic reprogramming that manifests in changes to TCA cycle flux. The respective increases of plasma malate, fumarate (Figure 3.6), and the gene for malate dehydrogenase 2 *(MDH2)* in EpKS are suggestive of increased anaplerotic flux into the TCA cycle. KSHV-infected endothelial cells were shown to have increased glutamine uptake which is required for glutaminolysis as it feeds a-ketoglutarate to the TCA cycle which promotes alternative energy production in cancer cells (21, 43). This appeared to accompany transcriptomic changes in glutamine metabolism (Figure 3.6), which has been suggested by others in KSHV in vitro infections (23). Because the Warburg effect results in the preferential production of lactate, the TCA cycle must derive its intermediates from alternative sources such as amino acids. Interestingly, lactate is inhibitory to T cell infiltration and function, which is consistent with the poor infiltration of CD8+ T cells that we have previously reported in KS tissues (44). However, as a function of chemoattractant chemokines by those same tissues, CD8 T cells are found on KS tumor margins (16), so it will be important in future studies using KS tissue to investigate the levels of lactate accumulation in correlation with lymphocyte infiltrations.

Purine metabolism is commonly dysregulated in viral infection and cancer as both conditions require increased nucleotide availability to sustain growth, replication, and survival (45). Indeed, nucleotide metabolism has long been an antiviral and antineoplastic therapeutic target (45). However, this shared characteristic may have

different metabolic underpinnings depending on latency, the presence of coinfections, and if/when KSHV progresses to KS. The opposing patterns observed in the mono-infection, coinfection, and KS progression comparisons may be attributed to competition for metabolic resources between infected cells, cancer cells, infected transformed cells, and normal cells. Chang et al. reported a metabolic competition for glucose between T cells and cancer cells in a mouse model of sarcoma that aided cancer progression (46). Similar patterns may be evident in the opposing hypoxanthine and uric acid patterns from the KSHV+/HIV- vs. KSHV+/HIV+ and EpKS vs. KSHV+/HIV+ comparisons. This is also supported by changes in allantoin, an oxidation product (non-enzymatic in humans) of uric acid, where we observed low levels in KSHV+/HIV+ and equal levels in KSHV+HIV- and EpKS. In the KSHV+/HIV- vs. KSHV+/HIV+ comparison, the increase in hypoxanthine and decrease in uric acid may indicate increased purine salvage. This was demonstrated by Vastag et al., who showed that pyrimidine metabolites peaked around 12 hours post HSV1 infection followed by a decrease (47). Elevated serum uric acid has been correlated with increased inflammation in cohort studies (48, 49). In KSHV+/HIV+ vs. EpKS comparison, the increase in *PNP* in tumors and uric acid in plasma may indicate increased inflammation, promoting tumorigenesis (50). Alternatively, the ability of uric acid to act as an antioxidant may serve to protect cancer cells, as it is well established that the increased metabolic requirements of tumor microenvironments produce higher levels of ROS (50). This increased metabolic rate is also suggested by the elevation in several TCA cycle genes and metabolites.

The patients' diet likely played a large role in which metabolites were detectable. During the statistical analysis, we identified citramalic acid as being increased in EpKS compared to the KSHV+/HIV+ group. Citramalic acid is a metabolite that does not typically appear in human metabolic studies; however, it is associated with eating or drinking fruit-based products or alcoholic beverages, as it is part of fermentation. Additionally, a study investigating the effects of chemotherapy on the plasma metabolome in breast cancer patients before and after chemotherapy found a loose association with lipid dysregulation and increased detection of citramalic acid (51). This supports what we have seen in KS where there is an abundance of lipid dysregulation observed in both the tumor transcriptome and the plasma metabolome. The difference in diets also posed a problem related to controls for this study, as we had initially included uninfected blood donors, albeit from the United States. Initial statistical analysis of this group compared to the KSHV+/HIV- group presented with over 100 differential metabolites, a result that indicated that our groups were far too different to be justifiably compared. Further studies with a larger cohort will be needed to investigate the importance of such rare metabolites and the overall impact of KSHV infection alone.

One final important aspect of KSHV/KS metabolic reprogramming is using amino acids as a source of energy and nitrogen. Of these, decreased valine was evident in KSHV+/HIV+ and even more in EpKS. Valine is a Branched-Chain Amino Acid (BCAA) that can be converted into Acetyl-CoA and further metabolized in the TCA cycle or diverted

as a precursor in lipogenesis. It is also a major nitrogen source for glutamine synthesis. As an essential amino acid, levels of valine reflect protein digestion, degradation, and uptake of amino acids. Decreasing levels in EpKS suggest increased cellular biogenesis and energy needs in neoplasia. Interestingly, another product of protein degradation, urea, exhibited decreased levels in KSHV+/HIV+ but returned to the KSHV+/HIV- levels in EpKS. This might be explained by reprogramming to maximize the utilization of nitrogen for anabolic macromolecule synthesis in tumorigenesis.

Conclusions

Overall, our data speak to discernable plasma metabolic differentials between KSHV infection and co-infection with HIV, as well as to plasma metabolites that mark the progression from co-infection to neoplastic growth of cutaneous KS tumors. These differentials reside in both polar and non-polar metabolites and show discrete linkages to transcriptomic dysregulation, likely as a function of dilution, as might be expected from plasma sampling tissue metabolites from the entirety of the human body. Unfortunately, our small sample sizes and the unavailability of normal healthy controls from Tanzania made it difficult to control for some confounding factors such as diet, lifestyle, or additional co-infections; however, we were able to demonstrate that there are changes in the overall metabolic profiles of KSHV-infected ASY and SYM individuals. Future studies will attempt to separate more generalized neoplastic markers (those present in any cancer, or any cancer with infectious etiology) from markers that may be specific for KS disease progression. Plasma lipid metabolites and their role as potential

biomarkers will need further refinement in coupled tissue and plasma analyses now that we have identified rationally targeted pathways and features. Similarly, we hope to be able to focus future investigations on more targeted polar metabolite biomarkers using the refined focus generated here, and coupled tumor, plasma, and perhaps other bodily fluid specimens.

Acknowledgments

The authors acknowledge all participants of this study and the supporting clinical and laboratory staff at the Ocean Road Cancer Institute where participants were recruited.

References

1. Chang Y, Cesarman E, Pessin MS, Lee F, Culpepper J, Knowles DM, et al. Identification of herpesvirus-like DNA sequences in AIDS-associated Kaposi's sarcoma. Science. 1994;266(5192):1865-9.

2. Moore PS, Chang Y. Detection of herpesvirus-like DNA sequences in Kaposi's sarcoma in patients with and those without HIV infection. N Engl J Med. 1995;332(18):1181-5.

3. Moore PS, Chang Y. Kaposi's sarcoma (KS), KS-associated herpesvirus, and the criteria for causality in the age of molecular biology. Am J Epidemiol. 1998;147(3):217-21.

4. Cesarman E, Damania B, Krown SE, Martin J, Bower M, Whitby D. Kaposi sarcoma. Nat Rev Dis Primers. 2019;5(1):9.

5. Grabar S, Costagliola D. Epidemiology of kaposi’s sarcoma. Cancers2021.

6. Castilho JL, Kim A, Jenkins CA, Grinsztejn B, Gotuzzo E, Fink V, et al. Antiretroviral therapy and Kaposi's sarcoma trends and outcomes among adults with HIV in Latin America. J Int AIDS Soc. 2021;24(1):e25658.

7. Friedman-Kien AE. Disseminated Kaposi's sarcoma syndrome in young homosexual men. Journal of the American Academy of Dermatology. 1981;5(4):468-71.

8. Friedman-Kien AE, Saltzman BR, Cao YZ, Nestor MS, Mirabile M, Li JJ, et al. Kaposi's sarcoma in HIV-negative homosexual men. Lancet. 1990;335(8682):168-9.

9. Grulich AE, Vajdic CM. The epidemiology of cancers in human immunodeficiency virus infection and after organ transplantation. Semin Oncol. 2015;42(2):247-57.

10. Mesri EA, Cesarman E, Boshoff C. Kaposi's sarcoma and its associated herpesvirus. Nat Rev Cancer. 2010;10(10):707-19.

11. Bower M, Dalla Pria A, Coyle C, Andrews E, Tittle V, Dhoot S, et al. Prospective stage-stratified approach to AIDS-related Kaposi's sarcoma. J Clin Oncol. 2014;32(5):409-14.

12. Ngalamika O, Munsaka S, Lidenge SJ, West JT, Wood C. Antiretroviral Therapy for HIV-Associated Cutaneous Kaposi's Sarcoma: Clinical, HIV-Related, and Sociodemographic Predictors of Outcome. AIDS Res Hum Retroviruses. 2021;37(5):368-72.

13. Tso FY, Kossenkov AV, Lidenge SJ, Ngalamika O, Ngowi JR, Mwaiselage J, et al. RNA-Seq of Kaposi's sarcoma reveals alterations in glucose and lipid metabolism. PLoS Pathog. 2018;14(1):e1006844.

14. Lidenge SJ, Kossenkov AV, Tso FY, Wickramasinghe J, Privatt SR, Ngalamika O, et al. Comparative transcriptome analysis of endemic and epidemic Kaposi's sarcoma (KS) lesions and the secondary role of HIV-1 in KS pathogenesis. PLoS Pathog. 2020;16(7):e1008681.

15. Gothland A, Jary A, Grange P, Leducq V, Beauvais-Remigereau L, Dupin N, et al. Harnessing Redox Disruption to Treat Human Herpesvirus 8 (HHV-8) Related Malignancies. Antioxidants (Basel). 2022;12(1).

16. Lidenge SJ, Tso FY, Ngalamika O, Kolape J, Ngowi JR, Mwaiselage J, et al. Lack of CD8(+) T-cell co-localization with Kaposi's sarcoma-associated herpesvirus infected cells in Kaposi's sarcoma tumors. Oncotarget. 2020;11(17):1556-72.

17. Lidenge SJ, Tso FY, Ngalamika O, Ngowi JR, Mortazavi Y, Kwon EH, et al. Similar Immunological Profiles Between African Endemic and Human Immunodeficiency Virus Type 1-Associated Epidemic Kaposi Sarcoma (KS) Patients Reveal the Primary Role of KS-Associated Herpesvirus in KS Pathogenesis. J Infect Dis. 2019;219(8):1318-28.

18. Lidenge SJ, Tso FY, Mortazavi Y, Ngowi JR, Shea DM, Mwaiselage J, et al. Viral and Immunological Analytes are Poor Predictors of the Clinical Treatment Response in Kaposi's Sarcoma Patients. Cancers (Basel). 2020;12(6).

19. Delgado T, Sanchez EL, Camarda R, Lagunoff M. Global metabolic profiling of infection by an oncogenic virus: KSHV induces and requires lipogenesis for survival of latent infection. PLoS Pathog. 2012;8(8):e1002866.

20. Lagunoff M. Activation of cellular metabolism during latent Kaposi's Sarcoma herpesvirus infection. Current Opinion in Virology2016.

21. Sanchez EL, Pulliam TH, Dimaio TA, Thalhofer AB, Delgado T, Lagunoff M. Glycolysis, Glutaminolysis, and Fatty Acid Synthesis Are Required for Distinct Stages of Kaposi's Sarcoma-Associated Herpesvirus Lytic Replication. J Virol. 2017;91(10).

22. Delgado T, Carroll PA, Punjabi AS, Margineantu D, Hockenbery DM, Lagunoff M. Induction of the Warburg effect by Kaposi's sarcoma herpesvirus is required for the

maintenance of latently infected endothelial cells. Proc Natl Acad Sci U S A. 2010;107(23):10696-701.

23. Sanchez EL, Carroll PA, Thalhofer AB, Lagunoff M. Latent KSHV Infected Endothelial Cells Are Glutamine Addicted and Require Glutaminolysis for Survival. PLoS Pathog. 2015;11(7):e1005052.

24. Pluskal T, Uehara T, Yanagida M. Highly accurate chemical formula prediction tool utilizing high-resolution mass spectra, MS/MS fragmentation, heuristic rules, and isotope pattern matching. Anal Chem. 2012;84(10):4396-403.

25. Lai Z, Tsugawa H, Wohlgemuth G, Mehta S, Mueller M, Zheng Y, et al. Identifying metabolites by integrating metabolome databases with mass spectrometry cheminformatics. Nat Methods. 2018;15(1):53-6.

26. Li B, Tang J, Yang Q, Cui X, Li S, Chen S, et al. Performance Evaluation and Online Realization of Data-driven Normalization Methods Used in LC/MS based Untargeted Metabolomics Analysis. Sci Rep. 2016;6:38881.

27. Pang Z, Chong J, Zhou G, de Lima Morais DA, Chang L, Barrette M, et al. MetaboAnalyst 5.0: narrowing the gap between raw spectra and functional insights. Nucleic Acids Res. 2021;49(W1):W388-W96.

28. Kind T, Wohlgemuth G, Lee DY, Lu Y, Palazoglu M, Shahbaz S, et al. FiehnLib: mass spectral and retention index libraries for metabolomics based on quadrupole and time-of-flight gas chromatography/mass spectrometry. Anal Chem. 2009;81(24):10038-48.

29. Wishart DS, Feunang YD, Marcu A, Guo AC, Liang K, Vazquez-Fresno R, et al. HMDB 4.0: the human metabolome database for 2018. Nucleic Acids Res. 2018;46(D1):D608-D17.

30. Chong J, Soufan O, Li C, Caraus I, Li S, Bourque G, et al. MetaboAnalyst 4.0: towards more transparent and integrative metabolomics analysis. Nucleic Acids Res. 2018;46(W1):W486-W94.

31. Paradies G, Paradies V, Ruggiero FM, Petrosillo G. Role of Cardiolipin in Mitochondrial Function and Dynamics in Health and Disease: Molecular and Pharmacological Aspects. Cells. 2019;8(7).

32. Bian X, Liu R, Meng Y, Xing D, Xu D, Lu Z. Lipid metabolism and cancer. J Exp Med. 2021;218(1).

33. Noorolyai S, Shajari N, Baghbani E, Sadreddini S, Baradaran B. The relation between PI3K/AKT signalling pathway and cancer. Gene. 2019;698:120-8.

34. Cirone M. Cancer cells dysregulate PI3K/AKT/mTOR pathway activation to ensure their survival and proliferation: mimicking them is a smart strategy of gammaherpesviruses. Critical Reviews in Biochemistry and Molecular Biology2021.

35. Olund Villumsen S, Benfeitas R, Knudsen AD, Gelpi M, Hogh J, Thomsen MT, et al. Integrative Lipidomics and Metabolomics for System-Level Understanding of the Metabolic Syndrome in Long-Term Treated HIV-Infected Individuals. Front Immunol. 2021;12:742736.

36. Ali ES, Ben-Sahra I. Regulation of nucleotide metabolism in cancers and immune disorders. Trends Cell Biol. 2023.

37. Long Y, Sanchez-Espiridion B, Lin M, White L, Mishra L, Raju GS, et al. Global and targeted serum metabolic profiling of colorectal cancer progression. Cancer. 2017;123(20):4066-74.

38. Zhao F, An R, Wang L, Shan J, Wang X. Specific Gut Microbiome and Serum Metabolome Changes in Lung Cancer Patients. Front Cell Infect Microbiol. 2021;11:725284.

39. Dai X, Wang D, Zhang J. Programmed cell death, redox imbalance, and cancer therapeutics. Apoptosis. 2021;26(7-8):385-414.

40. Vladimirova O, Soldan S, Su C, Kossenkov A, Ngalamika O, Tso FY, et al. Elevated iNOS and 3'-nitrotyrosine in Kaposi's Sarcoma tumors and mouse model. Tumour Virus Res. 2023;15:200259.

41. N SNC, Devi A, Sahu S, Alugoju P. Molecular mechanisms of action of Trehalose in cancer: A comprehensive review. Life Sci. 2021;269:118968.

42. Somsouk M, Estes JD, Deleage C, Dunham RM, Albright R, Inadomi JM, et al. Gut epithelial barrier and systemic inflammation during chronic HIV infection. AIDS. 2015;29(1):43-51.

43. Wang Z, Liu F, Fan N, Zhou C, Li D, Macvicar T, et al. Targeting Glutaminolysis: New Perspectives to Understand Cancer Development and Novel Strategies for Potential Target Therapies. Front Oncol. 2020;10:589508.

44. Watson MJ, Vignali PDA, Mullett SJ, Overacre-Delgoffe AE, Peralta RM, Grebinoski S, et al. Metabolic support of tumour-infiltrating regulatory T cells by lactic acid. Nature. 2021;591(7851):645-51.

45. Ariav Y, Ch'ng JH, Christofk HR, Ron-Harel N, Erez A. Targeting nucleotide metabolism as the nexus of viral infections, cancer, and the immune response. Sci Adv. 2021;7(21).

46. Chang CH, Qiu J, O'Sullivan D, Buck MD, Noguchi T, Curtis JD, et al. Metabolic Competition in the Tumor Microenvironment Is a Driver of Cancer Progression. Cell. 2015;162(6):1229-41.

47. Vastag L, Koyuncu E, Grady SL, Shenk TE, Rabinowitz JD. Divergent effects of human cytomegalovirus and herpes simplex virus-1 on cellular metabolism. PLoS Pathog. 2011;7(7):e1002124.

48. Lyngdoh T, Marques-Vidal P, Paccaud F, Preisig M, Waeber G, Bochud M, et al. Elevated serum uric acid is associated with high circulating inflammatory cytokines in the population-based Colaus study. PLoS One. 2011;6(5):e19901.

49. Spiga R, Marini MA, Mancuso E, Di Fatta C, Fuoco A, Perticone F, et al. Uric Acid Is Associated With Inflammatory Biomarkers and Induces Inflammation Via Activating the NF-kappaB Signaling Pathway in HepG2 Cells. Arterioscler Thromb Vasc Biol. 2017;37(6):1241-9.

50. Perillo B, Di Donato M, Pezone A, Di Zazzo E, Giovannelli P, Galasso G, et al. ROS in cancer therapy: the bright side of the moon. Exp Mol Med. 2020;52(2):192-203.

51. Lyon DE, Starkweather A, Yao Y, Garrett T, Kelly DL, Menzies V, et al. Pilot Study of Metabolomics and Psychoneurological Symptoms in Women With Early Stage Breast Cancer. Biol Res Nurs. 2018;20(2):227-36.

CHAPTER 4

CYTOKINE AND METABOLITE PROFILING OF KSHV SEROPOSITIVE PATIENTS WITH AND WITHOUT KS

Kaposi Sarcoma (KS) is a multifaceted disease caused by Kaposi Sarcoma-associated herpesvirus (KSHV) infection, or human herpesvirus 8 (HHV-8) (1). It presents a pressing need for further research due to its complex nature and ongoing clinical significance, specifically in sub-Saharan Africa where seroprevalence can exceed 90% in some countries. (1-5) KSHV belongs to the family Herpesviridae, which includes over 200 enveloped, double-stranded DNA viruses (6). Of these, KSHV stands out as one of the few that can lead to cancer in humans, although the mechanism of tumorigenesis has yet to be discovered. The virus mainly infects B cells, endothelial cells, epithelial cells, dendritic cells, and monocytes (7).

KSHV has a similar life cycle as other herpesviruses, characterized by latency and occasional lytic reactivation. Only a subset of viral proteins is expressed during latency, ensuring the virus's persistence within the host (1, 8, 9). Key latency proteins, such as latency-associated nuclear antigen (LANA) play crucial roles in tethering the viral genome to the host chromosome. Lytic reactivation, when it occurs, involves the expression of numerous viral genes, and leads to the production of infectious virus particles. The associated pathologies of KSHV infection include Kaposi Sarcoma, Multicentric Castleman's Disease (MCD), Pulmonary Effusion Lymphoma (PEL), and KSHV Inflammatory Cytokine Syndrome (KICS). Kaposi Sarcoma, with its distinctive

purple or red lesions, is the most well-known manifestation. It presents in various forms, including Classical KS, Endemic KS, Epidemic KS, and Iatrogenic KS, each with different risk factors and epidemiological distributions (1).

KSHV seroprevalence varies globally, with hotspots in regions like sub-Saharan Africa, South America, and parts of Asia. HIV co-infection significantly increases the risk of developing KS. However, the exact role of HIV in KS tumorigenesis is still not fully understood (1, 10-12). KS lesions are highly angiogenic, characterized by spindle-shaped cells, and the cellular origin of these tumor cells is still under investigation. They express markers typically associated with endothelial cells and mesenchymal stem cells (13-16).

The immune response to KSHV infection is complex. Both the innate and adaptive immune systems are involved in responding to the virus. Despite the increased production of T cell signaling cytokines like CXCL9, CXCL10, and CXCL11 within KS lesions, there is limited T cell infiltration, suggesting barriers to an effective T cell response (17-21). Here, we sought to investigate the state of plasma immune cytokine and metabolomic profiles in a large cohort of 58 Zambian individuals with and without KS to identify changes and potential signatures of the disease. The plasma may be reflective of the state of the periphery rather than the tumor itself; however, our preliminary data (data not shown) has suggested that plasma and tumor metabolic profiles are overlapping. Previous studies showed a lack of immune cell infiltration into KS tumors, the plasma cytokine profile may reflect potential reasons for this deficit of active T cells (18).

Here, we further investigate the relationship between plasma cytokines and metabolites in KSHV-positive patients with and without disease. Previous transcriptomic research in KS lesions identified increased T cell related proliferation and homing cytokines as well as dysregulation in many cellular metabolic processes including glucose metabolism, amino acid synthesis, and lipid synthesis In this study, cytokines associated with immune cell migration and replication were upregulated and amino acid synthesis was highly dysregulated in KS patients' plasma, which is similar to what our lab has previously found in KS lesion transcriptomics and plasma metabolomics (17, 20). The study described below revealed little correlation between cytokine or metabolic profiles which differed from what was observed in the KS lesion transcriptomics, suggesting the need for further studies of the KS lesions themselves rather than the circulating plasma.

Methods

Patient Recruitment

Approval to conduct this study was obtained from the review boards of Tanzania National Institute for Medical Research, Ocean Road Cancer Institute, the University of Zambia Biomedical Research Ethics Committee; the University of Nebraska-Lincoln (UNL) and the Louisiana State University Health Sciences Center-New Orleans' IRBs. Sample collection for this study was as described in Lidenge et al. (2020). Informed consent was obtained from all subjects involved in the study.

Olink Proteomics

As described in Bennett et al, 50uL of patient plasma were subjected to the Olink Target 96 Inflammation Panel. Briefly, plasma samples were randomly distributed into a 96-well plate, and the plate was sealed, frozen, and sent to Olink for a proximity extension assay. The assay provided normalized expression values (NPX) for each protein in the panel. Eight "bridge" samples were used to combine data from two plates, and the NPX values were bridge normalized using the Olink Analyze R package. Subsequent data analysis and visualization were performed using GraphPad Prism v9.3.1. Gene Ontology (GO) Enrichment Analysis was conducted for subsets of inflammatory mediators with specific conditions, and the most specific subclass of results was recorded from the analysis.

Metabolic Profiling

Plasma samples were analyzed as described in Chapter 3 (Privatt et al). Briefly, 20µL of plasma was collected from each individual to generate polar and non-polar metabolite fractions. Methanol and ribitol (used as an internal standard) were added to each plasma sample, followed by mixing and incubation. The samples were then centrifuged to separate polar and non-polar phases. The extracted polar metabolites were dried and prepared for GC-MS analysis, while the non-polar lipid metabolites were dried and dissolved in methanol for LC-MS analysis. Quality control samples and blanks were prepared for both platforms, and samples were analyzed in random order.

The lipid profiling was conducted using an HPLC system coupled to a high-resolution/accuracy mass spectrometer. Samples were injected onto a column, and

lipids were separated in a linear gradient elution. Data was collected in positive mode over a specific m/z range. The acquired data was processed with software tools like CompassXport and mzMine for peak detection, deconvolution, normalization, and alignment.

For polar metabolite analysis, dried samples were derivatized, and then MS acquisitions were performed using a GC-QTOF system with a specific column and temperature gradient. Data was converted and processed by MS-Dial. The generated data files included information about m/z values, retention times, and peak areas for each feature.

Statistical Analysis

Data analysis involved various statistical methods, including multivariate and univariate analyses. Heatmaps, principal component analysis (PCA), Kruskal-Wallace analysis, and volcano plots were used to visualize and compare data between different groups. Metabolites were tentatively identified using databases like the Fiehn database search and the Human Metabolome Database (HMDB). KEGG IDs were obtained for identified metabolites to analyze affected pathways. Additive counting was used when multiple ions were annotated to the same feature.

Results

Cohort Characteristics

58 participants from Zambia were recruited for this study and were divided into three groups: KSHV+HIV+ (N=23), EpKS (N=32), and EnKS (N=3) (Figure 4.1 A). The ages

of the KSHV+HIV+ group were significantly higher than the EpKS group at 40.9 years old on average as compared to 34.6 years old respectively (Figure 4.1 B). It is also important to emphasize that the KSHV+HIV+ group is split evenly between males and females, but the EpKS group is predominantly male, as is representative of the epidemiology of KS disease. 3 EnKS patients were recruited for this study, however, the small sample numbers rendered it impossible to statistically compare to the other groups. All 58 patients were included in the plasma metabolomics experiment and a subset of 47 patients (15 KSHV+HIV+ and 32 EpKS) were included in the plasma cytokine experiment.

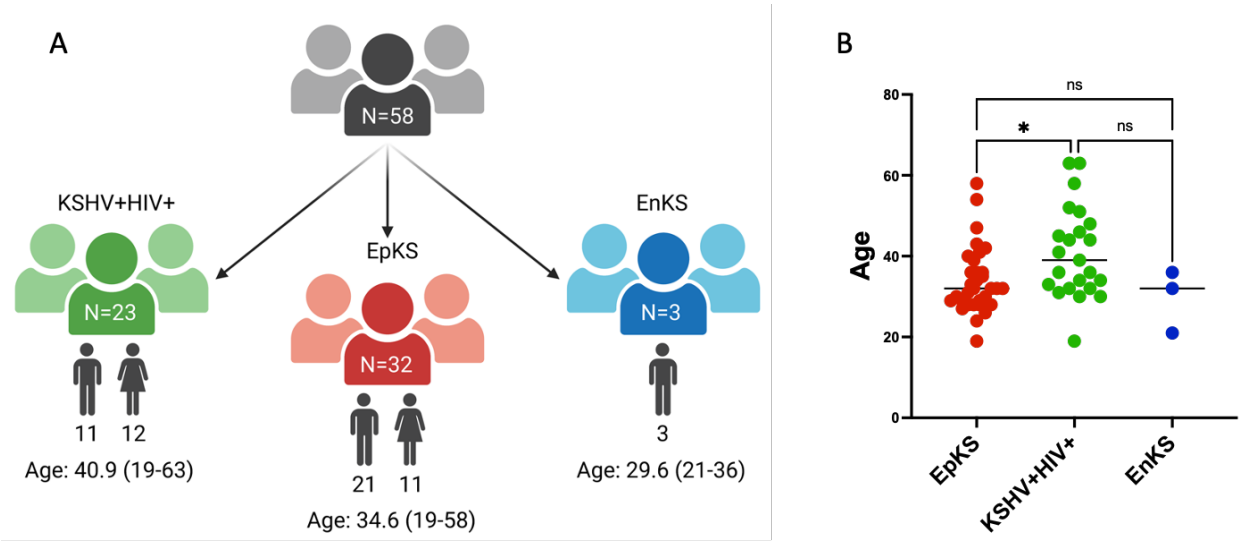

Figure 4.1. Cohort Characteristics. 58 individuals were segregated into three groups based on disease status: KSHV+HIV+, EpKS, and EnKS. The KSHV+HIV+ group was significantly older than either symptomatic group. The significance level is $p < 0.05$ *.

Plasma cytokines show increased immune cell migration and cell proliferation in EpKS patients

Utilizing the Olink Target 96 Inflammation Panel to detect up to 92 cytokines in human plasma, 74 different cytokines passed QC analysis and were used to compare 15

KSHV+HIV+ and 32 EpKS individuals. The cytokine profiles segregate into 3 distinct groups with mixtures of EpKS and KSHV+HIV+ individuals (Figure 4.2 A and B). However, group 2 is predominantly KSHV+HIV+ with only 4 EpKS. This group, in general, had lower levels of cytokines detected as compared to groups 1 and 3 which are made up of mostly EpKS individuals. KS disease presence is the only cofactor that correlates with cytokine segregation, as all other characteristics including age, gender, and CD4 count are evenly mixed. The partial separation of the KSHV+HIV+ and EpKS individuals can also be seen in the PCA plot, where KSHV+HIV+ samples cluster together with some overlap with EpKS.

When we compared the cytokine profiles of KSHV+HIV+ samples to EpKS, there were 30 out of 72 differential cytokines, 6 of which were downregulated. Unsurprisingly, the pathways that were upregulated in EpKS patients were related to immune cell migration for neutrophils, granulocytes, and lymphocytes largely associated with the upregulation of VEGF-A, INF-gamma, and CXCL5 as well as T cell signaling cytokines CXCL9, 10 and 11 (Figure 4.2 C). Several pathways related to cell proliferation were also upregulated as IL18, IL12b, SLAMF1, and CD274 were upregulated in KS. In conclusion, the cytokine profiles of KSHV+HIV+ and EpKS individuals are distinct and highlight changes in immune cell signaling suggesting global increases in immune cell proliferation and homing to infected sites; however, further studies with larger sample numbers and a more comprehensive cytokine panel are needed for better understanding of the systemic changes EpKS individuals are undergoing.

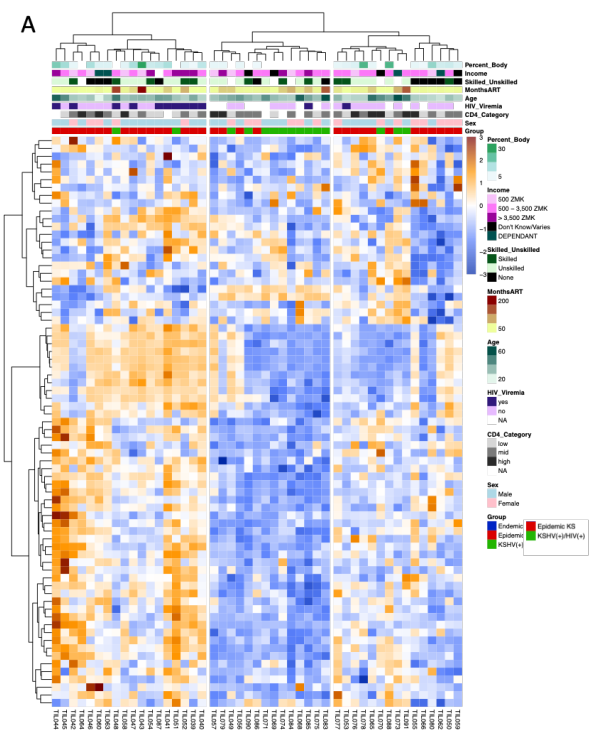

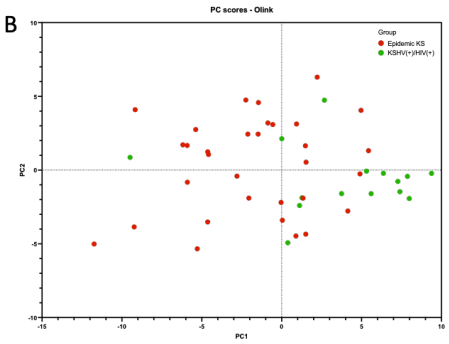

C

PANTHER GO-Slim Biological Process	Fold Enrichment	raw P value	FDR
antimicrobial humoral immune response mediated by antimicrobial peptide	> 100	5.84E-13	3.81E-11
neutrophil migration	> 100	8.45E-20	2.68E-17
granulocyte chemotaxis	> 100	1.26E-19	3.11E-17
cellular response to lipopolysaccharide	> 100	4.03E-14	3.89E-12
extrinsic apoptotic signaling pathway via death domain receptors	73.53	4.32E-04	1.08E-02
response to interleukin-1	71.49	1.51E-08	6.56E-07
cellular response to tumor necrosis factor	70.19	5.36E-10	2.83E-08
lymphocyte migration	57.19	1.05E-06	4.25E-05
regulation of angiogenesis	54.18	7.52E-04	1.70E-02
cytokine-mediated signaling pathway	49.02	3.41E-20	1.51E-17
inflammatory response	44.44	7.11E-17	1.13E-14
positive regulation of ERK1 and ERK2 cascade	43.81	2.84E-06	1.09E-04
ERK1 and ERK2 cascade	42.02	3.31E-06	1.23E-04
lymphocyte activation involved in immune response	41.18	1.25E-03	2.66E-02
regulation of lymphocyte proliferation	35.5	1.65E-03	3.35E-02
positive regulation of cell population proliferation	22.63	3.40E-05	1.06E-03
positive regulation of GTPase activity	15.48	1.41E-04	3.97E-03
positive regulation of protein phosphorylation	14.5	1.80E-04	4.95E-03
cell population proliferation	14.3	2.80E-05	9.02E-04
innate immune response	12.68	4.90E-05	1.47E-03
positive regulation of lymphocyte activation	11.7	2.27E-03	4.27E-02

Figure 4.2. Immune cytokine profiles show increased immune cell replication and migration signals. A. Hierarchal clustering revealed three distinct groups independent of KS status. B. PCA plot demonstrated little group separation of asymptomatic (green) and symptomatic (red) individuals. C. Upregulated cytokine pathways in KS patients.

<u>EpKS samples have increased dysregulation of amino acid metabolism compared to KSHV+HIV+</u>

Our lab also previously reported on the dysregulation of glucose metabolism and lipid synthesis based on bulk transcriptomic analysis of Kaposi Sarcoma lesions as well as the plasma metabolic profiles of a small Tanzanian cohort where we observed dysregulation of amino acid synthesis. Here, we utilized a cohort of 55 KSHV+ individuals with and without KS disease to further explore the effects of cancer development on systemic metabolites in a larger cohort of mixed genders. Unlike what was observed in Privatt et al (Chapter 3), asymptomatic and symptomatic individuals did not segregate

(Figure 4.3 A and B). The lack of segregation could be attributed to several different factors including sample handling and longer storage times, regional differences in diet or lifestyle between Zambia and Tanzania which has been shown to affect the quality of samples in studies related to metabolites (22). Future studies with more stringent study design to include patient fasting and consistent sample collection scheduling will be needed.

The metabolic profiles did separate into three distinct groups, however, there was no correlation to disease state, age, gender, HIV viremia, or any of the additional clinical characteristics analyzed. This clear discrepancy between the cohorts analyzed here and our previous study will require further research as there is no obvious difference other than sample size and recruitment location. There were still some similarities between the two studies. There were 35 differential metabolites between EpKS and KSHV+HIV+ samples; metabolites such as urea, glutamine, glutamate, and creatinine are involved in amino acid synthesis pathways for glutamine, glutamate, alanine, and aspartate, among others which were reflective of our conclusions from Privatt et al (Figure 4.3 C). Notably, urea and uric acid were also differential in this cohort and were dysregulated in KS patients.

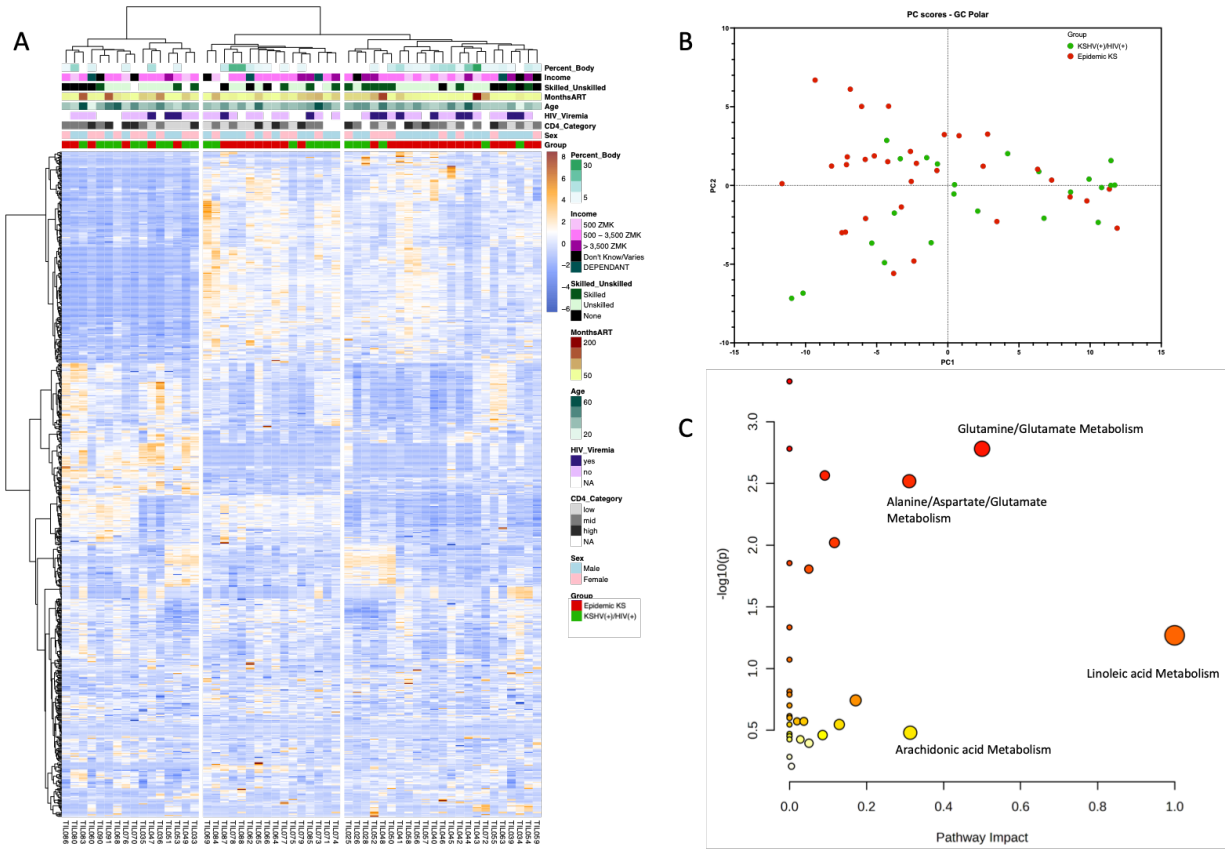

Figure 4.3. Polar metabolite profiles reveal changes in amino acid synthesis in EpKS patients. A. Hierarchal clustering revealed three distinct groups independent of KS status. B. PCA plot demonstrated little group separation of asymptomatic (green) and symptomatic (red) individuals. C. Dysregulated metabolic pathways in KS patients.

Conclusions

In this study, the analysis of plasma cytokines revealed distinct immune cell responses in EpKS patients compared to those with KSHV+HIV+. The data showed that cytokine profiles could differentiate between these two groups, with a partial overlap between them. Notably, the cytokine patterns in EpKS patients were associated with increased immune cell migration, particularly for neutrophils, granulocytes, and lymphocytes, as well as enhanced cell proliferation pathways. This is reflected by the

upregulation of T cell associated cytokines CXCL9, 10, and 11 as well as the upregulation of CXCL5 and CXCL8 which are associated with neutrophil migration. This suggests that EpKS individuals experience systemic changes in immune cell signaling, reflecting the impact of the disease. However, further investigations with larger sample sizes and a more comprehensive cytokine panel are essential for a more detailed understanding of these systemic alterations.

Additionally, the study highlighted increased dysregulation of amino acid metabolism in EpKS patients compared to KSHV+HIV+ individuals, consistent with previous findings, underscoring the importance of amino acid synthesis pathways in the context of EpKS. In this cohort, the separation between asymptomatic and symptomatic individuals was less pronounced than what was observed in Privatt et al. We hypothesize that changes in sample collection, storage, and shipment from Zambia to the US in addition to potential regional differences in diet could have impacted this difference. Additional differences between experiments could be due to changes in personnel executing the mass-spectrometry machinery. While both the cytokine and metabolites revealed three distinct groups regardless of KS status, there was no correlation between the two experiments, suggesting little correlation between plasma cytokines and metabolic profiles. Further studies focusing on the KS tumors themselves in comparison with plasma will be required to elucidate the precise mechanisms underlying these metabolic and cytokine changes and their implications for the disease

as the initial transcriptomic studies that suggested a connection were performed in KS tumors.

References

1. Cesarman E, Damania B, Krown SE, Martin J, Bower M, Whitby D. Kaposi sarcoma. Nat Rev Dis Primers. 2019;5(1):9.

2. Vladimirova O, Soldan S, Su C, Kossenkov A, Ngalamika O, Tso FY, et al. Elevated iNOS and 3'-nitrotyrosine in Kaposi's Sarcoma tumors and mouse model. Tumour Virus Res. 2023;15:200259.

3. Motlhale M, Sitas F, Bradshaw D, Chen WC, Singini MG, de Villiers CB, et al. Epidemiology of Kaposi's sarcoma in sub-Saharan Africa. Cancer Epidemiol. 2022;78:102167.

4. Ragi SD, Moseley I, Ouellette S, Rao B. Epidemiology and Survival of Kaposi's Sarcoma by Race in the United States: A Surveillance, Epidemiology, and End Results Database Analysis. Clin Cosmet Investig Dermatol. 2022;15:1681-5.

5. Grabar S, Costagliola D. Epidemiology of kaposi’s sarcoma. Cancers2021.

6. Liu L. Fields Virology, 6th Edition. Clinical Infectious Diseases. 2014;59(4):613-.

7. van der Meulen E, Anderton M, Blumenthal MJ, Schafer G. Cellular Receptors Involved in KSHV Infection. Viruses. 2021;13(1).

8. Sandhu PK, Damania B. The regulation of KSHV lytic reactivation by viral and cellular factors. Current Opinion in Virology2022.

9. Broussard G, Damania B. Regulation of KSHV Latency and Lytic Reactivation. Viruses2020.

10. Ngalamika O, Munsaka S, Lidenge SJ, West JT, Wood C. Antiretroviral Therapy for HIV-Associated Cutaneous Kaposi's Sarcoma: Clinical, HIV-Related, and Sociodemographic Predictors of Outcome. AIDS Res Hum Retroviruses. 2021;37(5):368-72.

11. Castilho JL, Kim A, Jenkins CA, Grinsztejn B, Gotuzzo E, Fink V, et al. Antiretroviral therapy and Kaposi's sarcoma trends and outcomes among adults with HIV in Latin America. J Int AIDS Soc. 2021;24(1):e25658.

12. Dandachi D, Morón F. Effects of HIV on the Tumor Microenvironment. Advances in Experimental Medicine and Biology. 12632020.

13. Naipauer J, Mesri EA. The Kaposi's sarcoma progenitor enigma: KSHV-induced MEndT-EndMT axis. Trends Mol Med. 2023;29(3):188-200.

14. Ding Y, Chen W, Lu Z, Wang Y, Yuan Y. Kaposi's sarcoma-associated herpesvirus promotes mesenchymal-to-endothelial transition by resolving the bivalent chromatin of PROX1 gene. PLoS Pathog. 2021;17(9):e1009847.

15. Choi D, Park E, Kim KE, Jung E, Seong YJ, Zhao L, et al. The Lymphatic Cell Environment Promotes Kaposi Sarcoma Development by Prox1-Enhanced Productive Lytic Replication of Kaposi Sarcoma Herpes Virus. Cancer Res. 2020;80(15):3130-44.

16. Bruce AG, Barcy S, DiMaio T, Gan E, Garrigues HJ, Lagunoff M, et al. Quantitative Analysis of the KSHV Transcriptome Following Primary Infection of Blood and Lymphatic Endothelial Cells. Pathogens. 2017;6(1).

17. Privatt SR, Braga CP, Johnson A, Lidenge SJ, Berry L, Ngowi JR, et al. Comparative polar and lipid plasma metabolomics differentiate KSHV infection and disease states. Cancer Metab. 2023;11(1):13.

18. Lidenge SJ, Tso FY, Ngalamika O, Kolape J, Ngowi JR, Mwaiselage J, et al. Lack of CD8(+) T-cell co-localization with Kaposi's sarcoma-associated herpesvirus infected cells in Kaposi's sarcoma tumors. Oncotarget. 2020;11(17):1556-72.

19. Lidenge SJ, Tso FY, Mortazavi Y, Ngowi JR, Shea DM, Mwaiselage J, et al. Viral and Immunological Analytes are Poor Predictors of the Clinical Treatment Response in Kaposi's Sarcoma Patients. Cancers (Basel). 2020;12(6).

20. Lidenge SJ, Kossenkov AV, Tso FY, Wickramasinghe J, Privatt SR, Ngalamika O, et al. Comparative transcriptome analysis of endemic and epidemic Kaposi's sarcoma (KS) lesions and the secondary role of HIV-1 in KS pathogenesis. PLoS Pathog. 2020;16(7):e1008681.

21. Tso FY, Kossenkov AV, Lidenge SJ, Ngalamika O, Ngowi JR, Mwaiselage J, et al. RNA-Seq of Kaposi's sarcoma reveals alterations in glucose and lipid metabolism. PLoS Pathog. 2018;14(1):e1006844.

22. Smith L, Villaret-Cazadamont J, Claus SP, Canlet C, Guillou H, Cabaton NJ, et al. Important Considerations for Sample Collection in Metabolomics Studies with a Special Focus on Applications to Liver Functions. Metabolites. 2020;10(3).

CHAPTER 5

OTHER WORKS: LONGITUDINAL QUANTIFICATION OF ADENOVIRUS NEUTRALIZING RESPONSES IN ZAMBIAN MOTHER-INFANT PAIRS: IMPACT OF HIV-1 INFECTION AND ITS TREATMENT

Abstract

Vaccination offers the most cost-effective approach to limiting the adverse impact of infectious and neoplastic diseases that reduce the quality of life in sub-Saharan Africa (SSA). However, it is unclear what vaccine vectors would be most readily implementable in the setting and at what age they should be applied for maximal efficacy. Adenoviruses (Ad) and Ad-based vectors have been demonstrated to induce effective humoral and cellular immune responses in animal models and in humans. However, because immunity associated with Ad infection is lifelong, there exists a debate as to whether pre-existing immunity might decrease the efficacy of Ad vectored vaccines.

To begin to rationally develop vaccination strategies for SSA, we have quantified neutralizing antibodies (nAb) against Ad4, Ad5, Ad7, Ad26, Ad28, Ad45, and Ad48 in 67 adult women and their infants. We are the first to define the decay kinetics of transferred maternal nAb in infants as well as the apparent initiation of *de novo* Ad responses. Our findings demonstrate that in Zambian adults, robust nAb responses exist against each of the Ads tested and are efficiently transferred to newborns. With few exceptions, neither the HIV-1 infection status of the mothers nor the antiretroviral

therapy (ART) treatment of HIV-1 disease had a significant impact on maternal Ad nAb responses or their transfer to infants. However, maternal Ad nAb decays in infants to a nadir at 12 months of age such that any of the seven Ad types could function as vaccine vectors. The definition of this 'window of opportunity' provides important foundational data for rational design and implementation of Ad vectors in this setting.

Introduction

Sub-Saharan Africa (SSA) is disproportionately affected by infectious diseases. The World Health Organization (WHO) has reported that two thirds of people living with HIV are in SSA (1). Similarly, there is increased prevalence of tuberculosis, malaria, and other communicable diseases, as well as higher incidence of infection-related cancers. The incidence of infectious disease associates with significantly higher mortality in comparison to developed regions (2-4). The public health impact of infectious diseases in SSA highlights the need for a more rational appreciation of vaccine designs with potential to reduce the regional disease burden. One important issue with vaccine design is the selection of suitable vector for the delivery of the vaccine, especially for infants in SSA, where effective childhood vaccinations could decrease disease incidence.

One promising investigational vaccine platform is Adenovirus (Ad). Adenoviruses are large double stranded DNA viruses that, through deletion of genetic content and propagation to high titers, can be used as gene-delivery tools or vaccine vectors (5). Historically, Ad vaccines and vectors were replication competent and thus had some risk of causing an Adenoviral infection (6, 7). Modern Ad constructs are typically replication

incompetent or produce single-cycle infections where no new Ad particles are produced but an inserted transgene of interest is efficiently expressed (8). These recombinant Ads have been used developmentally as vectors in many Phase 1 and 2 vaccine safety trials against a diverse cadre of pathogens, including Zika virus, HIV, influenza, and Ebola; however, safety and efficacy have only been demonstrated for non-recombinant vaccines used by the US military against Ad types 4 and 7 (9-16). Adenoviral vaccination typically produces a strong adaptive, Ad serotype-specific immune response (12, 17). The prevalence of pre-vaccination adenovirus-specific immunity needs to be considered when predicting potential efficacy for vaccination in infants and young children. For example, Adenovirus type 5 (Ad5) is commonly used in pre-clinical research and has been tested in human vaccine trials. Unfortunately, Ad5 has high worldwide seroprevalence suggesting that gene-delivery strategies based on that subtype could suffer from decreased effectiveness due to pre-existing neutralizing antibody (nAb) responses to the vector (18, 19). Consistent with this concept, the HIV-1 STEP trial, which utilized an Ad5 backbone to deliver the genes for HIV-1 *ga*g, *pol*, and *nef* proteins as potential immunogens, was prematurely discontinued when a correlation was observed between pre-existing Ad5 immunity and new HIV-1 infections (20). However, data from non-HIV targeted Ad vaccine efforts, as well as studies using other viral vector systems, such as measles or dengue, have demonstrated preclinical and clinical efficacy in the face of pre-existing neutralizing responses (21-24). Thus, the impact of pre-existing Ad nAb on increased infection may be a unique function of HIV biology since it

has not been consistently reported by other groups utilizing various vaccine targets delivered by Ad vectors (24).

There are currently more than 60 serotypes of circulating Ads, separated into 7 subspecies, A-G, with varying geographical prevalence (25). Adenoviruses are categorized based on infection-associated conditions, serology, propensity to cause tumors in rodents, and genome sequence. Here, we focus on the humoral immune responses to Ads from subgroups B, C, D and E. Adenovirus type D is the largest of the subspecies and most newly discovered Ads fit into this category, yet most research has been performed on types B, C, and E (26, 27). Subspecies B, C, and E adenoviruses are typically associated with acute respiratory infections and conjunctivitis which can cause serious disease in immunocompromised individuals (28, 29). However, very little is known about the adenoviral serotypes that are commonly found in Africa, and a better understanding of the existing immune response against adenovirus is important for the designing of vaccine which can be used in the setting. We have included four different type D viruses, Ad26, Ad28, Ad45 and Ad48, to expand on the limited knowledge of this subgroup. These adenovirus subspecies typically associate with respiratory diseases and conjunctivitis in humans and are likely responsible for many of the respiratory infections found in Africa and elsewhere (28, 30).

In the current study, we characterized the humoral immune response against seven different adenovirus serotypes in two Zambian cohorts consisting of mother-infant pairs collected at different time points. Many of the mothers were also HIV-1

infected. Investigation of immune responses in these cohorts will not only provide important information on the circulating adenoviral serotypes and the humoral immune response against adenovirus in the Zambian population, but also provide a better understanding of the pre-existing mother to infant transmission of anti-adenovirus antibodies, and the impact of untreated and treated HIV-1 infection on immune responses to adenoviral infections. Moreover, with the longitudinal infant follow-up specimens, we investigated the decay kinetics of maternal neutralizing antibodies (nAb) in infants and characterized the nadir of Ad seroreactivity prior to *de novo* response in those same infants. This information could form the foundation for rational selection of adenoviral gene delivery platforms for prophylactic or therapeutic application.

Our results suggest that in Zambian adults, pre-existing humoral immunity exists against all 7 Ads tested and is efficiently transferred to newborns. However, due to maternal Ab decay in infants, any of the 7 Ad types could function as vaccine vectors between 12-24 months of age, thereby defining the 'window of opportunity' for use of Ad vectors for vaccination of children in this setting.

Materials and Methods

Cohort description and sampling

Two cohorts were analyzed; the first cohort samples were collected between 1998 and 2003 in the pre-ART era as part of a prospective study investigating the effects of HIV-1 and KSHV infection among Zambian mothers and their infants at the University Teaching Hospital and the University of Zambia School of Medicine, Lusaka, Zambia.

Written informed consent was obtained from all participants. Blood samples were collected by venipuncture and blood was collected in acid citrate dextrose tubes and processed within 6 hours of being drawn. Samples were frozen at -80°C and shipped to the University of Nebraska-Lincoln for long-term storage. Protocols were reviewed and approved by the Institutional Review Boards at the University Teaching Hospital and the University of Nebraska-Lincoln.

The second cohort samples were collected between 2010 and 2013 when ART had become available in Zambia, and they were collected as part of an observational study investigating the effect of ART on KSHV transmission. Women with infants under the age of 12 months were enrolled into this study to examine the determinants of KSHV seroconversion. This study was approved by the Institutional Review Board of the University of Nebraska-Lincoln and the University of Zambia Biomedical Research Ethics Committee. From these cohorts, a subset of 63 mother-infant pairs (MIPs) were selected based on either mother HIV-1 infection status or ART treatment status. MIPs were also selected based on infant follow-up sample availability for nAb testing.

Recombinant Adenovirus Construction

All Ad constructs contain a green fluorescent protein-luciferase (*GFP-Luc*) fusion gene under a CMV promoter within either the *E3* gene or between *E1A* and *E1B*. The recombinant Adenovirus types 4 and 7 contain a *GFPLuc* reporter expression cassette in the *E3* gene and were constructed as described in Weaver, 2014 (31). Recombinant Adenovirus types 26, 28, and 48 construction was described in Weaver and Barry, 2013

(9). Recombinant adenovirus type 45 was produced as previously described (31). The recombinant Ad5-855 virus was constructed as described in [PMID: 10846098].

Recombinant Adenovirus Purification.

The recombinant adenovirus genomes containing the *GFP-Luc* insert were linearized and buffer exchanged using a Strataprep PCR purification kit (Agilent Technologies). The linearized recombinant gDNA was transfected into HEK293T cells using the PolyFect Transfection Reagent (Qiagen). Virus infection was indicated via plaque formation, at which time cells were harvested and infectious progeny virus was released by 3 freeze-thaw cycles. The recombinant Ad was amplified by sequential passages in HEK293T cells prior to final amplification in a Corning 10-cell stack (~6300 cm^2). Amplified virus was purified by two sequential CsCl ultracentrifuge gradients and desalted using Econo-Pac 10DG desalting columns (Bio-Rad). The virus particle quantity was determined by absorption at 260 nm on a NanoDrop Lite Spectrophotometer (Thermo Fisher). Virus aliquots were stored at -80°C in Ad-tris buffer (20 mM Tris-HCl, 100 mM NaCl2, 1 mM MgCl2•6H2O, 10% glycerol). HEK293T cells were grown in Dulbecco's modified Eagle's medium supplemented with 10% heat inactivated FBS and 1% penicillin-streptomycin at 37°C and 5% supplemented CO^2.

Adenovirus Neutralization Assay

Adenovirus-specific nAb activity was quantified by a reduction in luciferase activity. Briefly, maternal or infant sera were heat inactivated at 56°C for 60 minutes. Next, 20µL of serum was added to 380µL of DMEM containing 1.2 x 10^9 viral particles for

a final volume of 400uL, resulting in a final serum dilution of 1:20. The serum/virus mixture was incubated at 37°C for 60 min. 100µL was then added to 50µL of DMEM containing 1 x 10^5 293T cells per well in triplicate in a 96 well plate and allowed to incubate for 24 hours. The luciferase activity was determined using the reporter lysis 5X buffer and luciferase assay reagent (LAR) system (Promega, Madison, WI). 40µL of reporter lysis 5X buffer was added and allowed to incubate at room temperature for 20 min. Neutralization was defined as percent of virus only luciferase readout, which was then subtracted from 100%. We have defined neutralization as >90%, mild neutralization as 70-90% and non-neutralizing as <70%.

Statistical Analysis

Statistical analyses were conducted using GraphPad Prism 7 software. Non-parametric Mann-Whitney tests were used to determine statistical significance. P values ≤ 0.05 were considered statistically significant.

Results

Maternal Neutralizing Antibodies Against Subgroups B, C, E and D Adenoviruses

Adenovirus seroprevalence has not been evaluated in Zambian maternal-infant pairs (MIPs); therefore, the impact of HIV-1 infection, and its treatment with ART, on a) maternal nAb production, b) transfer of nAb to newborns, c) the decay of maternal Ab in neonates, and d) the development of infant *de novo* nAb responses, is incompletely understood. In order to estimate the seroprevalence of adenoviruses in Zambia, we tested 42 women in a pre-ART cohort and 25 women in a post-ART cohort for nAb

against recombinant Ad7 (Group B), Ad5 (Group C) and Ad4 (Group E) containing a *GFPLuc* reporter. Comparison of responses in the two temporally distinct cohorts allowed for evaluation of the change in breadth and magnitude of Ad nAb coincident with ART implementation in the region.

Other groups have defined neutralization with thresholds from 50% up to 90% (25, 32-35). We conservatively defined neutralization as ≥ 90% mean neutralization for n=3 replicates. The number of women who neutralized Ad5 was not significantly different between the pre- and post-ART maternal cohorts, 93% and 88% respectively. The majority of women in the pre-ART cohort (52%) had neutralizing activity exceeding 90% against Ad4 and Ad7. However, only 28% of women in the post-ART cohort exhibited nAb responses against those types. (Figure 5.1).

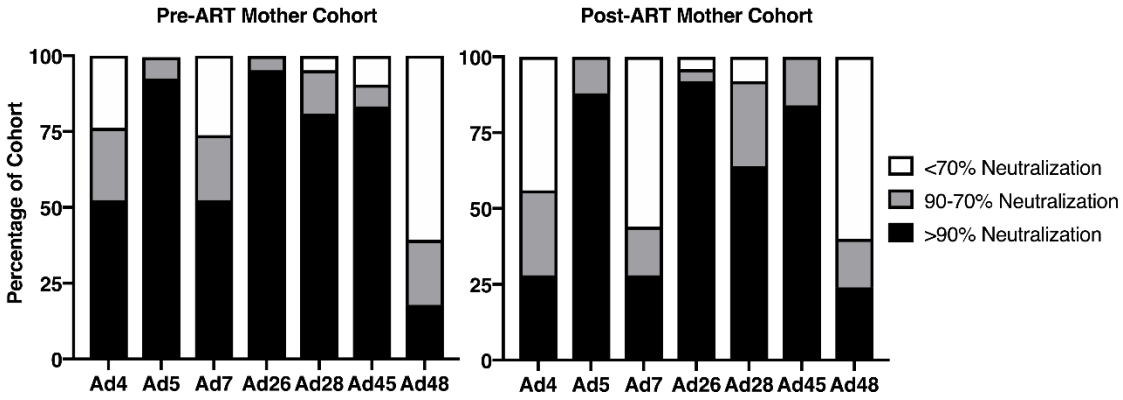

Figure 5.1. Neutralization profile of adult women in Zambia, Africa against Ad4, Ad5, Ad7, Ad26, Ad28 Ad45, and Ad48. 42 serum samples from the pre-ART cohort and 25 samples from the post-ART cohort were evaluated for neutralizing activity against Ad4, Ad5, Ad7, Ad26, Ad28, Ad45, and Ad48 at a 1:30 sera dilution by luciferase-based neutralization assay. Luciferase inhibition indicates viral neutralization by sera. Each sample was placed into one of three categories based on neutralization percentage

compared to virus only samples: >90%, 90-70% or <70% which equates to highly neutralizing, mildly neutralizing, or non-neutralizing, respectively.

Since species D adenoviruses were reported to be frequently isolated from immunosuppressed subjects and those with keratoconjunctivitis (36), and because this group was shown to have lower seroprevalence than Ads B, C, and E in other geographical regions, we tested for seroreactivity against four Group D Ads: Ad26, Ad28, Ad45 and Ad48 (26, 27). Given that these four Ads are members of the same Ad group, we anticipated levels of nAb to be similar in adults. Consistent with this concept, the majority of women in both the pre- and post-ART cohort did neutralize Ad26, Ad28 and Ad45 (Figure 5.1). The exception was Ad48 where less than 25% had detectable nAb (≥ 90%), irrespective of the cohort.

Transfer of Maternal nAb and the Impact of HIV Infection in the pre-ART Cohort

To evaluate patterns of maternal pre- and perinatally nAb transfer to infants, the percent neutralization for each adenovirus was quantified in sera collected from infants in 6-month intervals starting on the day of birth. The MIPs in the pre-ART cohort were recruited between 1998 and 2003, a time when Zambian women did not readily have access to ART treatment. Comparisons of the median nAb responses against each Ad subtype are shown in Figure 5.2 A-B. Median infant nAb responses were significantly lower than maternal against Ad4, Ad7, Ad26, and Ad28. In contrast, similar maternal and infant neutralizing responses were detected against Ad5 and Ad45. The median neutralization activity in infants against Ad5 and Ad45 was 99% and 99%, respectively. Because 4 of 28 maternal sera enhanced infection, median neutralizing activity against

Ad48 was not significantly different between mothers and infants. These findings suggest that pre-existing immunity could lower the effectiveness of a vaccine vectored with Ad5 or Ad45 if administered on the day of birth.

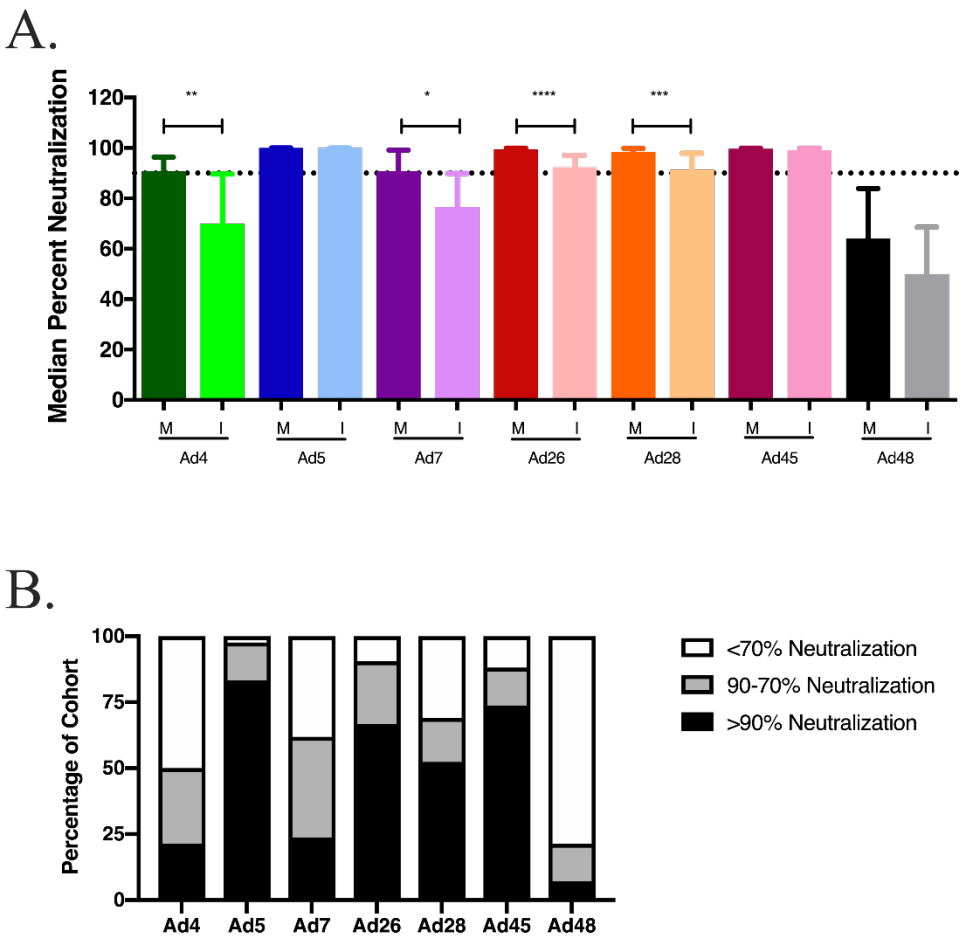

Figure 5.2. Mother-to-infant transfer of neutralizing antibodies in pre-ART cohort. A. Mother to infant nAb transfer in the pre-ART cohort. Neutralizing antibody transfer was evaluated by a comparison of total medians of percent neutralization between mother and infant pairs on day of birth. Statistical significance was determined by non-parametric Mann-Whitney tests. B. Infant neutralization profile in the pre-ART cohort. Each infant sample was placed into one of three categories based on neutralization percentage compared to virus only samples: >90%, 90-70% or <70% which equates to highly neutralizing, mildly neutralizing, or non-neutralizing, respectively. (* $P \leq 0.05$, ** $P \leq 0.01$, *** $P \leq 0.001$, **** $P \leq 0.0001$)

The pre-ART cohort was divided into two groups based on the HIV-1 status of the mothers, while the infants, irrespective of their infection status, were correspondingly grouped with their mothers. No significant difference was seen in overall maternal nAb activity between HIV-1 infected and uninfected women (Figure 5.3). Table 5.1 shows that maternal HIV-1 infection significantly reduced transplacental transfer of Ad nAb only for subtypes Ad7 and Ad26.

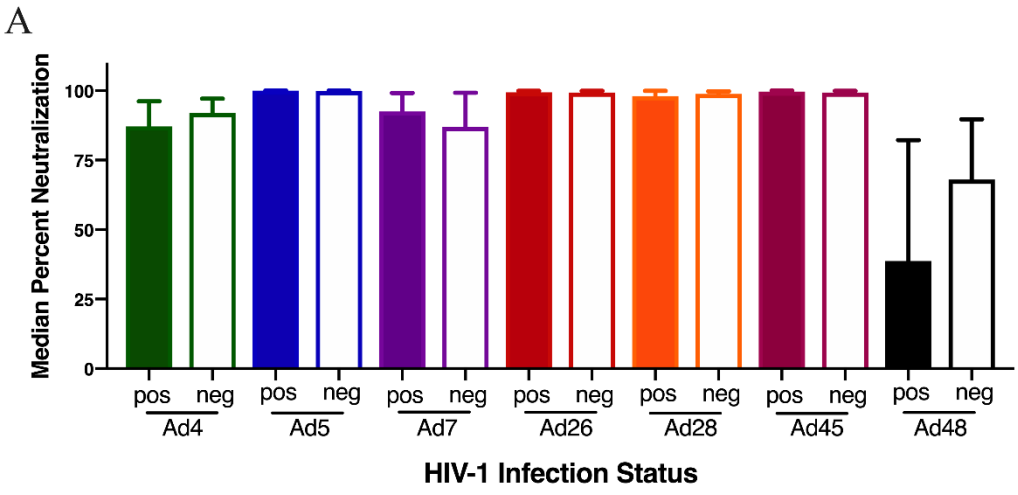

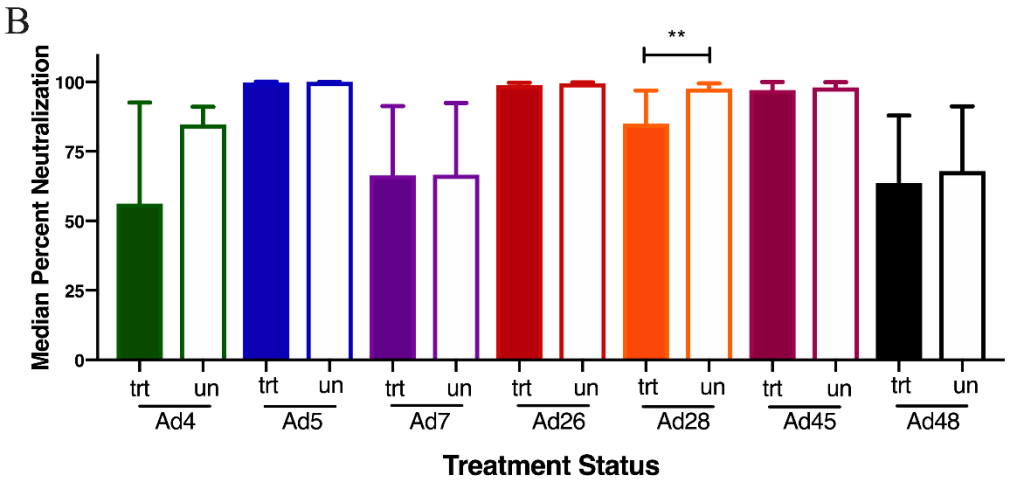

Figure 5.3. Median percentage of neutralization in the mothers against all seven Ads was analyzed for significance based on HIV-1 infection status **(A)** or ART treatment status **(B)**. (** P ≤ 0.01)

Table 5.1. Impact of maternal HIV infection on passive transfer of nAb on day of birth. For each MIP, the percent neutralization of the infant was divided by that of the cognate mother. The average of those ratios is reported for HIV-1 negative mothers (Column 2) versus positive (Column 3). Differences in the average of ratios based on HIV-1 status was statistically evaluated using non-parametric Mann-Whitney tests. A significant difference based on HIV-1 infection status was evident against Ad7 and Ad26. (* P ≤ 0.05)

Adenovirus	HIV-	HIV+	Significance	P-Value
Ad4	0.86	0.96	ns	0.230
Ad5	1.00	1.00	ns	0.914
Ad7	0.95	0.87	*	0.048
Ad26	0.96	0.91	*	0.039
Ad28	0.94	0.94	ns	0.907
Ad45	1.00	0.99	ns	0.995
Ad48	0.63	0.71	ns	0.658

Transfer of Maternal Neutralizing Antibodies and Impact of ART Treatment in post-ART Cohort

In the post-ART cohort, infants received significantly less maternal nAb against all 7 tested adenoviruses compared to the median values from the pre-ART cohort (Figure 5.4 A-B). The highest median neutralization in infants was against Ad5 at 93%, a value significantly lower than that from the pre-ART cohort (99%), but above the neutralization threshold. Median infant neutralizing activity against all other adenoviruses was below 90% and is therefore non-neutralizing or lacking in pre-existing immunity.

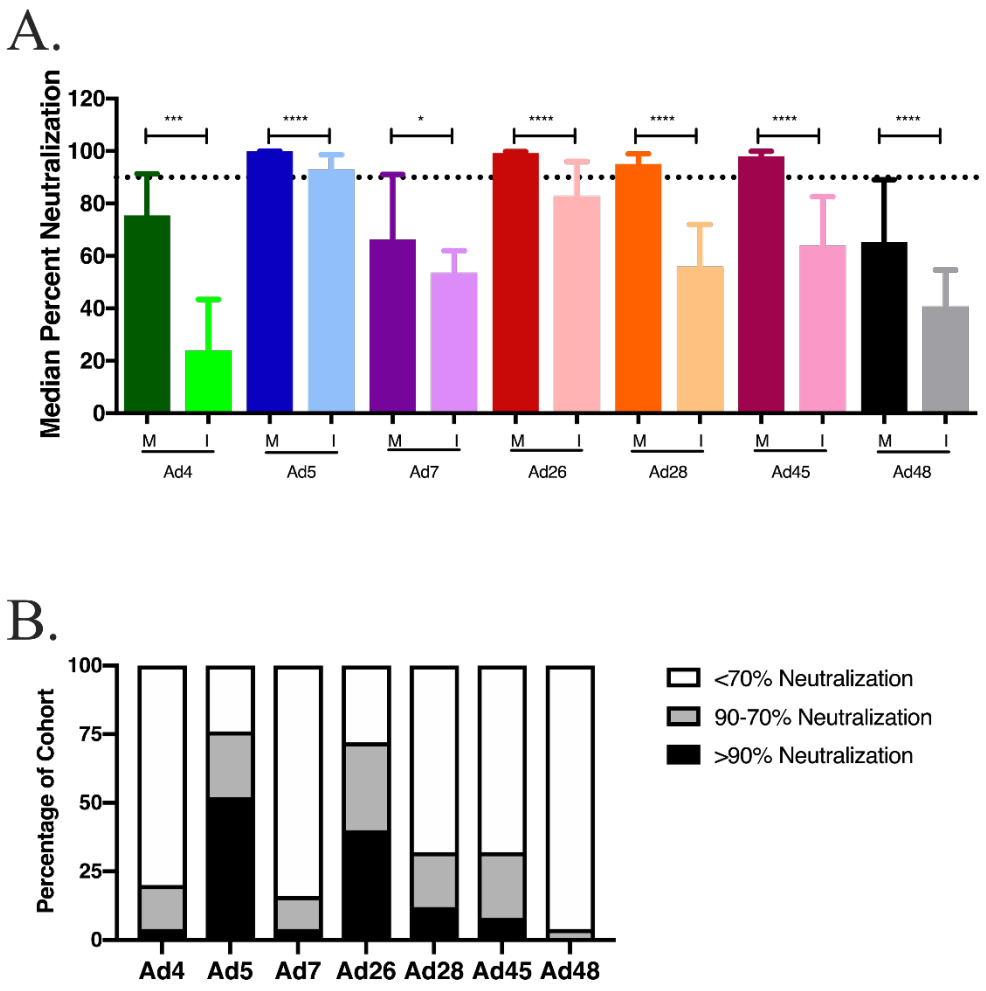

Figure 5.4. Mother to Infant transfer of neutralizing antibodies in post-ART cohort. A. Mother to infant nAb transfer in post-ART cohort. Neutralizing antibody transfer was evaluated by a comparison of total medians of neutralization between mother and infant pairs on day of enrollment (ENR) in the study. Infant ENR timepoint includes infants between 0-3 months of age. Statistical significance was determined by non-parametric Mann-Whitney tests. B. nAb profile of post-ART cohort infants. Each infant sample was placed into one of three categories based on neutralization percentage compared to virus only samples: >90%, 90-70% or <70% which equates to highly neutralizing, mildly neutralizing, or non-neutralizing, respectively. (* $P \leq 0.05$, *** $P \leq 0.001$, **** $P \leq 0.0001$)

To investigate whether or not ART treatment impacted the extent of nAb transfer to infants, the post-ART cohort was separated into ART-treated and -untreated

mothers along with their corresponding infants. HIV-1 treated and untreated women showed no significance in overall maternal nAb activity (Figure 5.3). Differential perinatal transfer was only evident for Ad5 nAb. This finding suggests that the overall decrease in Ad nAb in post-ART infants was not associated with ART-mediated maternal immune reconstitution (Table 5.2).

Table 5.2. Effect of maternal ART treatment on transfer of nAb from mother to infant. For each MIP, the percent neutralization of the infant was divided by that of the cognate mother. The average of those ratios is reported for ART-positive mothers (Column 2) versus negative (Column 3). Differences in the average of ratios based on treatment status were statistically evaluated using non-parametric Mann-Whitney tests. A significant difference based on ART treatment status was evident only against Ad5. (* P ≤ 0.05)

Adenovirus	ART+	ART-	Significance	P-Value
Ad4	0.47	0.45	ns	0.799
Ad5	0.97	0.80	*	0.021
Ad7	0.79	0.72	ns	0.903
Ad26	0.88	0.89	ns	0.249
Ad28	0.69	0.59	ns	0.217
Ad45	0.65	0.63	ns	0.562
Ad48	0.69	0.60	ns	0.411

Transfer of nAb between Mothers and Infants Coincident with ART Rollout

To quantify the differentials in maternal nAb transfer to infants between the pre- and post-ART cohorts, we calculated the median ratios of infant-to-mother neutralization after conversion of those ratios as a percentage. We found that transferred nAb against all Ads, except Ad48, was significantly reduced in post-ART cohort infants (Figure 5.5). Ad48 also showed lower nAb, but the difference was not significant. Since only modest variation in maternal Ad4 and Ad7 neutralization was

detected in response to HIV-1 infection or its treatment, this data suggests that neither variable altered the extent of nAb transferred to infants.

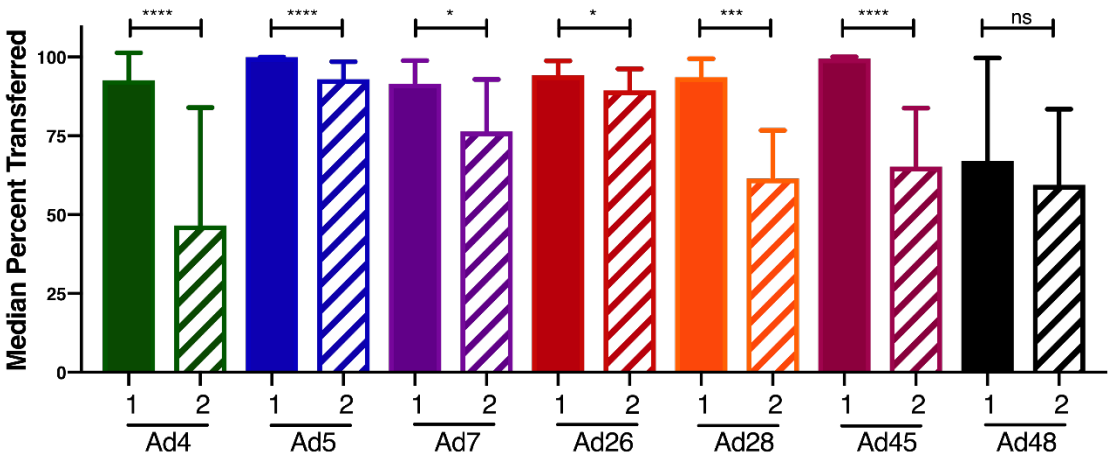

Figure 5.5. Maternal to Infant nAb Transfer in pre-ART (1) and post-ART (2) cohorts. An analysis of the change in nAbs transferred to infants over time was done by comparing the fold change between the pre-ART and post-ART cohorts. Fold change was calculated by dividing the infant neutralization percentage by that of the corresponding mother neutralization percentage. The medians are shown and Mann-Whitney tests were used to analyze statistical significance. (* $P \leq 0.05$, *** $P \leq 0.001$, **** $P \leq 0.0001$)

Degradation of Neutralizing Antibodies Over Time

In order to determine whether an optimal age for Ad-vectored infant vaccination might exist, and which Ad subtype(s) platform would be most efficacious, we quantified infant Ad nAb over time. Starting form from initial levels near those of the maternal donor, infant nAb levels decreased starting at 6 months after birth (Figure 5.6 A-B). All groups demonstrated a median neutralization below 70% at 12 months regardless of cohort or Ad. In both the pre- and post-ART cohorts, the highest median neutralization was against Ad5 at 68.6% and 52.5% respectively. The lowest median nAb response was

seen against Ad48 (26.1%) in the pre-ART cohort and against Ad4 (8.5%) in the post-ART cohort.

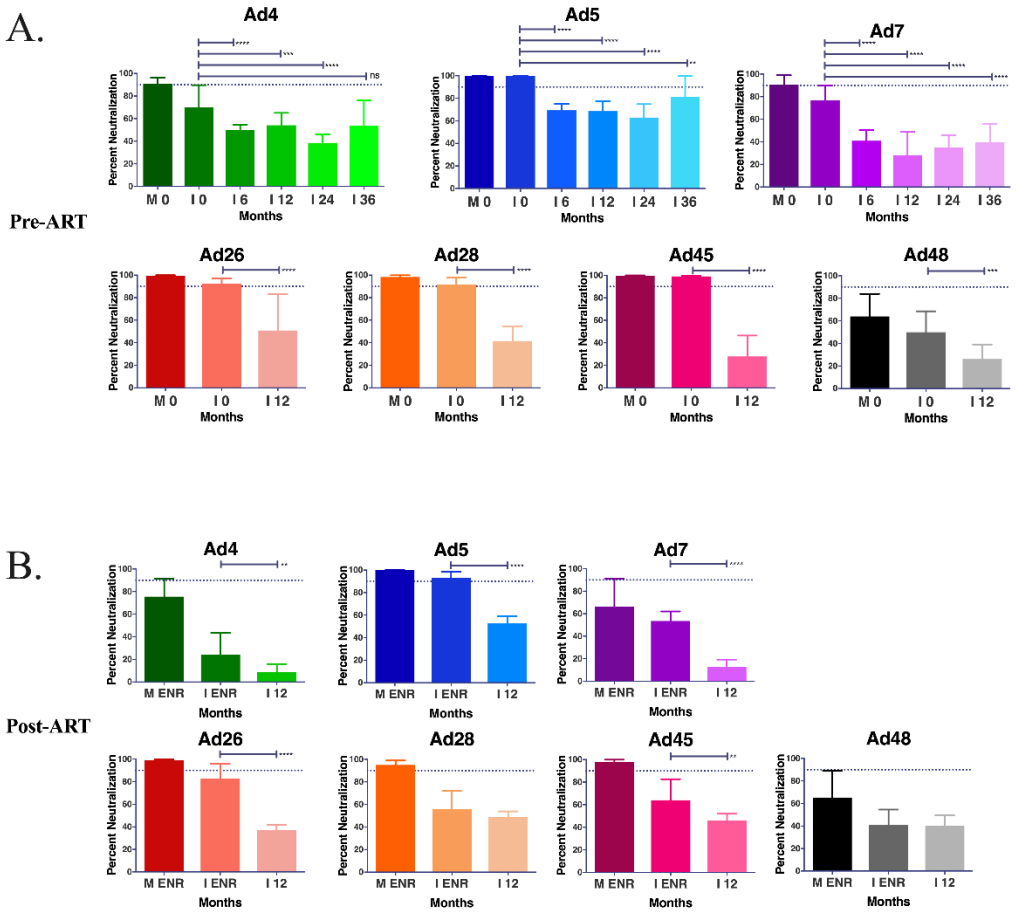

Figure 5.6. Neutralizing antibody decay over time in Zambian infants. Decay in neutralizing antibodies was evaluated at 0, 6, 12, 24 and 36 months for Ad4, Ad5, and Ad7 in the pre-ART cohort (A). Only the 12 month time point was analyzed for the pre-ART (A) for Ad26, Ad28, Ad45 and Ad48 and all Ads for the post-ART cohort (B) due to sampling limitations. Significant change in average neutralization was evaluated as a comparison to 0 months or enrollment (ENR) by Mann-Whitney analysis. (* $P \leq 0.05$, ** $P \leq 0.01$, *** $P \leq 0.001$, **** $P \leq 0.0001$)

In the pre-ART cohort, we were able to follow the nAb response against Ad4, Ad5, and Ad7 out to 36 months. The downward Ad nAb trend that starts at 6 months continued until 24 months of age but began to trend upwards at 36 months presumably

in response to *de novo* infections. This indicates that the infant population would be considered naïve and receptive to Ad vectored vaccines using any of the 7 adenoviruses.

Discussion

The WHO reports nearly 90% of the world's malaria infections, nearly 25% of TB cases, and 70% of HIV cases are located in Africa (2-4). Many of the diseases that are prominent in the region either have no vaccine available or are of very low efficacy, high cost, or with cold-chain dependent options that need improvement. Children in SSA, and elsewhere, are often exposed to infectious diseases at a young age, which makes infant vaccination crucial for effective disease control and child well-being and development. Indeed, our lab and others have demonstrated that seroconversion to Kaposi's Sarcoma Herpesvirus (KSHV) occurs in sub-Saharan infants at levels near the adult prevalence by 4 years of age (37, 38). Using adenoviruses as a vaccine vector has been shown to elicit strong T and B cell responses to inserted transgenes and could also confer immunity to the Ad used as the backbone, thereby decreasing the burden of adenovirus associated diseases in young children. Adenoviruses are relatively easy to manipulate and can be designed to be replication deficient where only the inserted transgene will be expressed in infected cells. Unlike many vaccine platforms, Ad based vaccines would not require cold storage. In combination with the fact that they can be grown to high titers in vitro at relatively low cost, this makes Adenovirus an ideal vector for vaccines that could realistically be implemented on a large scale in Africa (12, 25).

While Adenoviruses have been studied for over 20 years for their use as a vaccine and gene therapy, it has been suggested that pre-exposure can lead to decreased efficacy of the vector (14, 19, 20, 39). For this reason, we investigated the seroreactivity profile of Ad within Zambia to establish a targeted approach for future vaccine strategies in this region of SSA. Other groups previously investigated neutralization against several of these Ads in sub-Saharan adults, but the results have been variable, and were not conducted longitudinally in children, the most likely recipients of vaccinations. In 2007, Abbink *et al.* reported seroreactivity to Ad5, Ad26, and Ad48 in SSA at 100%, 21% and 3%, respectively (25). However, in 2011, Barouch *et al.* reported the South African adult Ad5, Ad26, and Ad48 seroprevalence to be 87.9-89.5%, 43.1–53.2%, and 13.3–24.6%, respectively (33). Our results are in agreement with these reports for some Ad subtypes whereas for others, the responses in our cohorts are distinct from those cited above. For example, while the median nAb responses to Ad 48 were also the lowest in both our cohorts, the magnitude of the response was 3-20-fold higher than the studies cited above, at 64% and 65.3% neutralization, respectively. In addition, low-level neutralization was readily detected in infants born to these mothers, whereas previous studies suggested that little Ad nAb was detected in young children (33). Nevertheless, the discrepant results could be a function of changes or differences in circulating Ad genotypes/serotypes in the region over time, or differences in experimental methods used for quantifying neutralization. For example, we see a decrease in maternal nAb responses against Ad4 and Ad7

between the pre- and post-ART cohorts which appears to correlate to a decrease in nAb transfer. This, however, does not explain the significant decrease in nAb transfer in the post-ART cohort against Ad5, Ad26, Ad28 or Ad45. The basis of methodological differences is also unclear since other studies quantified neutralizing responses by serial dilution but were unable to detect nAb at a 1:2 dilution, whereas we readily detected ≥90% neutralization at a 1:30 dilution of plasma.

Two other studies have investigated Ad5 seroprevalence in both HIV-1 positive and negative adult populations. Both reported no significant difference in Ad nAb between infected and uninfected populations (40, 41). These data suggest two possibilities. The first, and less likely, is that development of Ad nAb responses are not impacted by alterations to the CD4 T cell compartment since T cell depletion induced by HIV-1 infection did not diminish the neutralizing response. Alternatively, and perhaps more likely, the timing of infant *de novo* anti-adenoviral responses in our study suggests environmental exposure to adenoviral infection early in life, long before initiation of sexual activity. Thus, nAb responses had time to develop and mature immunological memory that likely is independent of CD4 T cell help in anamnestic responses. This second interpretation is supported by the lack of any statistically significant differential in Ad nAb responses in the mothers in our cohort as a result of ART treatment (i.e. CD4 T cell reconstitution).

Our study is the first to longitudinally quantify the prevalence of nAb against a subset of Ads in infants starting at the date of birth (DOB). This is a time point where

nAbs are most likely derived from the prenatal transfer of maternal nAb. In the pre-ART cohort infants, we found significantly decreased nAb against Ad4, Ad7, Ad26, and Ad28, in comparison to the cognate mothers suggesting inefficient transfer or perhaps insufficient titer in the mothers despite high % neutralization. In contrast, the infant DOB nAb levels to Ad5 and Ad45 approached adult levels, implying efficient transplacental transfer, whereas Ad48 nAb in infants was below 90%. In the post-ART cohort, transfer of nAb against the investigated Ads was decreased. Of note, the median DOB percent neutralization of Ad5 was still high at 93%, in contradiction to reports suggesting that infants lacked nAb against Ad5 (33).

A unique aspect of our study was the three-year follow-up of infants that allowed us to quantify the decay of maternally transferred nAb and to identify the timing of potential *de novo* responses to Ad infection. In both cohorts, median neutralization levels against all seven Ads were significantly lower by 12 months of age than at 0 months, and well below both the 90% and 70% threshold. Adenoviral infection and the resultant *de novo* humoral responses would explain the increases in infant nAb at 36 months seen against Ad4 and Ad5, this is consistent with post-weaning exposure to fecal-oral pathogens through solid food and increased social interactions. This study is the first to address the kinetics of nAb decay in infants where we potentially also identify exposure to the various Ads. Our findings implicate the existence of a window, between 12 and 24 months of age, that would support vaccination against regionally important pathogens without concern for pre-existing immunity.

In this study, the changes in adult seroreactivity to seven different Adenoviruses as well as the decay of nAb in children were examined to establish a timeline for vaccination in Zambia. We found that none of the seven Ads should be used in adults without pre-existing immunity being a major consideration as most adults neutralized the virus. In contrast, children have a window for vaccination between 12 and 24 months of age where maternally transferred antibodies decrease, and *de novo* infection has not yet occurred. All seven of the investigated Ads would work for this purpose since all showed low seroreactivity; but Ad4 and Ad7 are the most promising candidates as they had the lowest seroprevalence in the post-ART infants and have already been tested for efficacy against adult Ad4 and Ad7 diseases in the United States military.

Acknowledgments

The authors would like to graciously thank the Zambian mothers and infants who were participants in this study. We also thank Ms. Brigette Corder for assistance in preparation of the final manuscript. This study was supported in part of PHS grants from the National Institute of Health; National Cancer Institute grants (R01 CA75903), and National Institute of Allergy and Infectious Diseases Ruth L. Kirschstein National Research Service Award (T32 AI125207) to CW. SP is a Ruth L. Kirschstein fellow.

References

1. Anonymous. 2018. HIV/AIDS. https://www.who.int/news-room/fact-sheets/detail/hiv-aids. Accessed

2. Anonymous. 2019. Tuberculosis (TB), *on* World Health Organization. https://afro.who.int/health-topics/tuberculosis-tb. Accessed

3. Anonymous. 2016-12-13 00:58:00 2016. WHO | 10 facts on malaria, *on* World Health Organization. https://www.who.int/features/factfiles/malaria/en/. Accessed

4. Anonymous. 2018-12-18 10:36:54 2018. WHO | Data and statistics, *on* World Health Organization. https://www.who.int/hiv/data/en/. Accessed

5. Chen RF, Lee CY. 2014. Adenoviruses types, cell receptors and local innate cytokines in adenovirus infection. Int Rev Immunol 33:45-53.

6. Alexander J, Ward S, Mendy J, Manayani DJ, Farness P, Avanzini JB, Guenther B, Garduno F, Jow L, Snarsky V, Ishioka G, Dong X, Vang L, Newman MJ, Mayall T. 2012. Pre-clinical evaluation of a replication-competent recombinant adenovirus serotype 4 vaccine expressing influenza H5 hemagglutinin. PLoS One 7:e31177.

7. Stephenson KE, Keefer MC, Bunce CA, Frances D, Abbink P, Maxfield LF, Neubauer GH, Nkolola J, Peter L, Lane C, Park H, Verlinde C, Lombardo A, Yallop C, Havenga M, Fast P, Treanor J, Barouch DH. 2018. First-in-human randomized controlled trial of an oral, replicating adenovirus 26 vector vaccine for HIV-1. PLoS One 13.

8. Barry M. 2018. Single-cycle adenovirus vectors in the current vaccine landscape. Expert Rev Vaccines 17:163-73.

9. Weaver EA, Barry MA. 2013. Low seroprevalent species D adenovirus vectors as influenza vaccines. PLoS One 8:e73313.

10. Gach JS, Gorlani A, Dotsey EY, Becerra JC, Anderson CT, Berzins B, Felgner PL, Forthal DN, Deeks SG, Wilkin TJ, Casazza JP, Koup RA, Katlama C, Autran B, Murphy RL, Achenbach CJ. 2016. HIV-1-Specific Antibody Response and Function after DNA Prime and Recombinant Adenovirus 5 Boost HIV Vaccine in HIV-Infected Subjects. PLoS One 11:e0160341.

11. Baden LR, Liu J, Li H, Johnson JA, Walsh SR, Kleinjan JA, Engelson BA, Peter L, Abbink P, Milner DA, Jr., Golden KL, Viani KL, Stachler MD, Chen BJ, Pau MG, Weijtens M, Carey BR, Miller CA, Swann EM, Wolff M, Loblein H, Seaman MS, Dolin R, Barouch DH. 2015. Induction of HIV-1-specific mucosal immune responses following intramuscular recombinant adenovirus serotype 26 HIV-1 vaccination of humans. J Infect Dis 211:518-28.

12. Bullard BL, Corder BN, Gorman MJ, Diamond MS, Weaver EA. 2018. Efficacy of a T Cell-Biased Adenovirus Vector as a Zika Virus Vaccine. Sci Rep 8:18017.

13. Geisbert TW, Bailey M, Hensley L, Asiedu C, Geisbert J, Stanley D, Honko A, Johnson J, Mulangu S, Pau MG, Custers J, Vellinga J, Hendriks J, Jahrling P, Roederer M, Goudsmit J, Koup R, Sullivan NJ. 2011. Recombinant adenovirus serotype 26 (Ad26) and Ad35 vaccine vectors bypass immunity to Ad5 and protect nonhuman primates against ebolavirus challenge. J Virol 85:4222-33.

14. Dicks MD, Spencer AJ, Edwards NJ, Wadell G, Bojang K, Gilbert SC, Hill AV, Cottingham MG. 2012. A novel chimpanzee adenovirus vector with low human seroprevalence: improved systems for vector derivation and comparative immunogenicity. PLoS One 7:e40385.

15. Zhu FC, Wurie AH, Hou LH, Liang Q, Li YH, Russell JB, Wu SP, Li JX, Hu YM, Guo Q, Xu WB, Wurie AR, Wang WJ, Zhang Z, Yin WJ, Ghazzawi M, Zhang X, Duan L, Wang JZ, Chen W. 2017. Safety and immunogenicity of a recombinant adenovirus type-5 vector-based Ebola vaccine in healthy adults in Sierra Leone: a single-centre, randomised, double-blind, placebo-controlled, phase 2 trial. Lancet 389:621-628.

16. Choudhry A, Mathena J, Albano JD, Yacovone M, Collins L. 2016. Safety evaluation of adenovirus type 4 and type 7 vaccine live, oral in military recruits. Vaccine 34:4558-4564.

17. Fausther-Bovendo H, Kobinger GP. 2014. Pre-existing immunity against Ad vectors: humoral, cellular, and innate response, what's important? Hum Vaccin Immunother 10:2875-84.

18. Nwanegbo E, Vardas E, Gao W, Whittle H, Sun H, Rowe D, Robbins PD, Gambotto A. 2004. Prevalence of neutralizing antibodies to adenoviral serotypes 5 and 35 in the adult populations of The Gambia, South Africa, and the United States. Clin Diagn Lab Immunol 11:351-7.

19. Alonso-Padilla J, Papp T, Kajan GL, Benko M, Havenga M, Lemckert A, Harrach B, Baker AH. 2016. Development of Novel Adenoviral Vectors to Overcome Challenges Observed With HAdV-5-based Constructs. Mol Ther 24:6-16.

20. Buchbinder SP, Mehrotra DV, Duerr A, Fitzgerald DW, Mogg R, Li D, Gilbert PB, Lama JR, Marmor M, Del Rio C, McElrath MJ, Casimiro DR, Gottesdiener KM, Chodakewitz JA, Corey L, Robertson MN, Step Study Protocol T. 2008. Efficacy assessment of a cell-mediated immunity HIV-1 vaccine (the Step Study): a double-blind, randomised, placebo-controlled, test-of-concept trial. Lancet 372:1881-1893.

21. Flasche S, Jit M, Rodriguez-Barraquer I, Coudeville L, Recker M, Koelle K, Milne G, Hladish TJ, Perkins TA, Cummings DA, Dorigatti I, Laydon DJ, Espana G, Kelso J, Longini I, Lourenco J, Pearson CA, Reiner RC, Mier YT-RL, Vannice K, Ferguson N. 2016. The Long-Term Safety, Public Health Impact, and Cost-Effectiveness of Routine Vaccination with a Recombinant, Live-Attenuated Dengue Vaccine (Dengvaxia): A Model Comparison Study. PLoS Med 13:e1002181.

22. Halstead SB. 2017. Dengvaxia sensitizes seronegatives to vaccine enhanced disease regardless of age. Vaccine 35:6355-6358.

23. Pauly M, Hoppe E, Mugisha L, Petrzelkova K, Akoua-Koffi C, Couacy-Hymann E, Anoh AE, Mossoun A, Schubert G, Wiersma L, Pascale S, Muyembe JJ, Karhemere S, Weiss S, Leendertz SA, Calvignac-Spencer S, Leendertz FH, Ehlers B. 2014. High prevalence and diversity of species D adenoviruses (HAdV-D) in human populations of four Sub-Saharan countries. Virol J 11:25.

24. de Andrade Pereira B, Maduro Bouillet LE, Dorigo NA, Fraefel C, Bruna-Romero O. 2015. Adenovirus Specific Pre-Immunity Induced by Natural Route of Infection Does Not Impair Transduction by Adenoviral Vaccine Vectors in Mice. PLoS One 10:e0145260.

25. Abbink P, Lemckert AA, Ewald BA, Lynch DM, Denholtz M, Smits S, Holterman L, Damen I, Vogels R, Thorner AR, O'Brien KL, Carville A, Mansfield KG, Goudsmit J, Havenga MJ, Barouch DH. 2007. Comparative seroprevalence and immunogenicity of six rare serotype recombinant adenovirus vaccine vectors from subgroups B and D. J Virol 81:4654-63.

26. Duffy MR, Alonso-Padilla J, John L, Chandra N, Khan S, Ballmann MZ, Lipiec A, Heemskerk E, Custers J, Arnberg N, Havenga M, Baker AH, Lemckert A. 2018. Generation and characterization of a novel candidate gene therapy and vaccination vector based on human species D adenovirus type 56. J Gen Virol 99:135-147.

27. Farrow AL, Peng BJ, Gu L, Krendelchtchikov A, Matthews QL. 2016. A Novel Vaccine Approach for Chagas Disease Using Rare Adenovirus Serotype 48 Vectors. Viruses 8:78.

28. Lynch JP, 3rd, Kajon AE. 2016. Adenovirus: Epidemiology, Global Spread of Novel Serotypes, and Advances in Treatment and Prevention. Semin Respir Crit Care Med 37:586-602.

29. Scott MK, Chommanard C, Lu X, Appelgate D, Grenz L, Schneider E, Gerber SI, Erdman DD, Thomas A. 2016. Human Adenovirus Associated with Severe Respiratory Infection, Oregon, USA, 2013-2014. Emerg Infect Dis 22:1044-51.

30. Mayindou G, Ngokana B, Sidibe A, Moundele V, Koukouikila-Koussounda F, Christevy Vouvoungui J, Kwedi Nolna S, Velavan TP, Ntoumi F. 2016. Molecular epidemiology and surveillance of circulating rotavirus and adenovirus in Congolese children with gastroenteritis. J Med Virol 88:596-605.

31. Weaver EA. 2014. Vaccines within vaccines: the use of adenovirus types 4 and 7 as influenza vaccine vectors. Hum Vaccin Immunother 10:544-56.

32. Abbink P, Maxfield LF, Ng'ang'a D, Borducchi EN, Iampietro MJ, Bricault CA, Teigler JE, Blackmore S, Parenteau L, Wagh K, Handley SA, Zhao G, Virgin HW, Korber B, Barouch DH. 2015. Construction and evaluation of novel rhesus monkey adenovirus vaccine vectors. J Virol 89:1512-22.

33. Barouch DH, Kik SV, Weverling GJ, Dilan R, King SL, Maxfield LF, Clark S, Ng'ang'a D, Brandariz KL, Abbink P, Sinangil F, de Bruyn G, Gray GE, Roux S, Bekker LG, Dilraj A, Kibuuka H, Robb ML, Michael NL, Anzala O, Amornkul PN, Gilmour J, Hural J, Buchbinder SP, Seaman MS, Dolin R, Baden LR, Carville A, Mansfield KG, Pau MG, Goudsmit J. 2011. International seroepidemiology of adenovirus serotypes 5, 26, 35, and 48 in pediatric and adult populations. Vaccine 29:5203-9.

34. Yang WX, Zou XH, Jiang SY, Lu NN, Han M, Zhao JH, Guo XJ, Zhao SC, Lu ZZ. 2016. Prevalence of serum neutralizing antibodies to adenovirus type 5 (Ad5) and 41 (Ad41) in children is associated with age and sanitary conditions. Vaccine 34:5579-5586.

35. Zhang X, Wang J, Lu J, Li R, Zhao S. 2018. Correction to: Immunogenicity of adenovirus-vector vaccine targeting hepatitis B virus: non-clinical safety assessment in non-human primates. Virol J 15:137.

36. Lion T. 2014. Adenovirus infections in immunocompetent and immunocompromised patients. Clin Microbiol Rev 27:441-62.

37. Nalwoga A, Miley W, Labo N, Elliott A, Cose S, Whitby D, Newton R. 2018. Age of Infection with Kaposi Sarcoma-Associated Herpesvirus and Subsequent Antibody Values Among Children in Uganda. Pediatr Infect Dis J 37:e225-e228.

38. Olp LN, Minhas V, Gondwe C, Poppe LK, Rogers AM, Kankasa C, West JT, Wood C. 2016. Longitudinal analysis of the humoral response to Kaposi's sarcoma-associated herpesvirus after primary infection in children. J Med Virol 88:1973-81.

39. Saxena M, Van TT, Baird FJ, Coloe PJ, Smooker PM. 2013. Pre-existing immunity against vaccine vectors--friend or foe? Microbiology 159:1-11.

40. Kostense S, Koudstaal W, Sprangers M, Weverling GJ, Penders G, Helmus N, Vogels R, Bakker M, Berkhout B, Havenga M, Goudsmit J. 2004. Adenovirus types 5 and 35 seroprevalence in AIDS risk groups supports type 35 as a vaccine vector. Aids 18:1213-6.

41. Sun C, Zhang Y, Feng L, Pan W, Zhang M, Hong Z, Ma X, Chen X, Chen L. 2011. Epidemiology of adenovirus type 5 neutralizing antibodies in healthy people and AIDS patients in Guangzhou, southern China. Vaccine 29:3837-41.

CHAPTER 6

CONCLUDING REMARKS

Our recent research on Kaposi sarcoma has investigated the transcriptomic and metabolomic aspects of KS (1-3). To investigate potential biomarkers of KS, we utilized three different methods: bulk comparative tumor transcriptomics and subsequent marker validation in tissue, plasma metabolomics, and plasma proteomics. Through those transcriptomic studies, our laboratory showed that KS tumor tissues have gene expression alterations indicative of significant dysregulation of various metabolic pathways, including glucose utilization and anabolic and catabolic lipid metabolism (3). Because of the extent of these changes, we sought to identify targetable pathways or proteins for treatment (2) by defining upregulated cell surface glycoproteins in the KS tumor microenvironment that potentially could be used as targets or biomarkers for KS.

The transcriptomics study identified seven highly upregulated transcripts in the KS lesions that correlated with increased KSHV LANA expression, all of which encoded predicted cell surface proteins with potential as biomarkers for latent KSHV infection or KS-transformed cells. However, the absence of protein expression for OX40 and ZP2 indicates post-transcriptional decoupling from RNA expression levels for some genes. Several of the markers identified are indicative of an endothelial cell phenotype and consistent with the prevailing view that KS is an endothelial tumor; however, PROX1 and CD34 are typically attributed to distinct endothelial phenotypes, lymphatic and vascular, respectively. This emphasizes the need for further studies into the cellular origin of KS

tumors. The establishment of a mouse model accurately reflecting the KS environment may prove to be essential to further this research, however, none of the current animal models completely recapitulate endothelial phenotypes observed in human KS tumors. For example, we demonstrated that the L1T2 cell line, which is latently infected with KSHV, was unable to express characteristic endothelial cell markers Prox-1 and CD34 despite adopting a KS-like spindle cell morphology and retaining KSHV infection upon tumorigenesis.

Metabolomic studies in our lab have also shown metabolic differences between KSHV-infected individuals and those with KS specifically in the amino acid and purine metabolic pathways, these have been identified by others as potentially significant in KS disease progression in cell line studies as well (4). Here we also examined plasma metabolites to gain insights into the metabolic profiles associated with Kaposi sarcoma (KS) and its progression in a Tanzanian cohort. We found distinct metabolic profiles among the three experimental groups, with a clear separation between symptomatic and asymptomatic individuals (1). The lipid fraction of plasma showed significant effects on lipid metabolism, consistent with the transcriptomic data from bulk KS tumors which identified dysregulation of glucose metabolism. Glycerophospholipids and sphingolipids represented a substantial portion of the differential lipids when comparing both the asymptomatic groups and the group with KS. The study also highlighted changes in purine metabolism, with hypoxanthine decreased and uric acid increased in the symptomatic KS group. These findings suggest metabolic reprogramming in KS, with an

emphasis on lipid metabolism and purine utilization. The follow-up study in Zambian individuals yielded similar results, in that changes to amino acid synthesis pathways were also observed in the KS symptomatic group. Both studies demonstrated glutamine and glutamate pathways as being differentially dysregulated in KS, but the lack of overall cohesiveness between studies emphasizes the need for a more thorough and controlled metabolomics study.

The above studies provided insights into the metabolic alterations of lipid metabolism, amino acid, and glucose metabolism associated with KSHV infection and KS progression, offering potential avenues for further research and biomarker development. Targeted metabolomics of both plasma and KS tumors of the dysregulated pathways are needed as the sensitivity of untargeted metabolomics is not high enough to detect all important metabolites that have roles in tumorigenesis.

The Kaposi sarcoma (KS) research field faces several significant limitations that impede progress in understanding and effectively treating this complex disease. One of the foremost challenges is the lack of an animal model to study disease development. Currently, the only models utilize immunodeficient mice or latently infected epithelial cell lines (5). These models lack the complex immune systems humans have which impact tumor development and disease severity as well as the fundamental surface biomarkers that are characteristic of Kaposi Sarcoma such as CD34.

The second is the lack of reliable biomarkers for early detection, diagnosis, prognosis, and disease progression. KS often presents at advanced stages, making it

challenging to implement timely interventions. Developing sensitive and specific biomarkers for KS is critical to enable early diagnosis, assess disease severity, and guide treatment decisions. Identification of disease-related markers will not only lead to a study to better understand the pathogenesis of the disease but could potentially enhance patient outcomes by facilitating early therapeutic interventions and monitoring disease progression based on biomarker presence and levels. Before such testing could be implemented, a targeted cohort evaluating patients before, during, and after treatment is needed to understand the important metabolic features discriminating individuals who respond to treatment from those who do not. Such studies are difficult to perform in the African setting and will likely require an American cohort to overcome storage and sample handling discrepancies.

Another limitation is the heterogeneity of KS lesions, which can manifest in different clinical forms, including classic KS, endemic KS, iatrogenic KS, and epidemic KS. These variations in presentation suggest diverse underlying mechanisms and responses to treatment. EpKS often regresses when the individual is placed on ART; however, the only options currently available to HIV-negative EnKS patients are chemotherapy and palliative care, which have mixed outcomes where some patients who initially respond well will develop new tumors (6). Understanding and characterizing this heterogeneity at the cellular level within the TME is essential for tailoring personalized treatment strategies and improving therapeutic outcomes. However, limited access to patient samples in large enough quantities to support robust statistical comparisons and *in vitro*

and *in vivo* models that recapitulate this heterogeneity hinders research progress in this regard. Moreover, the infrequent occurrence of KS in certain areas and its prevalence mainly among specific populations, like those with HIV co-infection, makes it challenging to access patient samples. This shortage of real-world data hinders the identification of new therapeutic targets and the development of innovative treatment methods, given that most KSHV-related studies rely on in vitro models that may not fully capture the complexity of the disease. Overcoming these limitations requires collaborative efforts, increased research funding, and the establishment of biobanks and research networks to collect and share data, ultimately advancing our understanding of KS and improving patient care.

The work herein described studies identifying and validating potential biomarkers of KS tumorigenesis; however, the small sample sizes and untargeted approaches render the data difficult to resolve. Recent technology has moved from bulk transcriptomics and exploratory -omic studies to more accurate and precise deconvolution of tumor constituents and their spatial proximity in the TME. For example, highly multiplexed *in situ* protein marker detection at single-cell resolution offers the opportunity to define tumor components and their relationships more thoroughly with one another. Preliminary images of KS using the Lunaphore platform of low and high KSHV LANA-containing tumors is shown below (Figure 6.1). In these preliminary findings, we observed increased cell proliferation, indicated by Ki67 in green, increased monocytes and macrophages, indicated by CD68 in orange, and CD3

cells along the periphery of the KSHV LANA regions. This is contrasted with a KS lesion with very low LANA expression where little cell proliferation, macrophage infiltration, or T cell recruitment is seen. Indeed, it is suspected that this lesion may not have been a KS lesion, but rather one of the confounding skin conditions that occur at high incidence in sub-Saharan Africa in the HIV-1+ population. Extending from my studies, this technology will now be combined with spatial transcriptomics by others in the lab to resolve remaining questions relating to the tumor microenvironment such as the cellular origins and the cell landscape of KS, and the status and Ag-specificity of immune cells present in/near tumor. Such understanding could open avenues for therapies to reactivate or recruit functional immune cells.

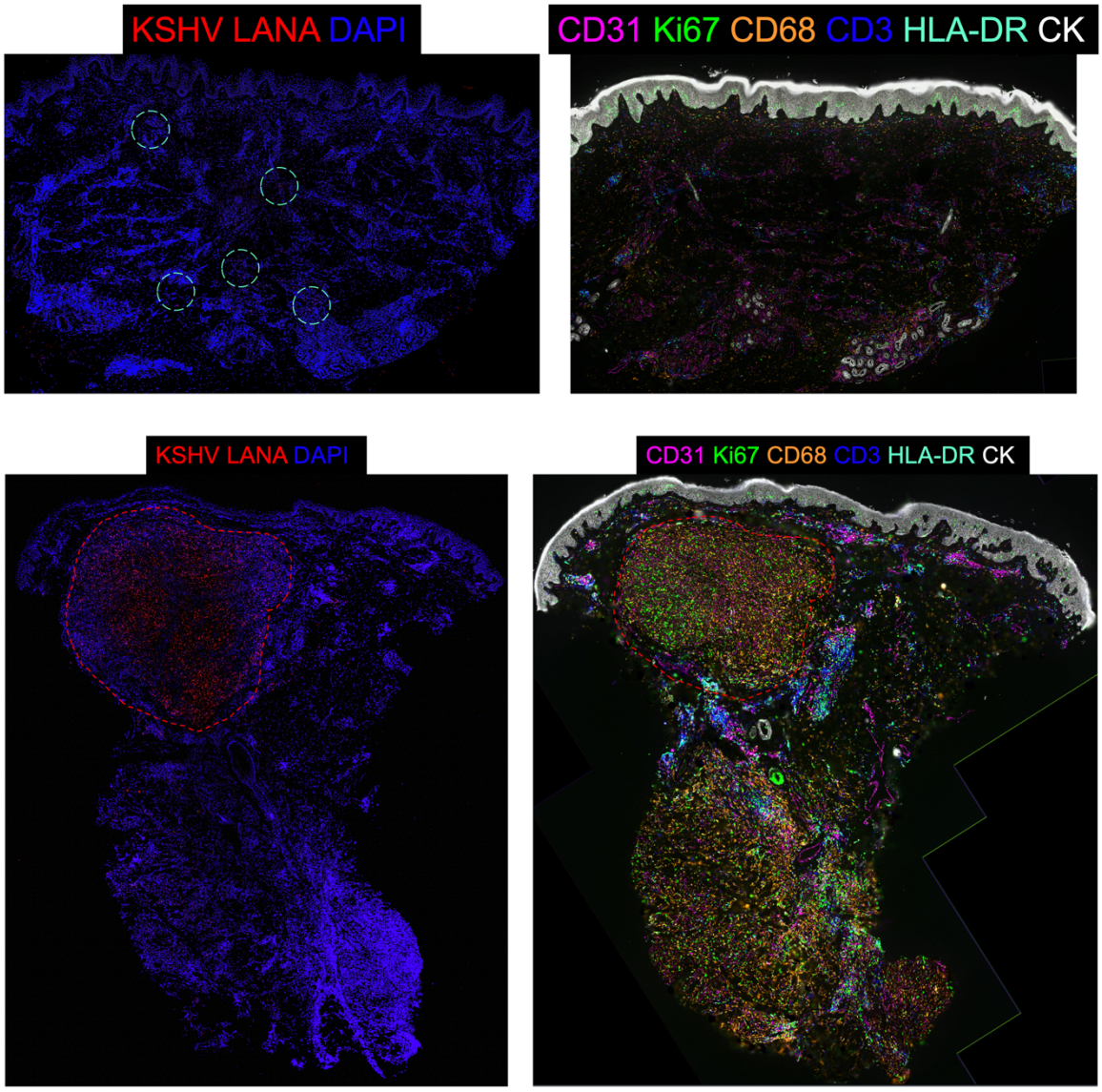

Figure 6.1. Preliminary spatial proteomics for two LANA positive KS lesions demonstrating the difference between a LANA low and LANA high tumor. Increased cell proliferation (Ki67) and CD68 are observed in the LANA high lesion.

Kaposi Sarcoma remains a complex and challenging disease that demands further research to study disease pathogenesis, identify the potential biomarkers for prognosis, and follow disease progression. Understanding the tumor environment, encompassing the diverse cell types present, particularly immune cells within and

surrounding tumors, is essential for advancing our comprehension of the immune response, its underlying causes, pathogenesis, and potential therapeutic strategies. Moreover, further investigations into the interplay between host and viral factors, their roles in mediating transformation and oncogenesis, how the host responds to KSHV infection and the development of cancers, as well as the metabolic changes during tumorigenesis are essential to advance our knowledge and develop more effective strategies for prevention and treatment of KS. Until we identify the interplay among important cellular and metabolic factors, we will not be able to develop new therapeutic strategies to treat or prevent KS.

A similar concept can be applied to investigate both spatial metabolic and transcriptomic profiles of KS tumors, allowing for a more accurate look into the state of tumor cells as opposed to metabolite profiles of circulating plasma. Here, we can differentiate between the metabolomic and transcriptomic profiles of KSHV-infected and uninfected cells within KS tumors as well as the metabolic states of the immune cells trapped on the exterior of the KS lesions. This technology can also be used to further explore the cellular origin of KS tumors. The proteomic and transcriptomic profiles at a single cell level may be able to differentiate cells that originate from circulating endothelial cells and stem cells. Identifying key pathways will open doors to investigating targeted therapeutics which may lead to more effective treatments and better outcomes for KS patients.

In conclusion, the results presented here describe a starting point for future research investigating the KSHV-infected cells in the tumor, the tumor-specific cellular markers, the tumor microenvironment, the role of infiltrating immune cells, and how various cell types interact with each other within the tumor. Studies with higher resolution at the single cell levels will further allow us to tease out the role of the infected cells, the importance of upregulated cellular pathways such as the VEGF and purine metabolism pathways while also allowing us to explore the state of the immune response in KS lesions to better understand the disease pathogenesis and possibly developing more effective therapeutic regimens.

References

1. Privatt SR, Braga CP, Johnson A, Lidenge SJ, Berry L, Ngowi JR, et al. Comparative polar and lipid plasma metabolomics differentiate KSHV infection and disease states. Cancer Metab. 2023;11(1):13.

2. Privatt SR, Ngalamika O, Zhang J, Li Q, Wood C, West JT. Upregulation of Cell Surface Glycoproteins in Correlation with KSHV LANA in the Kaposi Sarcoma Tumor Microenvironment. Cancers (Basel). 2023;15(7).

3. Lidenge SJ, Kossenkov AV, Tso FY, Wickramasinghe J, Privatt SR, Ngalamika O, et al. Comparative transcriptome analysis of endemic and epidemic Kaposi's sarcoma (KS) lesions and the secondary role of HIV-1 in KS pathogenesis. PLoS Pathog. 2020;16(7):e1008681.

4. Sanchez EL, Pulliam TH, Dimaio TA, Thalhofer AB, Delgado T, Lagunoff M. Glycolysis, Glutaminolysis, and Fatty Acid Synthesis Are Required for Distinct Stages of Kaposi's Sarcoma-Associated Herpesvirus Lytic Replication. J Virol. 2017;91(10).

5. Dittmer DP, Damania B, Sin SH. Animal models of tumorigenic herpesviruses--an update. Curr Opin Virol. 2015;14:145-50.

6. Ngalamika O, Mukasine MC, Kawimbe M, Vally F. Viral and immunological markers of HIV-associated Kaposi sarcoma recurrence. PLoS One. 2021;16(7):e0254177.